

Robert Lassfolk

Acyl Group Migration in Carbohydrates

Migration within the saccharide unit
and across the glycosidic linkage





Robert Lassfolk

Born 1992

Previous studies and degrees

M.Sc. in chemistry, 2017
Åbo Akademi University



Acyl Group Migration in Carbohydrates

Migration within the saccharide unit and across the glycosidic
linkage

Robert Lassfolk

Organic Chemistry
Faculty of Science and Engineering
Åbo Akademi University
Åbo, Finland, 2022

SUPERVISOR AND CUSTOS

Professor Reko Leino
Laboratory of Molecular Science and Engineering
Åbo Akademi University
Åbo, Finland

OPPONENT

Professor Paul Murphy
University of Galway
Galway, Ireland

REVIEWERS

Professor emeritus Harri Lönnberg
University of Turku
Åbo, Finland

And

Professor Carmen Galan
University of Bristol
Bristol, United Kingdom

ISBN 978-952-12-4233-5 (printed)
ISBN 978-952-12-4234-2 (digital)
Painosalama Oy – Åbo, Finland 2022

*Anyone who has never made a mistake
has never tried anything new*

— Albert Einstein

Preface

The work in this thesis was carried out between the years 2018-2022 at the Laboratory of Organic Chemistry, Åbo Akademi University. The Magnus Ehrnrooths foundation and Waldemar von Frenckells foundation are gratefully acknowledged for the financial support throughout the whole thesis.

I would deeply like to thank my supervisor Professor Reko Leino for giving me the opportunity to work in the field of carbohydrate chemistry. I am grateful for the trust and support that I have been given since my start at the laboratory. I would like to thank Professor Carmen Galan (University of Bristol) and Professor emeritus Harri Lönnberg (University of Turku) for reviewing my thesis, and Professor Paul Murphy (University of Galway) for taking the time to be my opponent.

My warmest thanks to Dr. Jani Rahkila for introducing me to world of carbohydrate chemistry and for the help you have given throughout the years. I would also like to thank my co-supervisor Dr. Filip Ekholm for the support. I would like to thank Professor Johan Wärnå for the collaboration. I would deeply like to thank the collaborators in Spain, from the University of Zaragoza: Professor Pedro Merino, Professor Tomás Tejero, and Manuel Pedrón; and from CIC bioGUNE: Professor Jesús Jiménez-Barbero, Dr. Ana Ardá, and Sara Bertuzzi. I would also like to thank Dr. Mikael Johansson (University of Helsinki).

I would like to thank my current and past coworkers and good friends at the Laboratory of Organic Chemistry, in no particular order: Dr. Patrik Eklund, Dr. Tiina Saloranta-Simell, Dr. Jan-Erik Lönnqvist, Professor Jorma Mattinen, Teija Tirri, Dr. Risto Savela, Dr. Lucas Lagerquist, Dr. Yury Brusentsev, Ida Mattsson, Dr. Otto Långvik, Patrik Runeberg, Veronika Badazhkova, Anton Örn, Atefeh Saadabadi, Annika Fougstedt, and many more. Big thanks to other Åbo Akademi colleges at the other laboratories with whom I have had many great discussions and for the support in my work.

My biggest thanks to my great friends Carl-Erik Strandberg, Dennis Granith, Edvard Söderback, Ville Anttinen, Robin Fagerudd, Oskar Lindberg, Riku Tuominen, and Tommi Kippola for the great times and giving me the opportunity to focus on other thing than the research.

My biggest gratitude to my parents, my brothers and sister and their families for the love and support throughout my studies. Finally, I would like to express my greatest gratitude to Sonja for all the love and care over these years.

Åbo, November 2022

A handwritten signature in black ink, appearing to read 'Robert Lassfolk'. The script is cursive and fluid, with the first name 'Robert' and last name 'Lassfolk' clearly distinguishable.

Robert Lassfolk

Abstract

Carbohydrates fulfill many biological roles in nature, all from giving cells their structure to cell signaling. Hemicelluloses form a group of polysaccharides found mostly in plant cells. These polysaccharides help to maintain the properties and functions of cell walls. Hemicelluloses can be further divided into mannans, xylans and glucans, depending on the main carbohydrate in the backbone. A common feature of the backbone is the β -(1 \rightarrow 4)-linkages between the main carbohydrate units. Branches are also common in hemicelluloses, usually consisting of carbohydrates other than the main one. Many hemicelluloses can be partially acetylated in nature and the acetyl groups are often crucial for the biological activity of the polysaccharides.

Acyl group migration is a phenomenon that can cause problems in synthesis, isolation, and purification of compounds. It was Fischer that first observed the migration in carbohydrates. The migration can take place in any compound with hydroxyl groups sufficiently close to each other but is most prominent in carbohydrates because of the close proximity of the hydroxyl groups. The migration has mostly been studied in monosaccharides and the migration in oligo- and polysaccharides has mostly been side notes in other studies. Many hemicelluloses are naturally acetylated and considering that the acetyl groups are used to regulate biological activity in nature, migration could be a method to enhance or suppress cell signaling and other biological activities.

This thesis explores the acyl group migration in monosaccharides as well as model compounds of hemicelluloses. A comprehensive investigation into the acyl group migration in monosaccharides has been performed. Furthermore, it is demonstrated that the acetyl group can migrate between two saccharide units in trisaccharide model compounds, towards the reducing end, from a secondary to the primary position. It is also demonstrated that the migration can take place in large polysaccharides. With the help of experimental evidence and computational calculations, a mechanism is proposed where the pH of the buffer and the pK_as of the hydroxyl groups have a significant role.

Abstrakt

Kolhydrater uppfyller många roller i naturen, allt från att ge celler deras struktur till cellsignaler. Hemicellulosa är en grupp polysackarider, som förekommer främst i växtceller. Hemicellulosor hjälper cellväggarna att upprätthålla sina egenskaper och funktioner. Hemicellulosor kan delas in i mannaner, glukaner och xylaner, beroende på den mest förekommande kolhydraten i huvudkedjan, som består främst av β -(1 \rightarrow 4)-kopplingar. Sidokedjor är vanliga och består främst av andra kolhydrater än huvudkolhydraten. Många hemicellulosor kan vara naturligt acetylerade och acetylgrupperna är viktiga för den biologiska aktiviteten hemicellulosor har.

Acylgruppsmigrationen är ett fenomen som ställer till med problem i syntes, isolering och rening av ämnen. Första beskrivningen av migrationen i kolhydrater gjordes av Fischer. Så länge hydroxylgrupper är nära varandra kan migrationen ske i vilka ämnen som helst, men migrationen observeras mest i kolhydrater på grund av att de innehåller flera hydroxylgrupper som är nära varandra. Migrationen har huvudsakligen studerats i monosackarider medan migration i oligo- och polysackarider har mestadels varit en bisak i andra studier. Migrationen kunde vara ett sätt att reglera cellsignaler och andra biologiska aktiviteter eftersom många hemicellulosor innehåller acetylgrupper, samt att acetylgrupper används för att reglera biologiska aktiviteter.

Denna avhandling utforskar acetylgruppsmigrationen i detalj i monosackarider, men också i modellförningar baserade på hemicellulosor. En utförlig studie på acetylgruppsmigration i monosackarider har gjorts för att ge en bättre helhetsbild. Avhandlingen påvisar även att acetylgrupper kan migrera från en sackaridenhet till en annan, mot den reducerande ändan, och även migrationen i en naturlig polysackarid, GGM, har undersökts. Med hjälp av experimentella metoder och databeräkningar har en mekanism för migrationen föreslagits, där buffertens pH och hydroxylgruppernas pK_a har en central roll för migrationshastigheten.

List of publications

Parts of the introductory chapter are based on the review article:

- I. A. A. Hettikankanamalage, R. Lassfolk, F. S. Ekholm, R. Leino, D. Crich, Mechanisms of Stereodirecting Participation and Ester Migration from Near and Far in Glycosylation and Related Reactions. *Chem. Rev.* **2020**, *120*, 7104 – 7151.

The experimental work reported in this thesis is based on the following original publications:

- II. R. Lassfolk, M. Pedrón, T. Tejero, P. Merino, J. Wärnå, R. Leino, Acyl group migration in pyranosides as studied by experimental and computational methods. *Chem. Eur. J.* **2022**, *28*, e202200499.
- III. R. Lassfolk, J. Rahkila, M. P. Johansson, F. S. Ekholm, J. Wärnå, R. Leino, Acetyl Group Migration across the Saccharide Units in Oligomannoside Model Compound. *J. Am. Chem. Soc.* **2019**, *141*, 1646–1654.
- IV. R. Lassfolk, S. Bertuzzi, A. Ardá, J. Wärnå, J. Jiménez-Barbero, R. Leino, Kinetic Studies of Acetyl Group Migration between the Saccharide Units in an Oligomannoside Trisaccharide Model Compound and a Native Galactoglucomannan Polysaccharide. *ChemBioChem* **2021**, *22*, 2986–2995.
- V. R. Lassfolk, M. Pedrón, T. Tejero, P. Merino, J. Wärnå, R. Leino, Acetyl group migration in xylan and glucan model compounds as studied by experimental and computational methods. *J. Org. Chem.* **Article ASAP**, DOI: 10.1021/acs.joc.2c01956.

Contribution of the author

The author of this thesis is the main author of the publications **II – V**. The author is also responsible for the experimental work presented in the thesis, with the following exceptions:

- Dr. J. Wärnå performed the calculation of the rate constants in publications **II – V**.
- Dr. M. P. Johansson performed the computational studies in publication **III**.
- Dr. P. Merino, Dr. T. Tejero, and M. Pedrón performed the computational studies in publication **II and V**.
- Dr. J. Jiménez-Barbero, Dr. A. Ardá, and S. Bertuzzi, performed the STD-NMR experiments in publication **IV**.

List of abbreviations

Ac	Acetyl
Bz	Benzoyl
CIP	Contact ion pair
DC-SIGN	Dendritic cell-specific intercellular adhesion molecule-3-grabbing non-integrin
DFT	Density functional theory
DNA	Deoxyribonucleic acid
DTT	Dithiothreitol
Et	Ethyl
GGM	Galactoglucomannan
HMBC	Heteronuclear multiple bond correlation
HSQC	Heteronuclear single quantum coherence
Me	Methyl
NMR	Nuclear magnetic resonance
Ph	Phenyl
Piv	Pivaloyl
RNA	Ribonucleic acid
SSIP	Solvent-separated ion pair
STD	Saturation transfer difference
TOCSY	Total correlation spectroscopy

Table of contents

List of publications.....	ix
Contribution of the author	x
List of abbreviations.....	x
Table of contents.....	xi
1. Introduction	1
1.1. The diversity of carbohydrates.....	1
1.1.1. The carbohydrate ring structure.....	3
1.2. Carbohydrate synthesis.....	6
1.2.1. Protecting group manipulation.....	7
1.2.2. Glycosylation	8
1.3. Carbohydrates in nature.....	11
1.3.1. Hemicelluloses.....	13
1.4. Acyl group migration	16
1.5. Objectives of the thesis.....	20
2. Experimental procedures	21
3. Results and discussion.....	23
3.1. Acyl group migration in monosaccharides.....	23
3.2. The first observation of the migration across the glycosidic linkage.....	29
3.2.1. The migration and characterization of new compounds	29
3.2.2. Computational investigation.....	32
3.3. Kinetics of the migration over the glycosidic bond.....	33
3.3.1. Kinetics of migration in the mannan trisaccharide	33

3.3.2.	Kinetics of migration in the glucan trisaccharide.....	37
3.3.3.	Kinetics of migration in the xylan trisaccharide.....	38
3.3.4.	Migration in GGM.....	40
3.4.	Elucidation of the migration mechanism.....	43
3.4.1.	Neutral mechanism	44
3.4.2.	Anionic Mechanism	45
3.4.3.	Experimental evidence.....	46
3.4.4.	The real model.....	47
3.4.5.	Applying the mechanistic model to trisaccharides	49
4.	Concluding discussion	52
4.1.	Summary and conclusions	52
4.2.	Future perspectives	53
5.	References	54
	Appendix: Original publications.....	63

1. Introduction

Carbohydrates are one of the most abundant group of molecules in the world. They take part in cell signaling and give cells their structures, but perhaps the most widely known function of carbohydrates is their ability to store energy. Carbohydrates are synthesized from water and carbon dioxide through photosynthesis that produces oxygen as a byproduct. This is a vital process for all life on earth, as carbohydrates serve not only as the major energy source for most animals but have biological applications in cells, too. Carbohydrates are part of some of the most important biopolymers for life itself: DNA and RNA. Deoxyribose, in DNA, and ribose, in RNA, are part of the monomeric structures, the nucleotides, in these important biopolymers. Carbohydrates have several key roles in the cells and understanding the chemistry of these molecules is vital for understanding many biological mechanisms.

The main components of cells consist of amino acids, nucleic acids, lipids, and carbohydrates. These components can be combined to form, for example, glycoproteins, glycolipids, peptidoglycans, and lipopolysaccharides. Many biopolymers have a linear chain due to the properties of the monomeric units, such as amino acids. Carbohydrates, on the other hand, can have several different linkages joining the monomers together, forming not only linear chains, but also branched structures, allowing them to have many different properties and fulfill several functions in the cells. Carbohydrates have also been used in pharmaceutical applications, demonstrating the versatility and importance of the sugars.

Early carbohydrate chemistry focused mainly on identifying the natural carbohydrates, while now the attention is more focused on synthesizing them and understanding their biological role. Understanding the possibilities of the carbohydrates is central for their utilization.

1.1. The diversity of carbohydrates

Carbohydrates can in general be broken down to the molecular formula $C_n(H_2O)_m$ ($n \geq m$), meaning they are hydrates of carbon. There are two main functionalities that divide the carbohydrates: ketone and aldehyde, giving ketoses and aldoses. Ketoses, e.g., fructose, can be derived from the chain extension of dihydroxy acetone. Aldoses, e.g., glucose, can be derived from the chain extension of glyceraldehyde (Figure 1.1). Carbohydrates are usually linked to one another and when there is just one carbohydrate unit the term monosaccharide is used,

when there are two to ten units linked together, the term oligosaccharide is used and when there are over ten saccharide units linked together, polysaccharide is used.

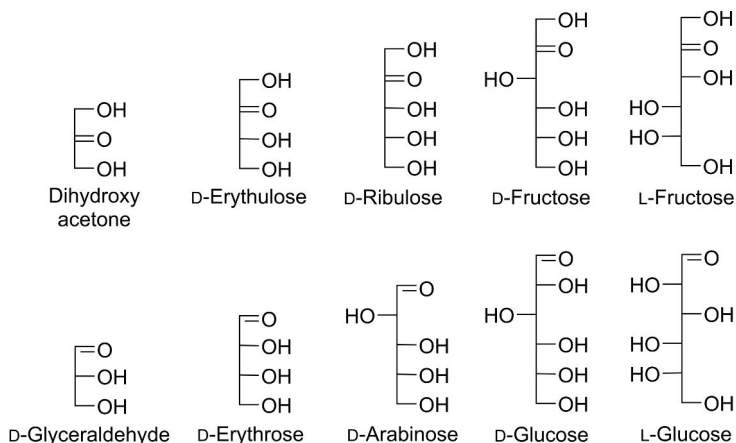


Figure 1.1. Fischer projections of selected carbohydrates.

One of the first to revolutionize the carbohydrate chemistry was H. E. Fischer. Fischer's most known accomplishment is the first total synthesis of D-glucose, in combination with the determination of the absolute stereochemistry of all the known sugars at the time.¹⁻³ This is a great achievement considering the methods available. The relatively small carbohydrate molecules can have a wide configurational variety because of the multiple stereocenters. Fischer was able to construct a carbohydrate family tree and gave the trivial names used today. The trivial names are a simpler way to name the complex molecules compared to the systematic way, where D-glucose would be named (2*R*,3*S*,4*R*,5*R*)-pentahydroxyhexanal. This convention of naming carbohydrates is clearly not practical, which is why the trivial names are preferred.

Fischer also laid the foundation for the carbohydrate nomenclature. The absolute configuration is decided by the highest numbered stereocenter, e.g., for glucose it is C5 (Figure 1.2). This center becomes the center of reference. In the Fischer projection, the denotation D is used for the absolute configuration when the center of reference is pointing to the right and L if it is pointing to the left. From the absolute configuration (D or L), the relative configuration (the trivial name) tells the stereochemistry of the other stereocenters in relation to the center of reference. As an example, in D-glucose the stereochemistry of C4 is the same as C5, *R*, meaning that in L-glucose where C5 is *S*, C4 is also *S*.

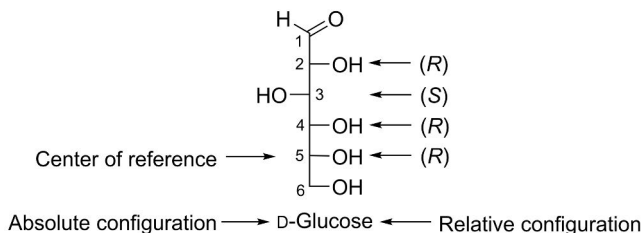
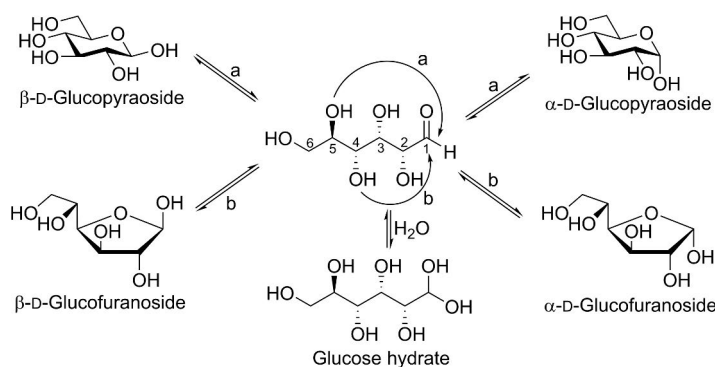


Figure 1.2. The absolute and relative configuration of D-glucose.

1.1.1. The carbohydrate ring structure

Carbohydrates exist mostly in a ring structure, which is attributed to the reactivity of the carbonyl group. It is well known that the carbonyl groups react readily with alcohols and water to form hemiacetals (for aldoses), hemiketals (for ketoses) and hydrates (when reacting with water). The intramolecular reaction of one alcohol group to the carbonyl carbon will thus form the ring structure. The size of the ring depends on which hydroxyl group attacks the carbonyl carbon. The most common rings in nature are the six-membered pyranose and five-membered furanose rings because these are both sterically and energetically favored. A new stereocenter is formed at the carbonyl carbon when the ring is formed. If the new alcohol group is *cis* to the most distant stereogenic center (the center of reference), the carbohydrate gets the prefix α and if the relationship is *trans* the prefix β is used, which can easily be observed in the Fischer projection. The furanose and pyranose configurations and the α/β configuration can interchange easily (Scheme 1.1). Starting from one single configuration in solution, an equilibrium will be achieved, which is easily observed in optical rotation, where pure β -D-glucopyranose has an optical rotation of $+18.7^\circ$ and pure α -D-glucopyranose has $+112.2^\circ$ and both will achieve an equilibrium with a value of $+52.7^\circ$ in water. This is called mutarotation.⁴



Scheme 1.1. Mutarotation in D-glucose.

The carbohydrates will in general uptake the pyranose form if it is possible. However, depending on the relative configuration, the carbohydrate can also exist in the furanose configuration to a significant degree such as in talose, idose (Figure 1.3) and altrose.⁵

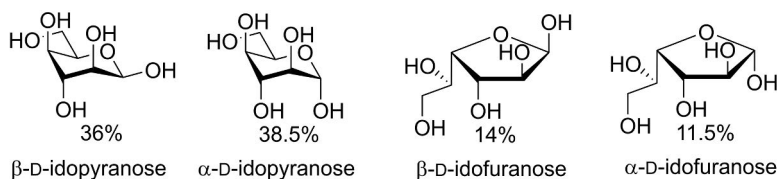


Figure 1.3. The ratios of pyranoses and furanoses of D-idose at 31 °C in water.

The ring structure of carbohydrates can have many different conformations, some energetically more favorable than others. Depending on the relative configuration, the preferred conformations can be present in an equilibrium. For pyranoses, the main conformations are *chair* (*C*), *half-chair* (*H*), *boat* (*B*), and *skew* (*S*) and for furanoses are *envelope* (*E*) and *twist* (*T*) the preferred conformations. (Figure 1.4). In pyranoses a plane of reference is formed by four atoms that exist in the same plane. In furanoses this plane can be formed by three or four atoms. Atoms above the plane of reference are written in superscript before the descriptor and atoms below the plane of reference are written in subscript after the descriptor. For example, the preferred conformation of D-glucopyranose, and many other carbohydrates, is the 4C_1 conformation. The relative configuration will have a significant effect on the preferred conformation of the ring. One example of this is the comparison between β -ribose and β -xylose. The axial O3 in ribopyranose allow it to uptake skew forms to significant degree in MeOH while the xylopyranose prefer the chair conformations almost selectively.⁶

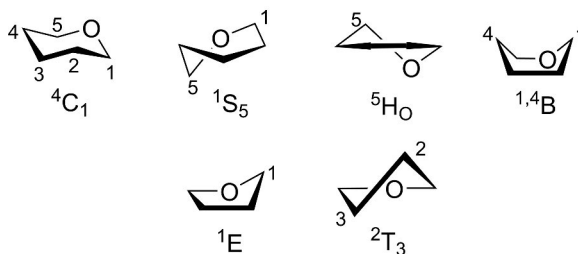
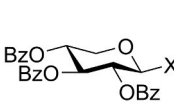
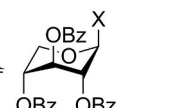


Figure 1.4. Selected ring conformations for pyranoses and furanoses.

In general, the bulkier substituent prefers to be equatorial over axial in a ring structure. Therefore, it would be expected that the anomeric position would be equatorial almost selectively, but that is however not the case as for D-glucopyranose approximately 62% uptake the β configuration and 38% the α .⁵ It was J. T. Edward that first described this phenomenon in 1955,⁷ and R. U. Lemieux later coined the term *anomeric effect*,⁸ also known as Edward-Lemieux effect. The substitution on the anomeric position will heavily affect the preferred conformation of the ring. The more polar the substituent is, the more is the axial conformation preferred. As seen in Table 1.1 when increasing the polarity of X, the preferred conformation goes from 4C_1 to 1C_4 .⁹⁻¹² The conditions, such as solvents, will influence the anomeric effect.

Table 1.1. The equilibrium ratios between 4C_1 and 1C_4 for 2,3,4-tri-*O*-benzoyl- β -D-xylopyranoside with different anomeric substitutions.

		\rightleftharpoons	
X = OMe	74%		26%
X = OAc	53%		47%
X = Cl	2%		98%
X = Br	0-10%		90-100%

There are two explanations for the anomeric effect: the dipole-dipole interaction and the stereoelectronic effect. The sp^3 hybridized ring oxygen has two free electron pairs that are part of the reason for both explanations. The free electron pairs at the ring oxygen give rise to a dipole at an exocyclic direction. The polarized bond between the anomeric carbon and the exocyclic heteroatom give rise to the other dipole. When the exocyclic heteroatom is equatorial the two dipole moments are almost parallel and will have a repulsive effect, while if the exocyclic heteroatom is axial the dipole moments will have almost opposite directions and the dipole-dipole interactions are small (Figure 1.5). One thing the dipole-dipole interaction fails to explain is that when the exocyclic heteroatom is axial, the bond between the ring oxygen and the anomeric carbon is shortened. Here comes the stereoelectronic effect with an explanation. The reason the bond is shortened is because the antiperiplanar electron lone pair of the ring oxygen is delocalized to the anti-bonding orbital of the bond between the anomeric carbon and the exocyclic heteroatom.¹³ This type of interaction can only occur when the exocyclic heteroatom is axial and leads to stabilization of the bonds. The anomeric effect can be observed in both pyranosides and furanosides.¹⁴

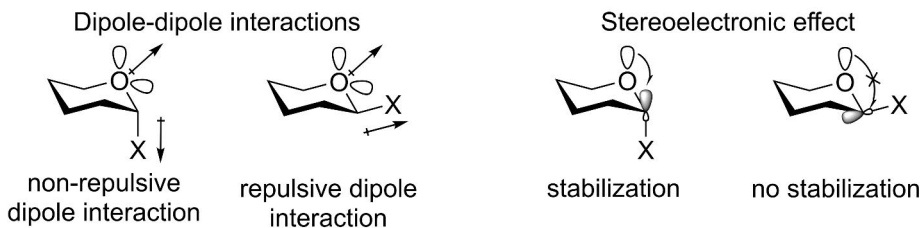


Figure 1.5. Stabilization by the dipole-dipole interactions and stereoelectronic effect.

There is also another conformational feature for many of the common carbohydrates, the rotation of the C5-C6 bond. The free rotation around the C5-C6 bond gives three low-energy conformations over the O5-C5-C6-O6 torsion angle: gg (gauche-gauche, -60°), gt (gauche-trans, 60°), and tg (trans-gauche, 180°) (Figure 1.6). The preferred torsion angle is heavily influenced by the steric effects surrounding the atoms.^{15–17} A clear example is given when the hydroxyl group at C4 is equatorial, as in glucopyranose, the gg:gt:tg conformation ratio is approximately 60:40:0, while, when the hydroxyl group at C4 is axial, as in galactopyranose, the ratio is approximately 15:70:15.¹⁷

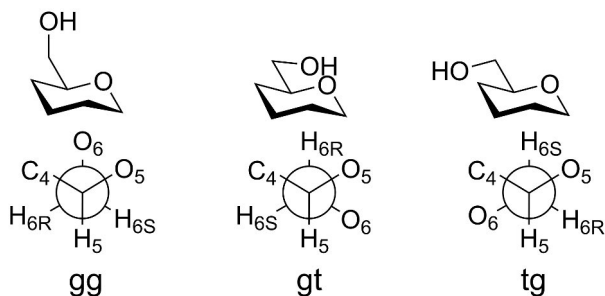


Figure 1.6. Low-energy conformation over the O5-C5-C6-O6 torsion angle in pyranosides.

1.2. Carbohydrate synthesis

One of the major problems that arise during carbohydrate synthesis is the differentiation of the hydroxyl groups. Selective methods and thorough planning are, therefore, needed, but a selective method is not always available to achieve the target molecule in a few steps. Protecting groups are usually utilized to overcome the selectivity problem and is therefore a major part of carbohydrate synthesis.

1.2.1. Protecting group manipulation

To arrive at the target molecule protecting group manipulations are most often required and therefore a good strategy is needed. The protecting groups can be divided into two main groups: permanent and temporary protecting groups. The permanent groups are not removed until the last step, while the temporary groups are added to facilitate further reactions. One important feature of the temporary groups is that they need to be stable until their removal. The most common protecting groups used are ethers, esters, silyls, and acetals.

Although the hydroxyl groups are similar, slight variations allow distinction between some of them. Three distinct types of hydroxyl groups can be found in the carbohydrates: anomeric, primary, and secondary hydroxyl groups (Figure 1.7). The anomeric hydroxyl group has a drastically different reactivity compared to the other hydroxyl groups because of the ring oxygen and can therefore be manipulated selectively under acidic conditions. The primary hydroxyl group is more reactive than a secondary hydroxyl group and can be selectively manipulated with bulky protecting groups. In general, the secondary hydroxyl groups can be differentiated on whether they are axial or equatorial. The equatorial is more reactive than the axial, but the conditions employed will significantly affect the selectivity.¹⁸

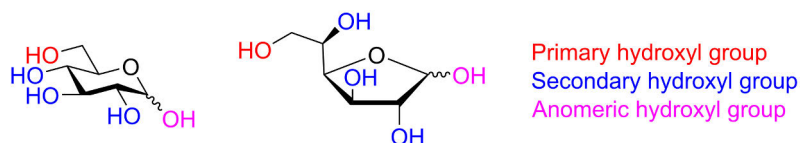
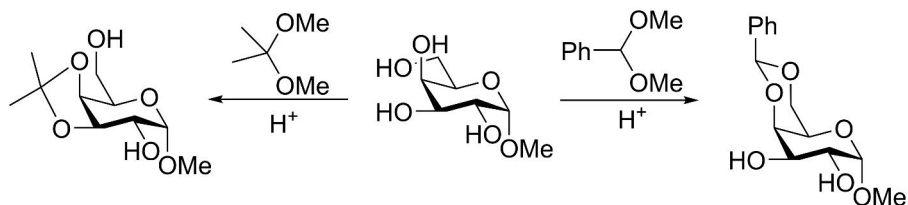


Figure 1.7. The distinct types of hydroxyl groups in glucopyranoside and -furanoside.

One example of selectivity can be seen in different acetal groups.¹⁹ Different ring sizes are preferred depending on the acetal. For example, the benzylidene acetal prefers to form a six-membered ring and will selectively form 4,6-*O*-benzylidene in hexapyranosides (Scheme 1.2). The isopropylidene acetal prefers a five-membered ring and will form acetals with vicinal *cis* diols, providing a method to distinguish between some secondary hydroxyl groups. By using the isopropylidene group in Me galactopyranoside, the primary and a secondary (O2) hydroxyl group is left unprotected, allowing selective methods to be used for further reactions. There are several different strategies that can be taken to arrive at the target compound. Several reviews and books cover this topic in depth.^{20–22}

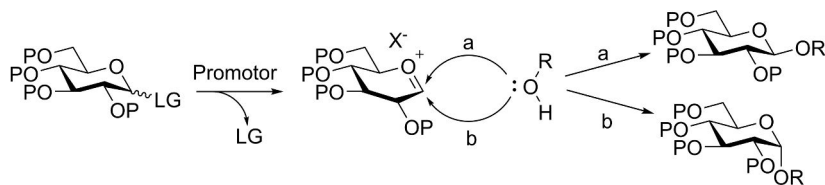


Scheme 1.2. The preferred position of the benzylidene and isopropylidene protecting groups in galactopyranoside.

1.2.2. Glycosylation

One of the most important reactions in carbohydrate synthesis is the formation of glycosidic linkages. Most of the carbohydrates in nature are not free monosaccharides but are linked to other carbohydrates or to other molecules called aglycons. Highly selective enzymes form the glycosidic bonds in nature. Enzymes have also been used by chemists to make glycosidic linkages. The main reason enzymes are attractive is the selectivity and there is no need for protecting groups. The main drawbacks are the narrow use of the enzymes, the low concentrations required, cost of the enzyme and difficulty to scale up. Because of these reasons, enzymatic glycosylation is often not viable for making the target saccharide and, therefore, chemical glycosylation is the preferred method by many chemists.

One of the first published glycosylations was by A. Michael, who made phenyl D-glucopyranoside from 2,3,4,6-tetra-*O*-acetyl-D-glucopyranosyl chloride and potassium phenolate.²³ Many different methods for chemical glycosylation have been developed over the years, each offering different benefits and shortcomings. What these methods have in common is how the glycosylation works. The use of a donor and acceptor or aglycon is the same for all glycosylation reactions. The donors have a leaving group at the anomeric position, which is activated with a promoter, typically a Lewis acid. The activation will form a planar oxocarbenium ion, which is then attacked by the acceptor. Depending on which side the oxocarbenium ion is attacked on, the α - or β -glycoside is formed (Scheme 1.3).



Scheme 1.3. The general mechanism of glycosylation.

One of the simplest examples of glycosylation is the Fischer glycosylation, where the anomeric position reacts with an alcohol in the presence of an acid catalyst.²⁴ The main product is often the α -anomer, but the selectivity depends on the thermodynamic stability of the products. In 1901 a new method was reported by W. Koenigs and E. Knorr.²⁵ This method utilized glycosyl halides that can be activated by heavy metal halophiles. This method is known as the Koenigs-Knorr glycosylation and is still used today. Several methods have been developed over the years and some selected donors can be seen in Figure 1.8.

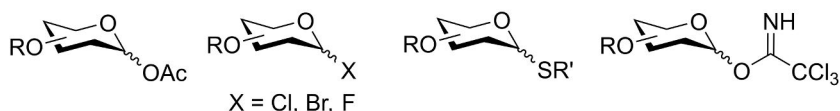
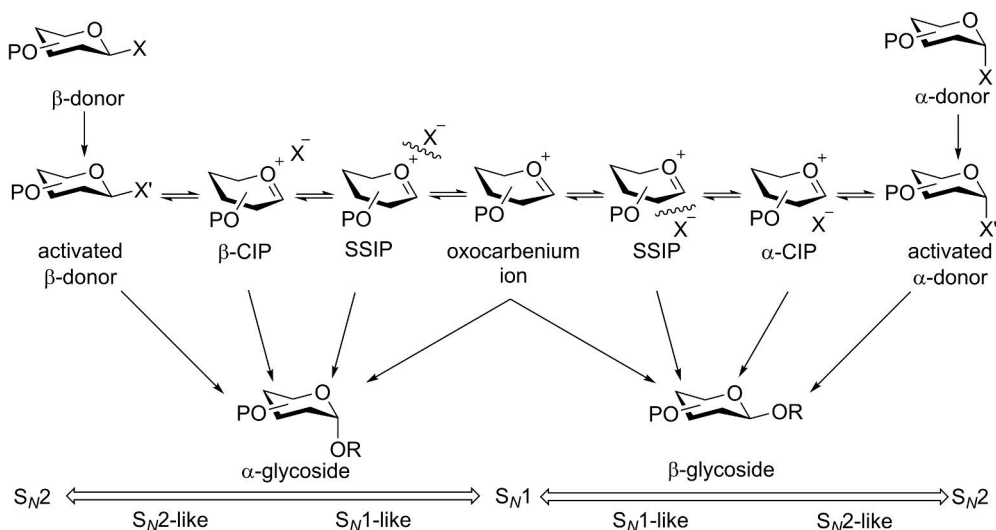


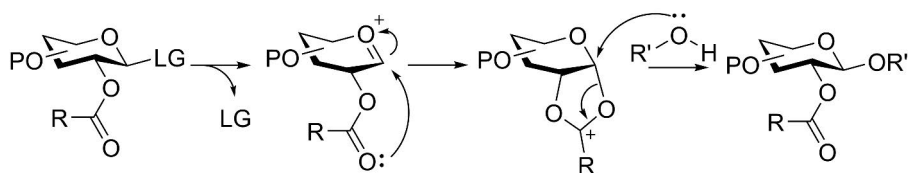
Figure 1.8. Selected donor leaving groups.

Several factors will affect the glycosylation mechanism and the true mechanism is not always a clear S_N1 or S_N2 type, but something in between, forming a mechanism continuum (Scheme 1.4).²⁶ Where a specific glycosylation lies on the continuum depends on the acceptor, donor, and conditions employed. For example, when using a more reactive acceptor the mechanism goes towards an S_N2 -like mechanism and when a less reactive acceptor is used a more S_N1 -like mechanism takes place.²⁷ The type of protecting groups applied on both the donor and acceptor have a big impact on the mechanism,^{28,29} indicating that all components contribute to the overall mechanism.



Scheme 1.4. Glycosylation mechanism continuum. SSIP: solvent separated ion pair, CIP: contact ion pair.

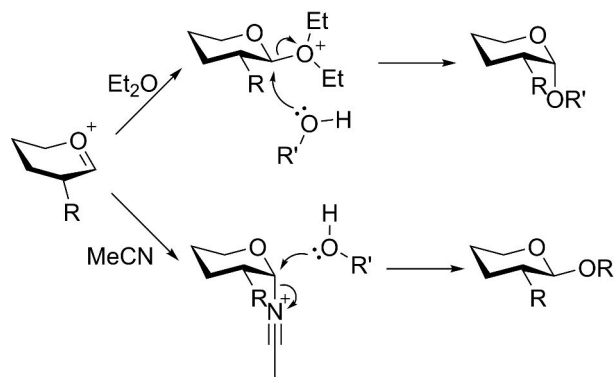
One way to steer the glycosylation product is by neighboring group participation. Having a protecting group, typically an ester, which can function as a nucleophile, at the position next to the anomeric center, will lead to participation (Scheme 1.5). The carbonyl oxygen will attack the anomeric position forming a temporary five-membered ring, blocking attack from one side of the ring. Using neighboring group participation as steering will result in 1,2-*trans* glycosides. Depending on the conditions and acceptor employed, the intermediate can form stable orthoesters.³⁰ This orthoester lowers the yield and has in some cases been responsible for the formation of 1,2-*cis* glycosides.^{31,32}



Scheme 1.5. Neighboring group participation.

The 1,2-*cis* glycosides are in general harder to prepare, but several protocols have been developed for higher selectivity towards these glycosides. There are some examples where neighboring group participation can steer the selectivity towards the 1,2-*cis* glycosides. Boons and coworkers showed that by using an (*S*)-phenyl-thiomethylbenzyl ether protecting group at C2 during glycosylation, the major product is the 1,2-*cis* glycosides.^{33,34} A six-membered ring between the (*S*)-phenyl-thiomethylbenzyl and the anomeric carbon is formed upon activation, blocking attack from the *trans* side.

Formation of the 1,2-*cis* glycosides usually needs more complex reaction systems. The stereoselectivity for a pure S_N1 reaction seems to prefer the 1,2-*cis* glycosides,³⁵ but achieving pure S_N1 reaction is not always viable. The glycosyl donor and the intermediate are the most important aspects of 1,2-*cis* glycosylation, and the conditions can shift the product towards the α - or β -glycoside. Solvents such as acetonitrile or diethyl ether can coordinate to the oxocarbenium ion and affect the selectivity (Scheme 1.6).^{36–38} Ethers tend to shift the stereoselectivity toward 1,2-*cis* glycosides and nitriles shift the selectivity towards equatorial glycosides. The utilization of these solvents could help shift the glycosylation to the target product.



Scheme 1.6. Solvent interaction in glycosylation.

The exact mechanism of the glycosylation can vary, and development of new methods and fine tuning of existing methods is always being investigated. The complexity of the glycosylation is a subject of several reviews,^{26,39-42} and it would be too much to cover everything here.

1.3. Carbohydrates in nature

The cells are covered by a multitude of different carbohydrates and the cell wall of plants consists mostly of cellulose and hemicellulose. The carbohydrates on the outside of the cells are markers of the cells and perform many roles in cell signaling. One of the most used examples of carbohydrates acting as cell signaling molecules, is the blood group system. The ABO blood groups are well known and the difference between these are the antigens on the surface of the red blood cells. A person with blood group O expresses the H antigen, a person with A blood group expresses A antigen, a person with B blood group expresses B antigen and a person with AB blood group expresses both A and B antigens (Figure 1.9). The A, B and O groups were discovered in 1900 by K. Landsteiner⁴³ and in 1902, A. von Decastello and A. Sturli discovered the AB group.⁴⁴ Up until the 1940s and 1950s it was not known that the differences between the antigens were linked to carbohydrates. Then the structures of the antigens were determined by W. T. J. Morgan and W. M. Watkins.⁴⁵⁻⁴⁷ Besides the ABO classification there are also many more blood groups, over 30, and many of these involve carbohydrates in some way.

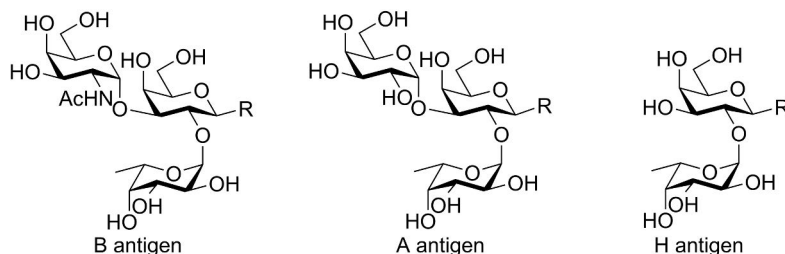


Figure 1.9. Structures of the ABO antigens

Polysaccharides are the most abundant form of carbohydrates. They have roles encompassing all from nutrition to giving structure to cells and participating in cell signaling. One of the most abundant polysaccharides is cellulose, which is the primary component of plant cell walls. Cellulose consists of β -(1 \rightarrow 4)-linked glucopyranoside units (Figure 1.10). Another well-known polysaccharide is starch. Starch consists also of glucose, but, unlike cellulose, starch consists of α -(1 \rightarrow 4)-linkages in the backbone and in the sidechains, which are attached with α -(1 \rightarrow 6)-linkages to the backbone. The different type of linkage is the reason humans can break down starch to glucose monomers and use it for energy, but not cellulose. This difference shows how large impact the linkages have in polysaccharides. There are several types of polysaccharides with different linkages and saccharide units. This allows the polysaccharides to have many different properties, depending on their function in the cells.

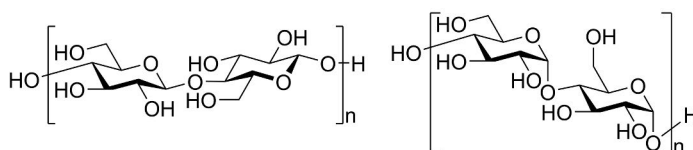


Figure 1.10. Backbone structure of cellulose (left) and starch (right).

Carbohydrates have also found a place as pharmaceuticals. The first carbohydrate based pharmaceutical, heparin, was used for its anticoagulant properties. It was J. McLean under W. Howell at John Hopkins University that have been credited for the discovery.⁴⁸ Heparin is a sulfated (1 \rightarrow 4)-linked polysaccharide consisting of glucosamine, iduronic acid and glucuronic acid. The first type of heparin had several side effects like headache, nausea, and fever. This problem was partly resolved by using heparin with lower molecular weight. The first total synthesis of the biologically active component (Figure 1.11) was achieved in the 1980s.^{49,50} Heparin is still used today to treat e.g., heart attacks and unstable angina. Carbohydrates are also part of several other pharmaceuticals with antibiotic, antiviral, anticoagulant, antithrombotic

properties and for treatment of epilepsy, diabetes and many more conditions.⁵¹ This short discussion was to show the wide use of carbohydrates and from now on the focus is turned to the relevant polysaccharides of this thesis: The *naturally acetylated β -(1 \rightarrow 4)-linked polysaccharides* or acetylated hemicelluloses

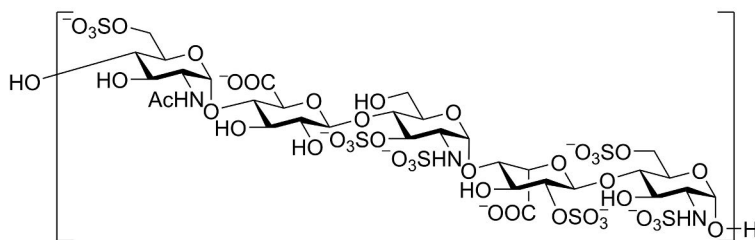


Figure 1.11. Structure of the biologically active pentasaccharide fragment of heparin.

1.3.1. Hemicelluloses

The plant cell walls consist mostly of cellulose, but other polysaccharides are also present to facilitate the properties the plant cell walls must have. Primary cell walls surround the growing cells, and some cells can develop secondary cell walls when the expansion have ceased. The plant cell walls are rigid and gives support to the plant, but they must also be metabolically active, and the primary cell wall must be flexible to allow cell expansion. Compounds and signals must be able to penetrate the cell walls for the cell to stay alive. These vital functions need a wide range of properties, requiring other compounds such as proteins, lignin, and other polysaccharides to be present in the cell walls. Besides cellulose, these polysaccharides can be divided into hemicelluloses and pectin. Pectin is a heteropolysaccharide consisting mostly of galacturonic acid. Hemicellulose is a collective name for several types of polysaccharides. The common features are the β -(1 \rightarrow 4)-linkages in the backbone with 500 – 300 saccharide units. Xylans, xyloglucans, mixed-link glucans, and mannans are the most common hemicelluloses. The hemicelluloses have many functions, such as providing cross-linking of cellulose microfibrils by interaction with cellulose, they also function as signaling molecules and as seed storage carbohydrates. By interacting with cellulose microfibrils, hemicelluloses allow the cell walls to attain the proper properties, giving strength and allowing for expansion.

1.3.1.1. Mannans

The main component of mannans is the β -(1 \rightarrow 4)-linked mannopyranoside backbone. Besides mannose, mannans can also have glucopyranosides in the backbone and galactopyranoside as sidechains, α -(1 \rightarrow 6)-linked to the mannose units. Acetyl groups are also common on the mannose units, especially at the O2

and O3 position, but have also been found at the O6 position.⁵²⁻⁵⁶ Examples of mannans are the linear mannan, galactomannan, glucomannan and galactoglucomannan (GGM) (Figure 1.12). These have been found in a wide variety of plants, all from Aloe vera to the orchid family (*Dendrobium officinale*) and Norway spruce (*Picea abies*).⁵²⁻⁵⁷

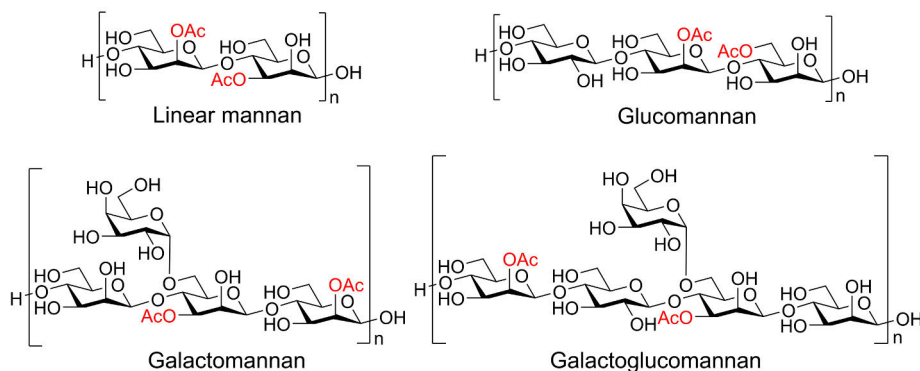


Figure 1.12. Structures of linear mannan, glucomannan, galactomannan, and galactoglucomannan.

In plants mannans have several roles, such as seed storage compound, molecular recognition sites for pathogens and acting as cell signaling molecules for plant growth and development.⁵⁸ Mannans also exhibit other biological activities such as antioxidant activities,^{59,60} immunomodulatory activities,⁶¹⁻⁶³ inhibiting the growth of cancer tumors,^{52,64,65} anti-inflammation activity,^{60,66} wound healing effects^{67,68} and more.⁶⁹ An interesting observation is that the acetyl groups are crucial for the biological activity of many mannans.⁶⁹⁻⁷²

1.3.1.2. Xylans

Xylans are one of the most common hemicelluloses and are found in several different plants.^{73,74} They are the major component of the xylem wall, the water conducting system of the plant. Xylans consist mostly of xylose in the backbone and the side chains can vary depending on the plant, but the most common side chains consist of α-(1→2)-linked glucuronosyl, 4-O-methyl glucuronosyl and α-(1→3) or (1→2)-linked arabinose residues.⁷⁵⁻⁷⁸ The xylans do not appear to have any repetitive pattern and there are many variations to the structures. Depending on the types of sidechains the xylans can be divided into glucuronoxylans, arabinoxylans and glucuronoarabinoxylans (Figure 1.13). The glucuronoxylans are the most common hemicellulose in the secondary cell wall of dicots, and the glucuronoarabinoxylans are the major hemicellulose in the primary cell wall of commelinid monocots.⁷⁷

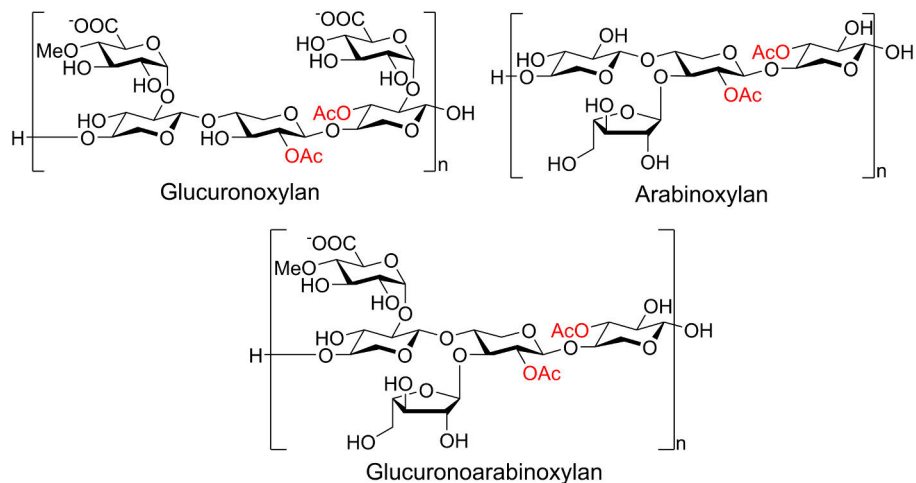


Figure 1.13. Structures of glucuronoxylan, arabinoxylan and glucuronoarabinoxylan.

Many xylans are naturally acetylated. Usually 30 – 60% of the xylose units are acetylated at the O2 and O3 positions. There are conflicting reports on the ratio between O2 and O3, with some reporting that O3 is the major acetylated one and others reporting O2 being the major.^{73,77–81} Interestingly, a study indicates that the acetyl groups have an even spread across the xylan chain.⁸² The acetyl groups are crucial regarding the structure and function of cell walls.⁸³ By gene manipulations, it was demonstrated that decreasing the plant's ability to acetylate the xylans, it would be detrimental to the plant. Xylans have shown some anti-carcinogenic properties and the ability to improve beneficial bacterial population growth in the colon.^{78,84}

1.3.1.3. Glucans

Xyloglucans can be found in almost every plant.^{85–88} The backbone of the glucans consists of β -(1 \rightarrow 4)-linked glucose with xylose as sidechains α -(1 \rightarrow 6)-linked to the backbone (Figure 1.14). The xylose units can then be further modified with other carbohydrates such as xylose, galactose, and fucose. There is a wide structural variety depending on the plant and tissue, but the xyloglucans usually consist of a repetitive pattern.⁷⁷ The degree of branching will affect the properties of the xyloglucans. The more branched the more soluble the xyloglucan is in water. The xyloglucans can also be partly acetylated with some acetyl groups attached to the O6 of the unbranched glucose units in the backbone.^{89–93}

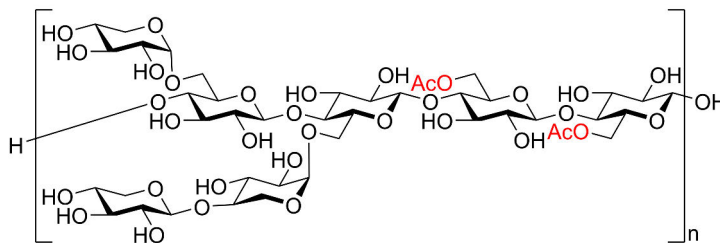


Figure 1.14. Structure of xyloglucan.

The xyloglucans are load-bearing components of the primary cell wall in the host plants.^{94–97} Although the load-bearing role of xyloglucans has been questioned it has been confirmed that they are implicated in the primary cell wall mechanics.⁹⁸ Xyloglucans have also displayed regulatory activities during plant cell growth and elongation.^{99,100}

Mixed link glucans are mostly found in grasses. These glucans consist of both β -(1 \rightarrow 4)- and β -(1 \rightarrow 3)-linkages, usually with three to five β -(1 \rightarrow 4)-linkages between each β -(1 \rightarrow 3)-linkage.¹⁰¹ This type of polysaccharide has a central role in the cell expansion of growing cells, and the concentration of the mixed link glucans is heavily dependent on the development stage of the cell.^{93,102,103} The mixed link glucans in grasses are broken down and replaced with glucuronoarabinoxylans, when the cell expansion stops.⁷⁷

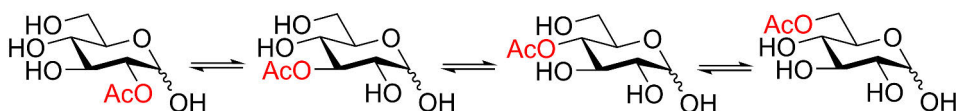
This chapter is intended to provide an overview of the polysaccharides described later in this thesis. A deeper dive into more specifics about these and other polysaccharides can be found in several reviews, such as those by Broadbelt *et al.*,⁷⁵ Scheller and Ulvskov,⁷⁷ and others.^{104,105}

1.4. Acyl group migration

Acyl groups, or ester protecting groups, are widely used in carbohydrate synthesis. Acetyl groups can also be found on polysaccharides in plant cells. Besides the polysaccharides, other molecules can also be partly acetylated such as gangliosides,¹⁰⁶ sialoglycoproteins¹⁰⁷ and their constituents.^{108,109} Acetyl groups are involved in the activation and deactivation of biologically active compounds,¹¹⁰ and also in metabolic reactions such as enzymatic acyl cleavage and acyl transfer processes.^{111–114} Acetylation is also used to enhance the lipid solubility of drugs, which leads to the enhanced blood-brain barrier permeability,¹¹⁵ e.g. the faster brain uptake of heroin compared to morphine. The degree of acetylation of the polysaccharides can alter their properties, hydrophobicity and conformation, and the degree of acetylation also changes

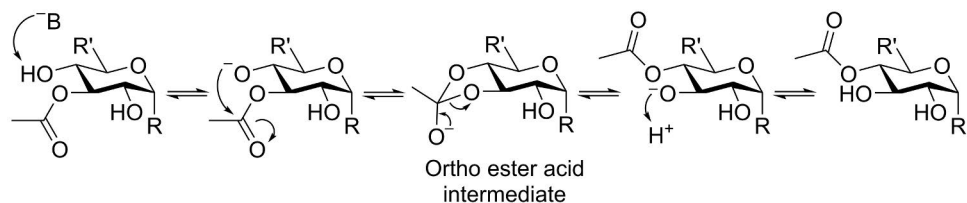
with the type of tissue and development stage.^{116–118} Interestingly, for many of the earlier discussed polysaccharides the acetyl groups are crucial for their function and biological activity.^{69–72,83} The degree of acetylation will impact the non-covalent interaction between the cell wall polymers.

When free hydroxyl groups are close in space to the carbonyl carbon of the acyl groups, migration might take place. This can take place in any molecule where the acyl groups are close enough to a free hydroxyl group, thiol, or amine.^{119,120} One observation is that the acyl groups do not migrate from amines to hydroxyls or thiols. The acyl group migration was first demonstrated by Fischer in 1920,¹²¹ and can be problematic during synthesis, purification, and isolation of compounds. In carbohydrates, the migration takes place between neighboring hydroxyl groups. Unsuccessful attempts to migrate an acetyl group across a myoinositol derivative directly, with protecting groups blocking the neighboring hydroxyl group, have been performed.¹²² Similar attempts have also been carried out in a mannopyranoside derivative (O2→O6 migration directly) without migration taking place.¹²³ Therefore, it can be said that the acyl groups migrate to the neighboring hydroxyl group (Scheme 1.7).



Scheme 1.7. The acyl group migration path for acetyl α -D-glucopyranose.

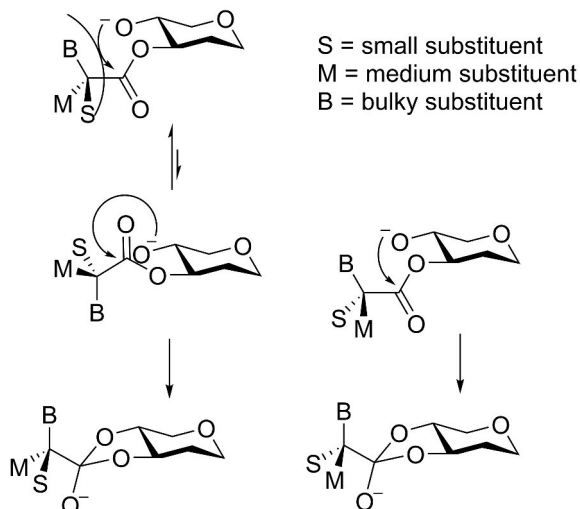
There have been several mechanisms suggested for the migration.^{124–126} One of these mechanisms stands out with experimental evidence^{127–130} and favorable computational calculations.^{131–133} This is a similar mechanism that Fischer suggested when he discovered the phenomenon. The mechanism has been tweaked over the years and in 1972 Oesterling and Metzler suggested that the migration starts off with deprotonation followed by the formation of an ortho ester acid (Scheme 1.8).¹²⁴ The ortho ester acid has even been isolated in one case.¹²⁷ The new carbonyl bond is formed by the breaking of the old C-O bond, which is followed by a protonation. Because the deprotonation is the first step in the mechanism, the base will significantly affect the rate. In buffers this can be noticed when the pH increases, the rate of migration will increase exponentially.^{128–130,134} The pH gives an indication of the deprotonation ability of the buffer and, therefore, provides evidence for the base catalyzed mechanism. Other mechanisms have also been suggested under other conditions,^{125,126} but these do not have as much supporting evidence.



Scheme 1.8. The base catalyzed acyl group migration mechanism.

The rate of migration in carbohydrates is dependent on several factors besides the ability of the solution to deprotonate the hydroxyl groups, such as the stereochemistry of the carbohydrates, size of acyl group and stereoelectronic properties of both acyl groups and the carbohydrate in question. The acyl groups are most stable at the primary hydroxyl groups in carbohydrates,^{108,109,135,136} due to the steric hindrance of the secondary hydroxyl groups and the flexibility of the primary position. When the primary position is not available, a more even spread typically arises, depending on other factors such as steric and electronic effects of both the carbohydrate and the acyl group. Several different studies have shown that the nature of the acyl group will affect the rate of migration and the most stable position.^{132,137–139} The most studied carbohydrate regarding the number of acyl groups is glucuronic acid due to its role in the metabolism of pharmaceuticals and other compounds.¹¹⁴ Although, it should be mentioned that these studies have focused on the stability of the 1-O-acyl glucuronide.^{132,134,140}

One of the factors that affects the rate is the steric hindrance around the carbonyl carbon, which slows down the rate of migration significantly.¹³⁶ Also the stereochemistry at the α -carbon will induce a steric effect,^{130,137,140–142} where, depending on the configuration, different migration transition states are preferred because of steric hindrance from one side (Scheme 1.9). The fact that the stereochemistry at the α -carbon affects the rate of migration is consistent with that the bulkier substituents have a slower rate of migration.¹³⁶ The electron withdrawing property of the substituents in the acyl groups is another factor that affects the rate of migration. When the electrons are drawn from the carbonyl carbon, it will be more positively charged and therefore more susceptible to nucleophilic attack from the hydroxyl group, increasing the rate of migration.



Scheme 1.9. Potential stereochemical interactions during acyl group migration.

The orientations of the hydroxyl groups play a key role on the rate of migration, which becomes clear when comparing the *cis* and *trans* relationships. The migration between secondary hydroxyl groups is faster when they have *cis* relationship compared to *trans*.^{136,143} The *cis* relationship offers a favorable transition state, as the five-membered ring in the transition state is more easily formed. In general, the acyl groups prefer the equatorial position, but the preference is heavily dependent on the conditions.¹²²

Migration has also been used in reactions to receive the desired product. Typically, Ag_2O and a base in an organic solvent have been used to facilitate the migration between two hydroxyl groups.^{126,144} This method has been assessed for the $\text{O2} \rightarrow \text{O3}$ migration in 4,6-O-benzylidene glucopyranoside and the $\text{O3} \rightarrow \text{O2}$ migration in 4,6-O-benzylidene galactopyranoside. These migrations often give fair yields of the intended products. Boranes are another group of compounds that can be used to steer the migration. Different inositol compounds have mostly been used with boranes.^{145–147} The boranes usually react with *cis* hydroxyl groups, which could help steer the migration product. In D-glucose a borane was used to migrate the acyl group straight to O3 by blocking the other hydroxyl groups.¹⁴⁸ Further development in boranes could result in selective methods for reaction with acyl groups in carbohydrates.

The discussion has so far been focused on pyranoses. The reason is that there is a lack of studies on the migration in furanoses (one study at the point of writing¹⁴⁹). Oligo- and polysaccharides are also lacking thorough migration

studies. It has mostly been concluded that the migration takes place within one saccharide unit, but the studies have been notations in larger studies.

1.5. Objectives of the thesis

The aim of this thesis is to shed more light on the acyl group migration in carbohydrates. No comprehensive studies on the acyl group migration in monosaccharides with several carbohydrates and several acyl groups had been performed prior to this work. The lack of comprehensive studies in monosaccharides makes it difficult to compare the migrations between the carbohydrates, since different conditions are usually utilized. How the configuration of the anomeric position and the overall configuration of the carbohydrate could affect the rate of migration have not been described in detail earlier.

Furthermore, the potential acetyl group migration between saccharide units in oligo- and polysaccharides has not been investigated earlier. In hemicelluloses the hydroxyl groups of neighboring saccharide units are close to each other and therefore it would be possible for the acetyl group to migrate between the saccharide units, which has not been shown earlier. The potential acetyl group migration over the glycosidic linkage in oligo- and polysaccharides (Figure 1.15), could be a way to regulate the biological activity of the polysaccharides.

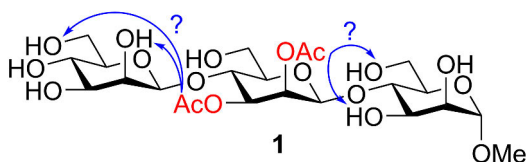


Figure 1.15. Possible migration in the model compound **1**.

2. Experimental procedures

The synthesis of the compounds used in this study can be found in the supporting information of the original publications. The main method for following and analyzing the acyl group migration was NMR-spectroscopy, because with this method it was possible to receive spectra at the correct interval and only small amounts of the compounds were needed.

Migration experiments

The migrations were conducted in phosphate buffers. The buffer strength lies between 10 – 500 mM. Most migrations were performed with the buffer strength of 100 mM and pH 8. The buffers are based on H₂O with 10% D₂O and in some cases are 100% D₂O buffers used. The concentration of compounds was 1 – 2 mg/ml.

Analysis of the migration

For following the migration process in the compounds under study, a Bruker Avance-III spectrometer operating at 500.20 MHz (¹H) and 125.78 MHz (¹³C) equipped with a Prodigy BBO CryoProbe or a Bruker Avance-III spectrometer operating at 500.20 MHz (¹H) and 125.78 MHz (¹³C) equipped with a Smartprobe: BB/1H was used. The migration was followed by normal ¹H-spectra for the D₂O buffer and water suppressed ¹H-spectra for the H₂O buffers. For identification and characterization of the migration products of the trisaccharides and for following the migration process of the polysaccharide a Bruker Avance-III spectrometer operating at 600.16 MHz (¹H) and 150.91 MHz (¹³C) equipped with a Prodigy TCI CryoProbe was used. The migration in the polysaccharide was followed by water suppressed ¹H-NMR, water suppressed Multiplicity edited HSQC and 1D HMBC.

The acetyl peaks in the NMR-spectra of the trisaccharides and the polysaccharide, GGM, investigated were sufficiently separated to allow for analysis of the migration and hydrolysis. For the acyl group migration in monosaccharides, peaks that were sufficiently separated were used, i.e., OMe, Ac, CH₃ of the Piv group, the CH₂ in the 2-Ph-propyl, and sometimes the H2 and H6 of the Ph in Bz. To acquire the ratios of the migration and hydrolysis products, the NMR simulation software ChemAdder/SpinAdder¹⁵⁰ was used.

Kinetics

The equations used for calculating the rate constants can be found in the original publications. Errors shown are standard error = variance/(N^{1/2}) (N number of

samples), and within 95% confidence interval. With the use of experimental methods and mathematical kinetic modelling, experimental points, or complete experiments, which do not fit the model can be identified and reanalyzed, or the experiment may be repeated.

The potential changes in pH had to be accounted for when calculating the rate constants, since the pH significantly affects the rate of migration. The pH in the migrations of the trisaccharides and the polysaccharide were therefore followed by pH-meter. The starting pH of the buffer used in these studies was 8, but as seen in Figure 2.1 the first pH measurement starts at a different point. The pH decreased after a while for most starting points and immediately for both **60a** and **60b**. The change in pH was accounted for by adding a factor to the rate constants. The factor was easily calculated since the rate is linear with the $[\text{OH}^-]$ concentration. The factor was calculated as $C(\text{OH})/C(\text{OH})_{\text{start}}$ and is 1 at $\text{pH} = 8$ and decreases with lower pH.

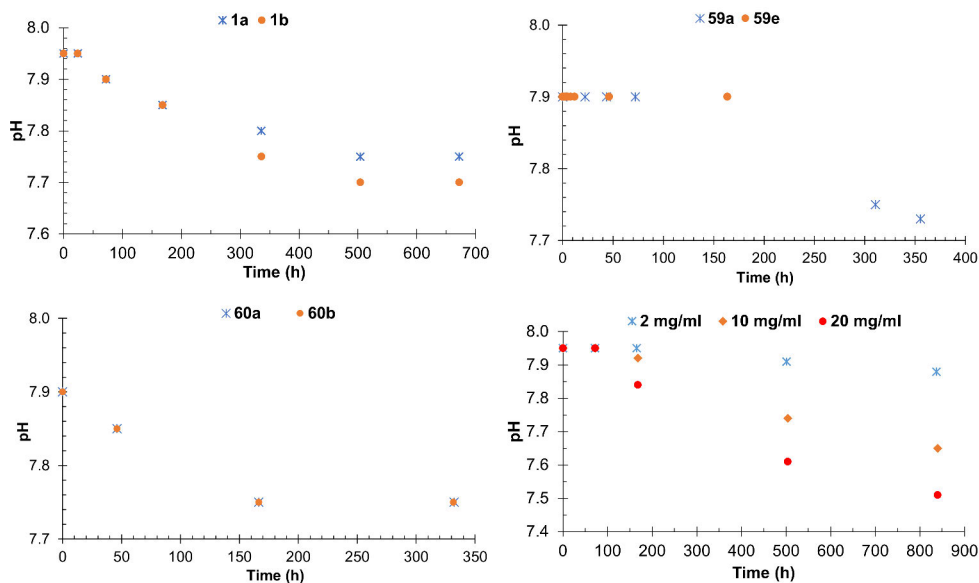


Figure 2.1. The changes in pH over time for the starting compound **1a** and **1b**, **59a** and **59e**, **60a** and **60b**, and the migration in GGM at different concentrations.

3. Results and discussion

3.1. Acyl group migration in monosaccharides

In the review article I it was noticed that there is a clear void on comprehensive studies on the migration in monosaccharides, where several carbohydrates and acyl groups are investigated, allowing for proper comparison. Here, the pyranoside ring structures are in focus of some selected common carbohydrates. The carbohydrates are combined with five different acyl groups, Ac, Bz, Piv, (*R*)- and (*S*)-2-Ph-propanoyl (Figure 3.1), making this a broad study of the migration, where some interesting observations were made.

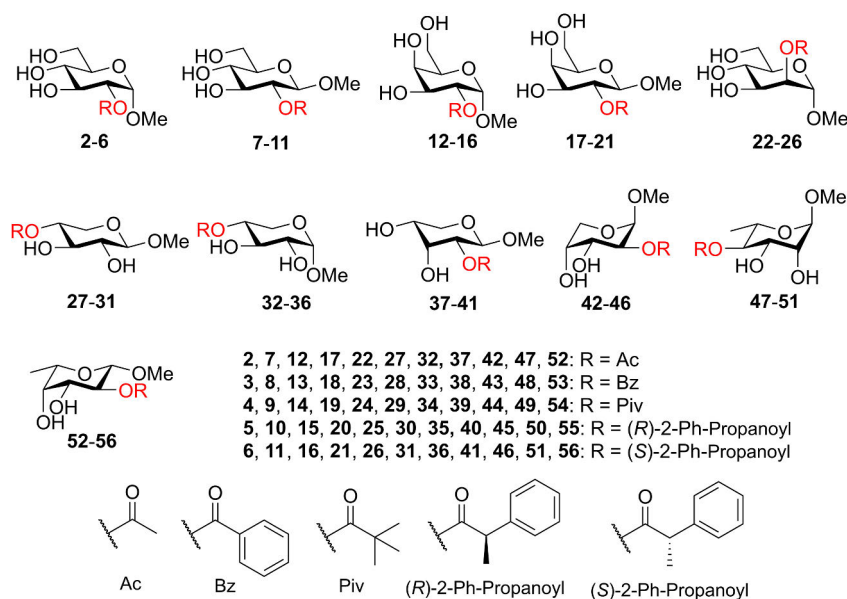
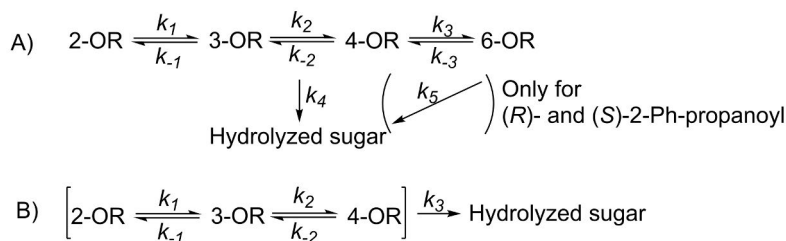


Figure 3.1. Starting compounds of the investigated acyl group migrations.

When calculating the rate constants, the two paths in Scheme 3.1 were used. Path A was used for glucopyranoside, galactopyranoside, and mannopyranoside derivatives and B was used for the remaining carbohydrates. The hydrolysis was set to be the same from all hydroxyl groups for Ac, Bz, and Piv, but for (*R*)- and (*S*)-2-Ph-propanoyl the hydrolysis from the primary position was separate to fit the experimental data better. This constant, k_5 , varies a lot between the carbohydrates. One reason could be the degree of freedom O6 has and that it would place the acyl group in a position where the hydrolysis would be sterically hindered.



Scheme 3.1. The reaction schemes used for calculating the rate constants.

One of the most surprising observations is that there is a significant difference in the rate of migration between the axial and equatorial anomeric OMe, which was observed in gluco-, galacto- (Table 3.1) and xylopyranosides (Table 3.2). When there is a *trans* relationship between the hydroxyl groups involved, the migration is 22 – 58% slower for the pyranosides with axial anomers (Figure 3.2). Interestingly, the *cis* relationship is not affected, in fact, the rate is slightly increased for the pyranosides with axial anomer as observed in the galactopyranoside derivatives (**12** – **21**). The reason for the observed difference in the *trans* relationship is the anomeric affect. The shortening of the bond between the cyclic oxygen and C1 will add strain to the ring, making it more difficult to form the transition state. Hydroxyl groups with a *cis* relationship are not affected due to the already favorable orientations, in fact the extra strain to the ring seems to help the transition state, but the difference is not large and could be due to other reasons such as electronic effects or errors in the measurements.

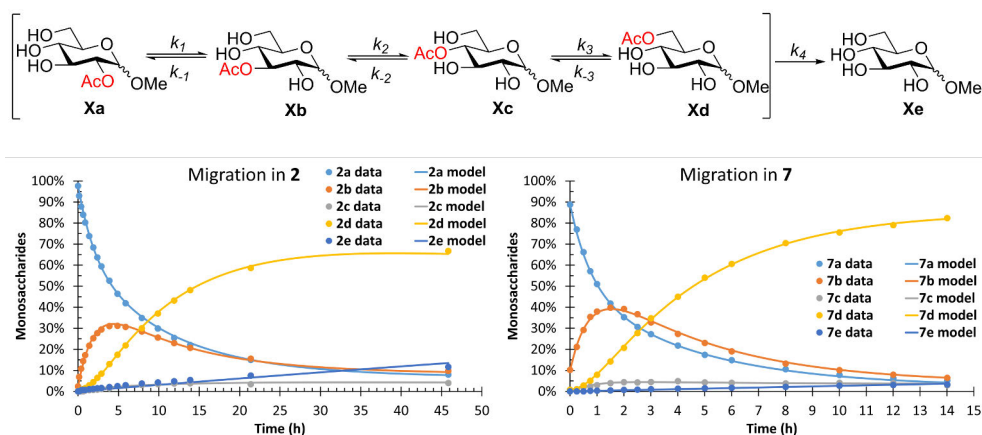


Figure 3.2. The acetyl group migration in Me α- and β-D-glucopyranoside displaying the experimental data and kinetic model. Conditions: 100 mM phosphate buffer with 10% D₂O, pH 8, 25 °C.

Table 3.1. The migration rate constants of the acetyl, benzoyl, pivaloyl, (*R*)- and (*S*)-2-Ph-propanoyl groups in Me α - and β -D-glucopyranoside, Me α - and β -D-galactopyranoside and Me α -D-mannopyranoside.^a

Acyl group	Ac	Bz	Piv	(<i>R</i>)-2-Ph-propanoyl	(<i>S</i>)-2-Ph-propanoyl
Start	2	3	4	5	6
<i>Me</i> α -D-Glc					
k ₁ (h ⁻¹)	2.26E-1 \pm 7.14E-3	1.43E-1 \pm 2.60E-3	1.09E-2 \pm 3.54E-4	5.64E-2 \pm 8.22E-4	3.79E-2 \pm 7.10E-4
k ₋₁ (h ⁻¹)	1.84E-1 \pm 1.42E-2	7.64E-2 \pm 3.98E-3	1.07E-2 \pm 6.98E-4	6.44E-2 \pm 2.26E-3	2.66E-2 \pm 2.26E-3
k ₂ (h ⁻¹)	1.82E-1 \pm 1.23E-2	9.24E-2 \pm 6.10E-3	9.52E-3 \pm 1.02E-3	3.22E-2 \pm 6.38E-3	8.62E-2 \pm 9.92E-3
k ₋₂ (h ⁻¹)	3.64E-1 \pm 1.09E-1	1.41E-1 \pm 4.52E-2	1.04E-2 \pm 2.48E-3	1.38E-1 \pm 9.26E-2	1.46E-1 \pm 3.62E-2
k ₃ (h ⁻¹)	4.34E+0 \pm 2.20E+0	7.63E-1 \pm 9.42E-2	9.72E-3 \pm 7.64E-4	3.75E-1 \pm 7.18E-2	2.02E-1 \pm 1.89E-2
k ₋₃ (h ⁻¹)	2.82E-1 \pm 1.79E-1	4.63E-2 \pm 1.32E-2	2.71E-4 \pm 3.76E-4	6.86E-3 \pm 4.00E-3	1.27E-2 \pm 2.40E-3
k ₄ (h ⁻¹)	3.17E-3 \pm 2.70E-4	8.40E-4 \pm 1.56E-4	2.72E-4 \pm 1.63E-5	5.01E-3 \pm 1.35E-4	5.05E-3 \pm 1.73E-4
k ₅ (h ⁻¹)	-	-	-	2.92E-4 \pm 2.36E-4	5.97E-4 \pm 2.20E-4
Start	7	8	9	10	11
<i>Me</i> β -D-Glc					
k ₁ (h ⁻¹)	7.28E-1 \pm 1.77E-2	4.59E-1 \pm 1.24E-2	3.28E-2 \pm 1.13E-3	1.19E-1 \pm 1.95E-3	7.95E-2 \pm 2.56E-3
k ₋₁ (h ⁻¹)	4.00E-1 \pm 2.26E-2	2.48E-1 \pm 1.54E-2	1.92E-2 \pm 1.20E-3	1.27E-1 \pm 4.24E-3	5.84E-2 \pm 7.98E-3
k ₂ (h ⁻¹)	4.14E-1 \pm 1.69E-2	2.06E-1 \pm 1.06E-2	1.61E-2 \pm 1.25E-3	5.73E-2 \pm 2.86E-3	1.20E-1 \pm 1.20E-2
k ₋₂ (h ⁻¹)	4.62E-1 \pm 1.16E-1	2.12E-1 \pm 4.70E-2	1.89E-2 \pm 3.10E-3	1.13E-1 \pm 2.18E-2	1.19E-1 \pm 4.30E-2
k ₃ (h ⁻¹)	3.95E+0 \pm 4.46E-1	1.09E+0 \pm 1.13E-1	1.97E-2 \pm 8.78E-4	5.17E-1 \pm 5.76E-2	4.21E-1 \pm 6.24E-2
k ₋₃ (h ⁻¹)	1.64E-1 \pm 3.50E-2	9.65E-2 \pm 1.86E-2	1.42E-3 \pm 2.50E-4	2.92E-2 \pm 5.76E-3	2.75E-2 \pm 7.74E-3
k ₄ (h ⁻¹)	2.66E-3 \pm 3.62E-4	9.76E-4 \pm 2.42E-4	3.09E-4 \pm 1.51E-5	4.09E-3 \pm 1.76E-4	4.42E-3 \pm 4.12E-4
k ₅ (h ⁻¹)	-	-	-	5.65E-4 \pm 1.88E-4	1.36E-3 \pm 2.66E-4
Start	12	13	14	15	16
<i>Me</i> α -D-Gal					
k ₁ (h ⁻¹)	1.19E-1 \pm 2.34E-3	9.20E-2 \pm 1.59E-3	5.49E-3 \pm 8.62E-5	2.99E-2 \pm 5.48E-4	3.41E-2 \pm 9.80E-4
k ₋₁ (h ⁻¹)	9.55E-2 \pm 8.98E-3	9.12E-2 \pm 7.36E-3	4.29E-3 \pm 2.56E-4	3.26E-2 \pm 4.10E-3	4.15E-2 \pm 4.62E-3
k ₂ (h ⁻¹)	8.74E-1 \pm 9.98E-2	1.17E+0 \pm 1.56E-1	8.24E-2 \pm 1.41E-2	1.97E+0 \pm 6.28E-1	1.65E+0 \pm 9.72E-1
k ₋₂ (h ⁻¹)	8.73E-1 \pm 1.44E-1	8.13E-1 \pm 1.38E-1	5.14E-2 \pm 9.60E-3	9.81E-1 \pm 3.58E-1	1.33E+0 \pm 8.44E-1
k ₃ (h ⁻¹)	1.02E+0 \pm 1.02E-1	2.02E-1 \pm 6.98E-3	1.29E-3 \pm 1.46E-4	8.43E-2 \pm 4.22E-3	4.78E-2 \pm 2.64E-3
k ₋₃ (h ⁻¹)	1.97E-1 \pm 2.62E-2	4.78E-2 \pm 3.52E-3	4.47E-5 \pm 6.14E-4	2.01E-2 \pm 1.58E-3	4.90E-3 \pm 9.90E-4
k ₄ (h ⁻¹)	7.40E-3 \pm 4.52E-4	1.52E-3 \pm 3.18E-4	2.43E-4 \pm 1.04E-5	5.05E-3 \pm 1.26E-4	3.90E-3 \pm 2.30E-4
k ₅ (h ⁻¹)	-	-	-	1.09E-8 \pm 1.16E-4	6.51E-4 \pm 3.86E-4
Start	17	18	19	20	21
<i>Me</i> β -D-Gal					
k ₁ (h ⁻¹)	5.28E-1 \pm 1.38E-2	3.00E-1 \pm 3.78E-3	2.09E-2 \pm 1.07E-3	7.76E-2 \pm 9.96E-4	3.01E-1 \pm 3.48E-3
k ₋₁ (h ⁻¹)	2.19E-1 \pm 1.64E-2	1.55E-1 \pm 8.04E-3	1.17E-2 \pm 1.62E-3	7.33E-2 \pm 5.56E-3	1.53E-1 \pm 7.32E-3
k ₂ (h ⁻¹)	8.73E-1 \pm 3.30E-2	1.15E+0 \pm 4.60E-2	8.35E-2 \pm 1.78E-2	9.77E-1 \pm 6.92E-2	1.16E+0 \pm 4.22E-2
k ₋₂ (h ⁻¹)	6.20E-1 \pm 4.06E-2	5.40E-1 \pm 3.02E-2	3.87E-2 \pm 9.32E-3	4.05E-1 \pm 4.04E-2	5.41E-1 \pm 2.76E-2
k ₃ (h ⁻¹)	7.55E-1 \pm 2.18E-2	1.38E-1 \pm 2.24E-3	1.02E-3 \pm 2.38E-4	8.57E-2 \pm 1.75E-3	1.37E-1 \pm 2.16E-3
k ₋₃ (h ⁻¹)	2.06E-1 \pm 9.36E-3	4.31E-2 \pm 1.76E-3	1.33E-4 \pm 1.15E-5	1.99E-2 \pm 9.80E-4	4.28E-2 \pm 1.69E-3
k ₄ (h ⁻¹)	1.36E-2 \pm 1.33E-3	4.27E-3 \pm 5.56E-4	9.40E-4 \pm 1.32E-4	4.36E-3 \pm 1.82E-4	1.58E-3 \pm 2.28E-4
k ₅ (h ⁻¹)	-	-	-	8.65E-4 \pm 1.58E-4	2.28E-13 \pm 1.90E-4
Start	22	23	24	25	26
<i>Me</i> α -D-Man					
k ₁ (h ⁻¹)	1.91E+0 \pm 6.60E-2	2.19E+0 \pm 1.77E-1	2.04E-1 \pm 1.07E-2	2.08E+0 \pm 6.88E-2	1.53E+0 \pm 7.52E-2
k ₋₁ (h ⁻¹)	1.39E+0 \pm 5.60E-2	1.91E+0 \pm 1.67E-1	1.62E-1 \pm 9.66E-3	1.41E+0 \pm 5.06E-2	1.32E+0 \pm 7.46E-2
k ₂ (h ⁻¹)	1.41E-1 \pm 1.16E-2	1.35E-1 \pm 1.55E-2	1.16E-2 \pm 1.27E-3	2.76E-2 \pm 1.33E-3	5.44E-2 \pm 3.98E-3
k ₋₂ (h ⁻¹)	5.63E-1 \pm 1.50E-1	4.63E-1 \pm 1.15E-1	2.23E-2 \pm 3.86E-3	8.32E-2 \pm 1.25E-2	1.08E-1 \pm 1.97E-2
k ₃ (h ⁻¹)	1.69E+0 \pm 1.66E-1	5.95E-1 \pm 4.52E-2	1.19E-2 \pm 1.02E-3	1.77E-1 \pm 9.78E-3	1.51E-1 \pm 1.31E-2
k ₋₃ (h ⁻¹)	7.48E-2 \pm 1.88E-2	3.82E-2 \pm 6.88E-3	2.49E-3 \pm 5.48E-4	1.34E-2 \pm 1.95E-3	1.58E-2 \pm 2.36E-3
k ₄ (h ⁻¹)	3.02E-3 \pm 2.20E-4	6.08E-4 \pm 1.31E-4	2.90E-4 \pm 2.02E-5	3.97E-3 \pm 7.84E-5	4.97E-3 \pm 1.61E-4
k ₅ (h ⁻¹)	-	-	-	4.61E-12 \pm 7.14E-8	5.33E-15 \pm 7.98E-6

^a Conditions: 100 mM phosphate buffer with 10% D₂O, pH 8, 25 °C.

Table 3.2. The migration rate constants of the acetyl, benzoyl, pivaloyl, (*R*)- and (*S*)-2-Ph-propanoyl groups in Me α - and β -D-xylopyranoside, Me β -D-ribofuranoside, Me β -D-arabinopyranoside, Me α -L-rhamnopyranoside, and Me β -L-fucopyranoside.^a

Acyl group	Ac	Bz	Piv	(<i>R</i>)-2-Ph-propanoyl	(<i>S</i>)-2-Ph-propanoyl	
Me β-D-Xyl	Start	27	28	29	30	31
	k ₁ (h ⁻¹)	5.94E-1 ± 3.16E-1	4.05E-1 ± 6.88E-2	2.58E-2 ± 1.04E-3	1.22E-1 ± 3.74E-2	1.72E-1 ± 3.08E-2
	k ₋₁ (h ⁻¹)	2.64E-1 ± 1.22E-1	2.16E-1 ± 2.96E-2	1.83E-2 ± 6.40E-4	1.31E-1 ± 3.46E-2	1.28E-1 ± 1.80E-2
	k ₂ (h ⁻¹)	3.28E-1 ± 3.10E-2	1.62E-1 ± 8.62E-3	8.73E-3 ± 1.03E-4	4.95E-2 ± 5.00E-3	1.02E-1 ± 6.68E-3
	k ₋₂ (h ⁻¹)	2.81E-1 ± 1.71E-2	1.51E-1 ± 4.00E-3	8.13E-3 ± 4.94E-5	4.20E-2 ± 2.02E-3	8.24E-2 ± 2.68E-3
	k ₃ (h ⁻¹)	5.87E-3 ± 1.06E-3	1.35E-3 ± 3.96E-4	2.20E-4 ± 4.48E-6	2.91E-3 ± 1.42E-4	3.57E-3 ± 1.97E-4
Me α-D-Xyl	Start	32	33	34	35	36
	k ₁ (h ⁻¹)	2.11E-1 ± 2.50E-2	1.76E-1 ± 1.27E-2	8.67E-3 ± 1.58E-3	4.68E-2 ± 1.06E-2	2.92E-2 ± 4.36E-3
	k ₋₁ (h ⁻¹)	1.53E-1 ± 1.44E-2	1.06E-1 ± 6.30E-3	6.68E-3 ± 7.96E-4	4.99E-2 ± 8.98E-3	4.74E-2 ± 9.22E-3
	k ₂ (h ⁻¹)	7.30E-2 ± 2.94E-3	5.32E-2 ± 1.26E-3	5.53E-3 ± 3.30E-4	2.20E-2 ± 2.20E-3	3.76E-2 ± 4.36E-3
	k ₋₂ (h ⁻¹)	8.41E-2 ± 1.35E-3	6.06E-2 ± 6.10E-4	5.15E-3 ± 1.29E-4	1.93E-2 ± 7.60E-4	4.22E-2 ± 1.82E-3
	k ₃ (h ⁻¹)	2.17E-3 ± 1.45E-4	4.68E-4 ± 6.48E-5	1.64E-4 ± 1.63E-5	2.26E-3 ± 1.01E-4	2.66E-3 ± 8.74E-5
Me β-D-Rib	Start	37	38	39	40	41
	k ₁ (h ⁻¹)	3.04E+1 ± 8.16E-1	1.21E+1 ± 5.92E-2	3.62E-1 ± 3.30E-3	7.50E+0 ± 9.92E-2	1.01E+1 ± 6.18E-2
	k ₋₁ (h ⁻¹)	1.13E+1 ± 4.00E-1	3.35E+0 ± 3.60E-2	1.05E-1 ± 2.82E-3	2.94E+0 ± 5.60E-2	3.76E+0 ± 3.20E-2
	k ₂ (h ⁻¹)	1.85E+1 ± 7.70E-1	4.92E+0 ± 6.98E-2	1.92E-1 ± 6.22E-3	4.68E+0 ± 1.11E-1	4.68E+0 ± 3.92E-2
	k ₋₂ (h ⁻¹)	2.20E+1 ± 9.96E-1	8.50E+0 ± 1.41E-1	3.27E-1 ± 1.41E-2	7.45E+0 ± 2.02E-1	6.55E+0 ± 6.40E-2
	k ₃ (h ⁻¹)	n.d.	n.d.	n.d.	n.d.	n.d.
Me β-D-Ara	Start	42	43	44	45	46
	k ₁ (h ⁻¹)	1.02E-1 ± 1.03E-3	7.22E-2 ± 9.94E-4	4.16E-3 ± 8.32E-3	2.74E-2 ± 1.23E-3	2.52E-2 ± 1.11E-3
	k ₋₁ (h ⁻¹)	5.40E-2 ± 3.06E-3	5.25E-2 ± 3.24E-3	3.86E-3 ± 7.72E-3	2.44E-2 ± 3.48E-3	3.80E-2 ± 4.46E-3
	k ₂ (h ⁻¹)	1.72E+0 ± 1.96E-1	1.53E+0 ± 2.50E-1	1.92E-1 ± 3.84E-1	2.00E+0 ± 2.76E+0	2.00E+0 ± 2.22E+0
	k ₋₂ (h ⁻¹)	1.31E+0 ± 1.60E-1	8.94E-1 ± 1.58E-1	9.65E-2 ± 1.93E-1	1.29E+0 ± 1.81E+0	1.06E+0 ± 1.21E+0
	k ₃ (h ⁻¹)	2.27E-3 ± 2.27E-3	5.54E-4 ± 1.67E-4	1.61E-4 ± 3.22E-4	2.23E-3 ± 1.54E-4	2.09E-3 ± 1.30E-4
Me α-L-Rha	Start	47	48	49	50	51
	k ₁ (h ⁻¹)	1.46E+0 ± 6.42E-2	1.63E+0 ± 1.93E-1	1.36E-1 ± 1.08E-1	6.98E-1 ± 1.73E-1	2.74E+0 ± 1.62E+0
	k ₋₁ (h ⁻¹)	1.05E+0 ± 4.30E-2	1.38E+0 ± 1.56E-1	1.35E-1 ± 1.02E-1	7.54E-1 ± 1.73E-1	2.21E+0 ± 1.29E+0
	k ₂ (h ⁻¹)	1.27E-1 ± 1.93E-3	9.18E-2 ± 2.86E-3	9.60E-3 ± 1.25E-3	4.82E-2 ± 3.14E-3	2.94E-2 ± 1.14E-3
	k ₋₂ (h ⁻¹)	2.89E-1 ± 1.54E-3	1.49E-1 ± 1.47E-3	1.32E-2 ± 6.54E-4	5.32E-2 ± 1.41E-3	4.68E-2 ± 5.70E-4
	k ₃ (h ⁻¹)	3.73E-3 ± 1.37E-4	1.58E-3 ± 1.86E-4	2.47E-4 ± 6.74E-5	4.75E-3 ± 1.55E-4	3.47E-3 ± 7.56E-5
Me β-L-Fuc	Start	52	53	54	55	56
	k ₁ (h ⁻¹)	4.25E-1 ± 1.13E-3	2.17E-1 ± 9.16E-4	1.18E-2 ± 4.54E-5	6.22E-2 ± 9.10E-4	5.75E-2 ± 9.20E-4
	k ₋₁ (h ⁻¹)	1.41E-1 ± 1.33E-3	9.97E-2 ± 1.88E-3	5.98E-3 ± 9.82E-5	4.87E-2 ± 2.72E-3	6.35E-2 ± 3.84E-3
	k ₂ (h ⁻¹)	4.39E-1 ± 2.00E-3	5.33E-1 ± 4.72E-3	2.83E-2 ± 2.10E-4	8.16E-1 ± 8.86E-2	3.95E-1 ± 2.26E-2
	k ₋₂ (h ⁻¹)	2.25E-1 ± 1.59E-3	1.86E-1 ± 2.56E-3	8.19E-3 ± 9.88E-5	3.42E-1 ± 4.16E-2	1.33E-1 ± 1.05E-2
	k ₃ (h ⁻¹)	2.50E-3 ± 6.12E-5	1.02E-3 ± 7.42E-5	7.32E-5 ± 3.26E-6	1.34E-3 ± 8.52E-5	1.57E-3 ± 1.02E-4

^a Conditions: 100 mM phosphate buffer with 10% D₂O, pH 8, 25 °C. n.d.: not determined

It is also observed that similar types of migration have similar rate constants. For example, the O2 \rightleftharpoons O3 migration in α -gluco-, α -galacto-, and α -xylopyranoside have similar rate constants. The minor differences observed can be related to the orientation of the other hydroxyl groups inducing steric hindrance and electronic effects.

One carbohydrate that differs significantly from the others is Me β -D-ribofuranoside. The migration is several times faster in ribofuranoside

compared to the other carbohydrates. Most of the acyl groups achieved equilibrium after 15 – 30 min in ribopyranoside, and the pivaloyl group reached equilibrium after 14 h. The carbohydrate closest to ribose, with regards to how fast equilibrium was achieved, was fucose (Figure 3.3). One reason for the fast migration in Me β -D-ribofuranoside could be the preferred conformations. It was shown that the Nap β -D-ribofuranoside has several preferred conformations of which several are the skew conformation in combination with two chair conformations.⁶ The preferred conformations clearly have a significant impact on the rate of migration, but it seems that the acyl groups also have an impact on the ratio of the preferred conformations. Comparing the rate constants in ribopyranoside to rate constants of other carbohydrates containing *cis* hydroxyl groups, it becomes apparent that the rate in ribopyranoside varies a lot, all from being 50 times faster to having similar rates. This could be due to the acyl groups affecting the ratio of conformations, resulting in different rate of migration.

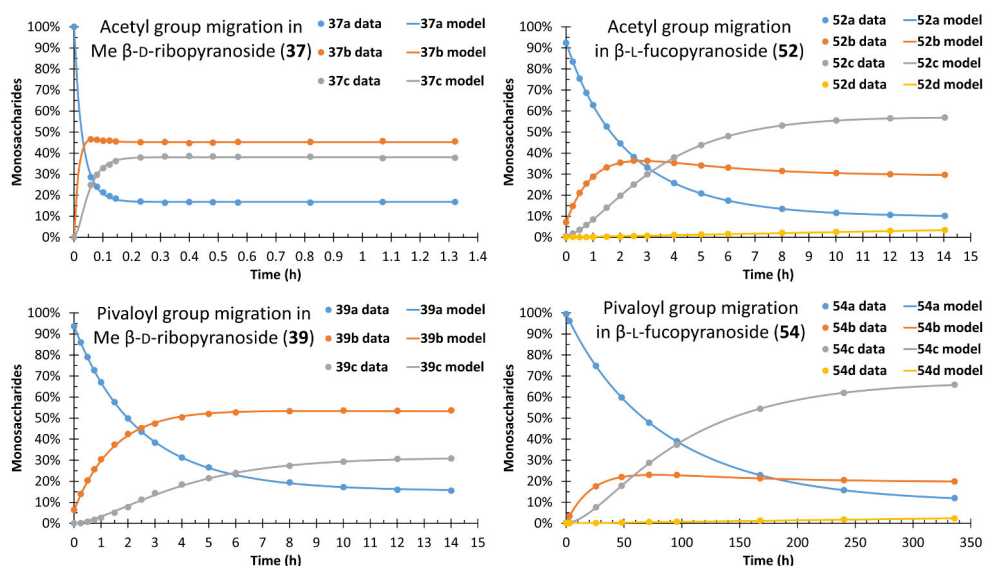


Figure 3.3. Migration of the acetyl group and pivaloyl group in Me β -D-ribo- and Me β -L-fucopyranoside displaying the experimental data and kinetic model. Conditions: 100 mM phosphate buffer with 10% D₂O, pH 8, 25 °C.

The favorable transition state over the *cis* relationship becomes evident when comparing the rate constants for the different acyl groups. The benzoyl group is faster than the acetyl groups over hydroxyl groups with *cis* relationship and in some cases is the 2-Ph-propanoyl as fast as the migration rate of the acetyl group over hydroxyl groups with *cis* relationship. It seems that for migration over *cis* hydroxyl groups, the steric hindrance of the acyl groups impacts the rate less

than for migration over a *trans* hydroxyl groups, which is most likely due to less strain of the transition state.

As expected, clear differences between the migration of (*R*) and (*S*)-2-Ph-propanoyl can be noticed. The reasoning can be seen in Scheme 1.9, where the attack can be blocked from one side by the substituents, meaning the acyl group must rotate to allow the nucleophilic attack from the other side. It is demonstrated in Figure 3.4 where the Me and Ph are not blocking the attack from O3 as much for **21a** as for **20a**, resulting in the faster **21a** → **21b** migration than **20a** → **20b** migration.

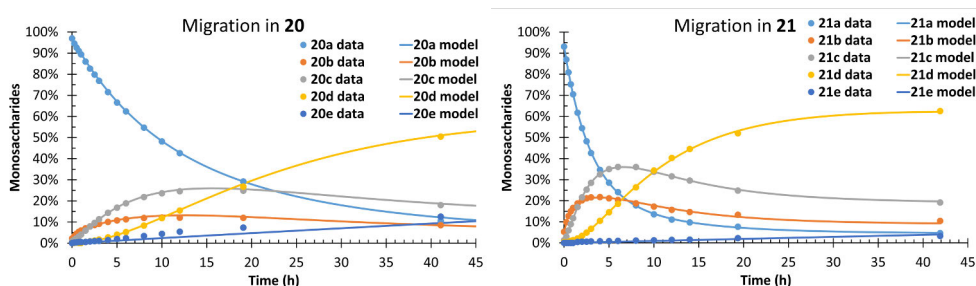


Figure 3.4. The migration of (*R*)- (**20**) and (*S*)-2-Ph-propanoyl (**21**) in Me α -D-galactopyranoside displaying the experimental data and kinetic model. Conditions: 100 mM phosphate buffer with 10% D₂O, pH 8, 25 °C.

The influence of the buffer strength on the migration was also investigated. This was achieved by following the acetyl group migration in Me α -D-mannopyranoside (**22**) in phosphate buffers with buffer strengths of 50, 100 and 500 mM. The migration was significantly slower at lower buffer strength. Coefficients could be calculated to match the rate constants in the 50 and 500 mM buffer strengths to the 100 mM buffer strength. The rate of migration in 500 mM buffer is 1.49 times that of the 100 mM and the 50 mM buffer is 0.87 that of the 100 mM. The higher concentration of phosphate in the buffers could stabilize the anion, giving more time for the migration to take place. This demonstrates how easily the migration can be manipulated and that rate constants cannot be directly compared unless similar buffers are used in two different migration studies.

3.2. The first observation of the migration across the glycosidic linkage

Most of the previous studies on the acyl group migration have been investigating the migration in monosaccharides and the investigations in oligo- and polysaccharides have only shown that the migration takes place within one saccharide unit.^{151,152} Although the earlier studies show no migration between the saccharide units of larger oligo- and polysaccharides, more thorough studies are required to say for certainty whether the migration between saccharide units is possible. In mannans the most common positions of the acetyl groups are at the O2 and O3 positions of the mannose units, and the acetyl groups have also been found at the O6 position of the mannose units to a lesser extent. It could be argued that the acetylated O6 is a result from migration, meaning that the migration would take place between different saccharide units as the O2→O6 migration within the saccharide unit is not possible.¹²³

3.2.1. The migration and characterization of new compounds

The possible migration between saccharide units in oligosaccharides started with the investigation of trisaccharide **1** and disaccharide **57** (Figure 3.5). Migration to a neighboring hydroxyl group is blocked in trisaccharide **1** and any observed migration is therefore new. For disaccharide **57** there is the possibility for migration to a neighboring hydroxyl group in the same saccharide unit, but it will also help to determine what happens in **1**, if anything happens.

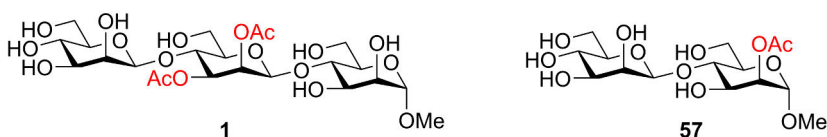


Figure 3.5. The structures of the mannan model compounds studied.

Some peaks are growing slowly during the migration in **1** (Figure 3.6). After 6 weeks these peaks had reached a point when analysis was possible. From the ¹H-spectra it becomes clear that several products have formed. For example, peaks around 4.2 and 4.4 ppm have appeared. These signals usually correspond to the H6:s when O6 is acetylated.¹³⁶ There is also peaks arising close to the original H2' and H3' of **1**.

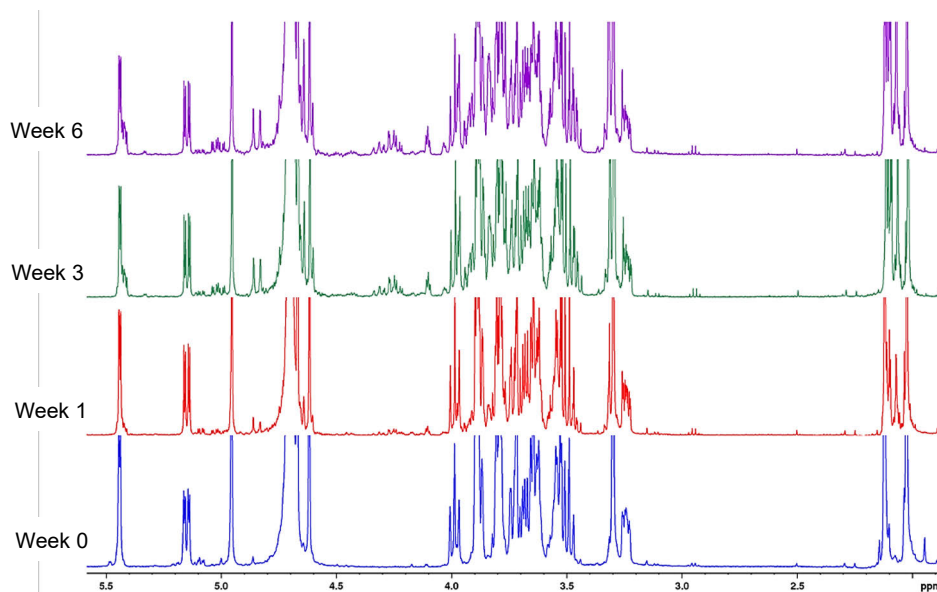


Figure 3.6. ^1H -NMR spectra of the migration at various times of the migration. Conditions: 10 mM D_2O phosphate buffer, starting pD = 8, 25 $^\circ\text{C}$.

Some of the new peaks could be selected for 1D-TOCSY spectra to get a clearer view of the formed saccharide units (Figure 3.7). It can clearly be observed from the 1D-TOCSY spectra that the new saccharide units come in pairs, with some of the shifts being slightly off from each other, e.g., the saccharide units A and B have an acetyl group at the O2 position, G and H have no acetyl groups, and, most importantly, E and F have an acetyl group at the O6 position. This means that at least one acetyl group has migrated to a neighboring saccharide unit. With the help of HSQC of the anomeric signals and HMBC, it can be concluded that the acetyl group has been relocated to the O6 of the reducing end, because the saccharide units with an acetyl group at O6 are connected to the OMe group.

The long migration time will lead to hydrolysis, and it could be argued that the observed change in position of the acetyl groups is due to hydrolysis followed by reattachment to another hydroxyl group. This was ruled out by having Me α -D-mannopyranoside and NaOAc (1 eq) dissolved in the same buffer for a week. No acetyl group had been attached to the saccharide. Furthermore, the reattachment of an acetyl group would not be regiospecific and would not explain the new saccharide units and their correlations.

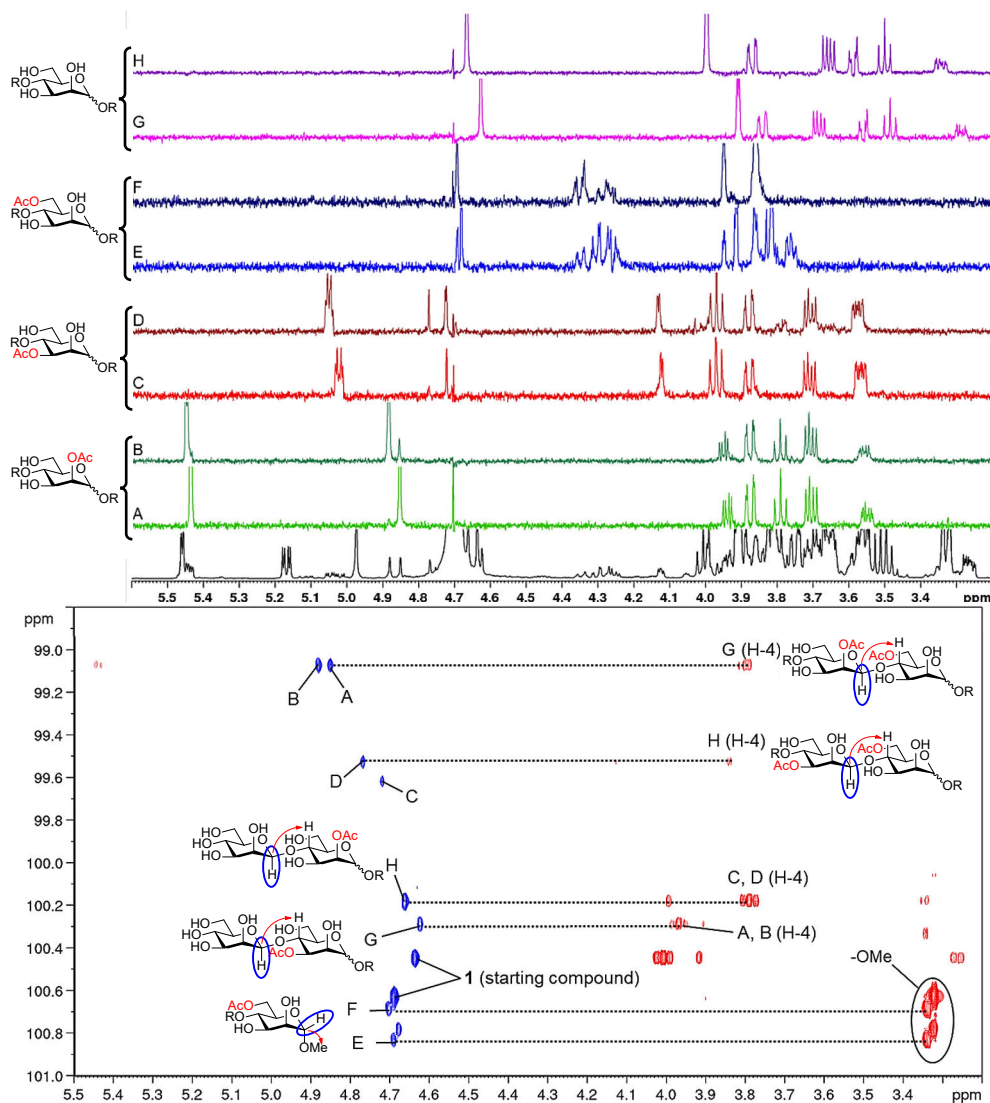


Figure 3.7. The upper spectra: 1D-TOCSY of selected peaks after 6 weeks of migration in 10 mM D₂O phosphate buffer with a starting pD of 8. The lower spectra: correlations between HSQC of the anomeric signals (blue) and HMBC (red) of the saccharide units in the 1D-TOCSY spectra.

Coordination through hydrogen bonding between the trisaccharides could possibly take place and might allow for the migration to take place intermolecularly. To investigate this possibility three different concentrations of **1** (1, 5 and 10 mg/ml) were followed for six weeks. There was no significant difference between the rates of these concentrations, meaning that the migration takes place intramolecularly, towards the reducing end.

The migration across the saccharide bond towards the reducing end is also supported by the migration in **57**. The only migration observed in **57** is the O2 \rightleftharpoons O3 migration. It becomes clear that the migration between neighboring hydroxyl groups is fast because at the first measuring point over 20% have already migrated and after 5 h, an equilibrium has been reached (Figure 3.8).

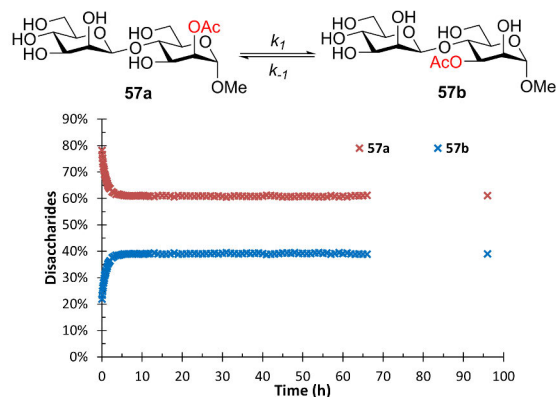
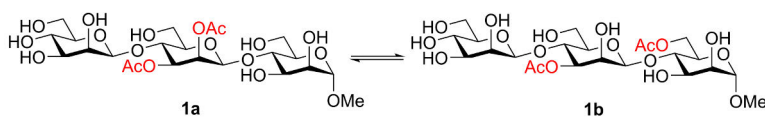


Figure 3.8. The migration in **2**. Conditions: 10 mM D₂O phosphate buffer, starting pD = 8, 25 °C. $k_f = 0.389 \pm 0.00550 \text{ h}^{-1}$ and $k_{-f} = 0.606 \pm 0.00882 \text{ h}^{-1}$.

With all the support above it can be concluded that the migration takes place from the O2 of the middle unit towards the O6 of the reducing end (Scheme 3.2). This is the first time this type of migration has been shown to take place and the implications could be significant regarding the regulation of the biological activity of polysaccharides.

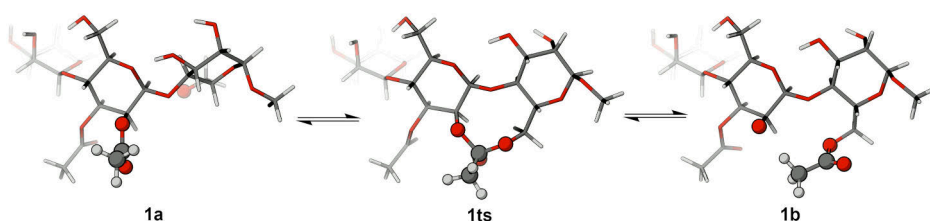


Scheme 3.2. The migration path across the glycosidic linkage.

3.2.2. Computational investigation

To provide further support for the migration, modelling of the process was implemented. Quantum chemical simulations of the possible migration mechanism were performed, by studying the process of migration between **1a** and **1b**. These simulations show that the deprotonation is a crucial step for the migration process and therefore an anionic mechanism is assumed. The barrier for the migration without deprotonation is too high to take place at room temperature. This is consistent with earlier works showing that the migration slows down at neutral pH and is close to nonexistent at acidic pH.^{130,136} The

migration is also limited by the distances between the two oxygens involved and, therefore, the dynamics of the trisaccharide are crucial. Oligomannosides usually uptake a similar conformation to cellulose,^{153,154} and retain flexibility. The reducing end saccharide unit can turn and get close enough for the migration to take place because of the flexibility. The distance between the two oxygens involved is 2.7 Å at the transition state, when a nine-membered ring is formed (Scheme 3.3). Then the distance shortens even more, to 2.5 Å before the old C-O bond is broken. The activation energy of the migration when considering the already deprotonated hydroxyl group is 13 kcal/mol at room temperature. This activation energy corresponds to a short reaction time, a half-life of milliseconds, but this is clearly not the case. The limiting factor for the migration is, therefore, the dynamics of the trisaccharide and the deprotonation (the pK_a of the hydroxyl group). Deeper investigations into the true mechanism can be found in section 3.4.



Scheme 3.3. The migration across the saccharide linkage.

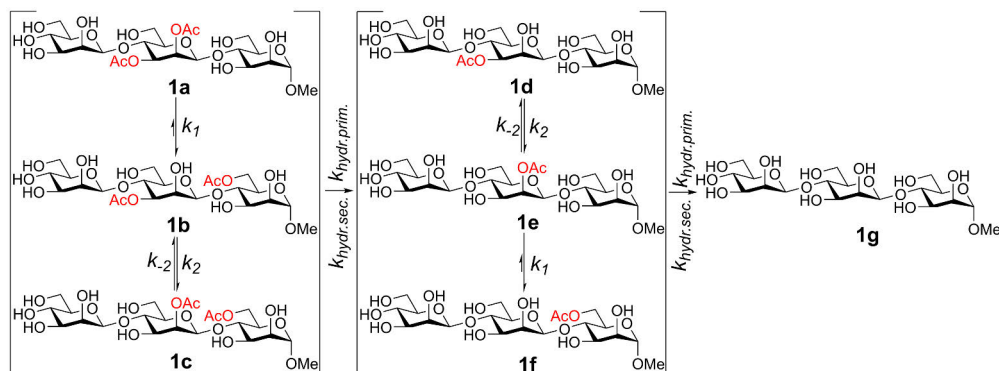
3.3. Kinetics of the migration over the glycosidic bond

To know the potential biological relevance of the new migration phenomenon, it is important to know how fast the migration is. Since the migration is faster in a H₂O buffer than a D₂O buffer (see section 3.4), a 100 mM phosphate H₂O buffer with 10% D₂O was used instead of the 10 mM D₂O buffer. The stronger buffer will tolerate the hydrolysis better, but the pH was also followed so it could be accounted for when it inevitably changed. Besides the mannan trisaccharide, two other types of trisaccharides were also investigated: xylan and glucan. With these three model trisaccharides, the migration in the backbone of the most common hemicelluloses is covered.

3.3.1. Kinetics of migration in the mannan trisaccharide

Two starting point was selected to follow the migration in the mannan trisaccharide; **1a** and **1b**. More accurate rate constants could be calculated with the two points, and the possible O6→O2 migration could be investigated

thoroughly, and if it takes place, the rate of this migration could be determined. It becomes evident that the migration system is complex (Scheme 3.4), which is why similar reactions, e.g., the O2 \rightleftharpoons O3 migrations and hydrolysis form primary positions, were set to have the same rate constants to minimize the errors, since these rates, although not exactly the same, would be similar.



Scheme 3.4. The proposed migration pathway in the manna model trisaccharide.

It becomes apparent that the O2 \rightarrow O6 migration is almost non-existent. There is almost no formation of **1a** when starting from **1b**, only approximate 0.4% (Figure 3.9). The dynamics of the trisaccharide, in combination with the stability of the acetyl group at the primary position,^{129,136} could prevent the migration back to O2. Similar tendencies in another mannan trisaccharide, **58** (Figure 3.10), were observed. Hydrolysis was the most prominent reaction taking place in **58**. Other compounds also formed but these compounds had too low concentration (under 1%) to be characterized by NMR spectroscopy.

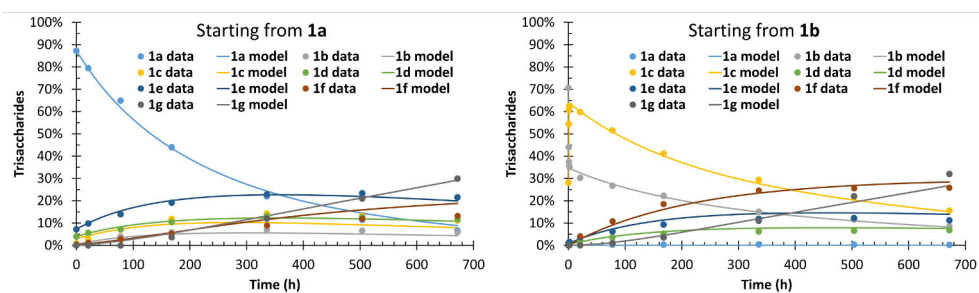


Figure 3.9. The acetyl group migration starting from the model compounds **1a** and **1b**, displaying the experimental data and kinetic model. Conditions: 100 mM phosphate solution with 10% D₂O, pH = 8, 25 °C.

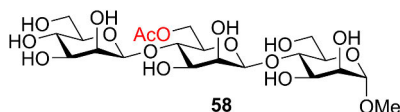


Figure 3.10. Structure of trisaccharide **58**.

There is a fast increase in **1d** and **1e** when starting from **1a**, which cannot be explained by the **1a** → **1b** migration followed by hydrolysis alone. When starting from **1b**, **1f** increased faster than **1d** and **1e**. The hydrolysis from the secondary position must, therefore, be considered when calculating the rate constants. The hydrolysis from secondary positions is almost as fast as from the primary positions. As expected, the O2 ⇌ O3 migration is fast, approximately 1000 times faster than any other migration and hydrolysis in the trisaccharides (Table 3.3). The O2:O3 ratio in the trisaccharides is 65:35, which is similar to the reported ratios in natural mannan polysaccharides.^{52–56} The migration between the saccharide units is slightly faster than the hydrolysis from the primary position, meaning that the concentration of 6-OAc products will not become high. The total amount of trisaccharides with a 6-OAc (**1b**, **1c** and **1f** together) do not exceed 32% when starting from **1a**, which might be one of the reasons the acetyl group is not found to a significant degree at the O6 position in natural mannans.

Table 3.3. The rate constants at pH 8 for the acetyl group migration in Scheme 3.4.^a

Rate constants for the mannan trisaccharides (h ⁻¹)	
k_1	2.06E-3 ± 1.85E-4
k_2	1.88E+0 ± 2.96E-1
k_{-2}	1.01E+0 ± 1.84E-1
$k_{hydr. prim}$	1.93E-3 ± 1.29E-4
$k_{hydr. sec.}$	1.56E-3 ± 7.56E-5

^a Conditions: 100 mM phosphate solution with 10% D₂O at 25 °C, starting pH = 8.

3.3.1.1. Influence of lectin on the migration

The influence of a lectin on the migration in a mannan model compound was also investigated by using DC-SIGN EDC (extracellular domain). DC-SIGN is one of the most widely studied human C-type lectin. The lectin is located in a solvent-exposed surface of the carbohydrate recognition domain and participates in crucial biological processes, mostly related to the immune response.^{155–157} The binding between the lectin and D-mannose and L-fucose sugar units have been extensively studied.^{158–161}

Compounds **1a**, **1b** and **58** were investigated in the presence of DC-SIGN at t_0 and after 30 days (t_1) by acquiring ¹H NMR, ¹H-¹³C HSQC and saturation transfer difference-NMR (STD-NMR) experiments, which were used to investigate the

interaction with the lectin. STD-NMR will give information of the interaction between a receptor and a ligand of low affinity ligand-protein systems, by transferring magnetization from the protons of the protein to the protons of the studied ligand in close contact to the protein surface. Thus, providing structural information about the molecular recognition event.^{162–165} The coordination of the trisaccharides to the primary Ca^{2+} ion via the O3 and O4 of the non-reducing end of the trisaccharides (residue C) takes place for all tree trisaccharides (Figure 3.11). This agrees with the mannose-recognition mode described for DC-SIGN.^{166,167} The O2 and O3 signals from residue A in **1a** overlaps with the O3 and O4 signals in residue C, which could mean coordination to residue A, but this was excluded by docking analysis. It becomes clear that there is no substantial difference between the t_0 and t_1 . It seems that the migration in **1a** is slower here than the buffer used earlier. Different buffers are used which may affect the rate of migration. For compound **58** minor migration and hydrolysis took place. The migration and hydrolysis did not affect the interactions with lectin. The presence of DC-SIGN might slow down the migration because of the interactions, which might not allow the right conformation of the trisaccharides to form.

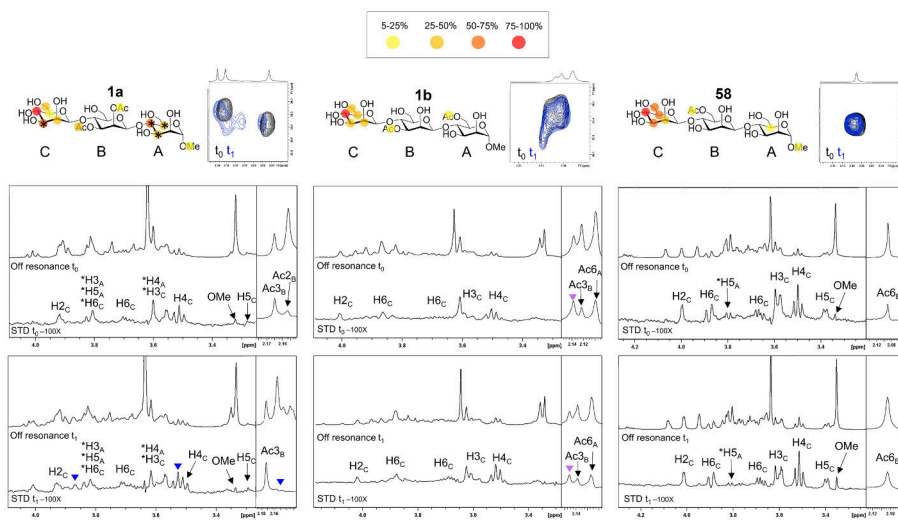
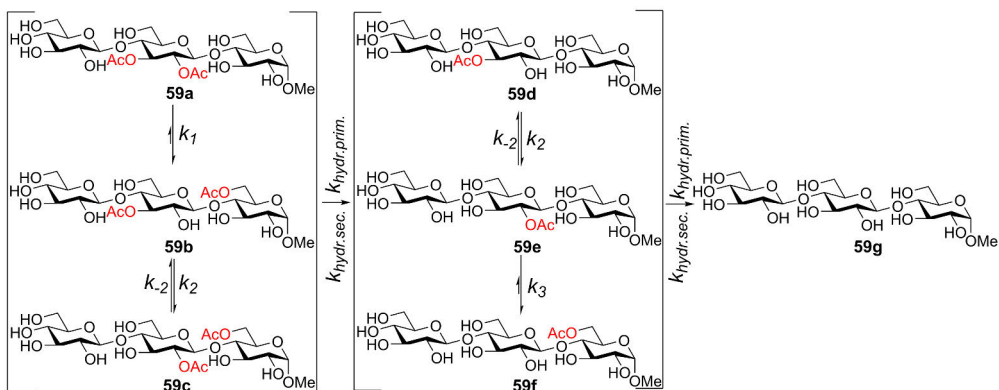


Figure 3.11. NMR experiments of compounds **1a**, **1b** and **58** with DC-SIGN ECD. Top figure: epitope mapping of the ^1H - ^{13}C HSQC of the respective acetyl region; STD-NMR spectra: off-resonance spectrum and STD spectrum with irradiation at δ 0.8 ppm at t_0 (upper) and t_1 (lower). *: signals that cannot be unequivocally assigned due to signal overlapping. \blacktriangledown : new signals in the STD spectrum at t_1 . \blacktriangledown : signals that appeared at t_0 because of fast migration.

3.3.2. Kinetics of migration in the glucan trisaccharide

Because the xyloglucans can be found in almost every plant,^{85–88} the potential migration over the glycosidic bond in these polysaccharides could have a huge impact on how their biological roles are regulated. The equatorial O2 will most likely have a large impact on the rate of migration, compared to the axial O2 in mannan. The migration over the glycosidic bond in glucans was investigated starting from the compounds **59a** and **59e** and a similar scheme as for the mannan trisaccharides was used to calculate the rate constants (Scheme 3.5).



Scheme 3.5. The proposed migration pathway in the glucan model trisaccharide.

The **59a** → **59b** migration is much faster than for the corresponding mannan trisaccharide (**1a** → **1b**). Already after 24 h have more than 50% of **59a** migrated to **59b** and further to **59c**, but the **59e** → **59f** migration is clearly not as fast (Figure 3.12). Therefore, when calculating the rate constants of the O2→O6 migrations, k_3 could not be equal to k_1 . The O6→O2 migration was at first calculated but was insignificantly low and was therefore excluded.

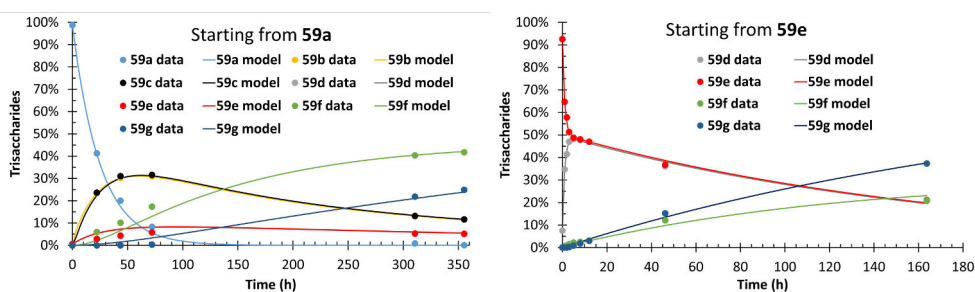


Figure 3.12. The acetyl group migration starting from compounds **59a** and **59e**, displaying the experimental data and kinetic model. Conditions: 100 mM phosphate solution with 10% D₂O, pH = 8, 25 °C.

The difference between the rates of **59a** → **59b** and **59e** → **59f** migrations, a factor of 7, is surprising (Table 3.4). The fast **59a** → **59b** migration could be due to some stabilization or destabilizing putting the O6 close to the O2. The **59e** → **59f** migration is closer to that of the manna trisaccharide but is still two times faster, because of the equatorial O2, hence the orientation of O2 will have a significant impact on the rate of migration across the glycosidic bond.

Table 3.4. The rate constants at pH 8 for the acetyl group migration in Scheme 3.5.^a

Rate constants for the glucan trisaccharides (h ⁻¹)	
k_1	3.33E-2 ± 1.62E-3
k_2	4.92E-1 ± 5.46E-2
k_{-2}	4.82E-1 ± 4.58E-2
k_3	4.85E-3 ± 5.08E-4
$k_{hydr. prim.}$	1.35E-3 ± 1.55E-4
$k_{hydr. sec.}$	3.24E-3 ± 1.50E-4

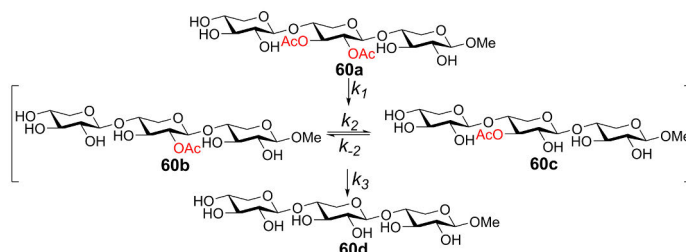
^a Conditions: 100 mM phosphate solution with 10% D₂O at 25 °C, starting pH = 8.

A surprising note is that the hydrolysis from the primary hydroxyl group is slower than the hydrolysis from the secondary. One plausible reason could be that when the acetyl group is located at the primary position, the free rotation could put the acetyl group in a more protected conformation, hindering hydrolysis. The fast migration between the saccharide units in the glucans and the slower hydrolysis from O6 could be one of the reasons that the natural glucans are mainly acetylated at the O6 position.

3.3.3. Kinetics of migration in the xylan trisaccharide

The xylans differentiate a lot from mannans and glucans. The lack of primary positions destabilizes the chain, and the conformations of xylans are different in comparison to the glucans and mannans. The absence of primary hydroxyl groups will also affect the migration, meaning if migration takes place over the glycosidic bond, it must be from a secondary to a secondary hydroxyl group. Migration between saccharide units in xylans will be much slower if even taking place at all. The selected starting points **60a** and **60b** makes it easier to analyze whether the migration across the glycosidic linkage can take place. For example, if the migration across the glycosidic linkage takes place in **60b**, it will be difficult to analyze the product since it is a migration from a secondary to a secondary hydroxyl group. With the help of **60a** the potential migration across the linkage can easily be noticed by comparing the ratios and the shifts of the acetyl peaks in the ¹H NMR-spectra.

The migration to a new saccharide unit did not take place. The only migration observed in the xylan trisaccharides is the $O2 \rightleftharpoons O3$ migration within the same saccharide unit (Scheme 3.6 and Figure 3.13). This is not surprising because the migration between saccharide units in the glucan and mannan trisaccharides was slow compared to other migrations and similar to hydrolysis, which was a migration from a secondary to a primary position.



Scheme 3.6. The proposed migration pathway in the xylan model trisaccharide.

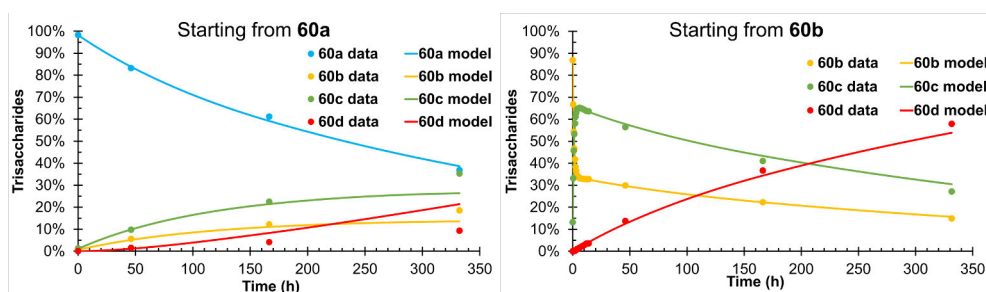


Figure 3.13. The acetyl group migration and hydrolysis starting from **60a** and **60b**, displaying the experimental data and kinetic model. Conditions: 100 mM phosphate solution with 10% D₂O, pH = 8, 25 °C.

The hydrolysis from **60a** compared to hydrolysis from **60b** and **60c** are a bit different (Table 3.5). The difference is most likely due to the steric hindrance the two acetyl groups impose on each other, resulting in the slower hydrolysis from **60a**. The rate of hydrolysis is similar to that of the glucans. The hydrolysis from O2 and O3 could not be differentiated due to the fast migration.

Table 3.5. The rate constants at pH 8 for the acetyl group migration in Scheme 3.6.^a

Rate constants for the xylan trisaccharides (h ⁻¹)	
k_1	$1.82\text{E-}3 \pm 1.28\text{E-}4$
k_3	$3.01\text{E-}3 \pm 1.94\text{E-}4$
k_2	$6.33\text{E-}1 \pm 5.32\text{E-}2$
k_{-2}	$3.25\text{E-}1 \pm 3.58\text{E-}2$

^a Conditions: 100 mM phosphate solution with 10% D₂O at 25 °C, starting pH = 8.

Comparing the ratio between O2 and O3 in the xylan, glucan, and mannan trisaccharides, it becomes clear that hydrogen bonding and steric hindrance will affect the ratio of acetylation. The acetylated O2:O3 ratio in the glucan trisaccharides is 1:1, while in the xylan trisaccharides this ratio is 1:2. The steric hindrance from the O6 of the non-reducing end or possible hydrogen bonding might influence the preferred position of the middle unit. For the mannan trisaccharides the O2:O3 ratio is about 2:1, which is even more in favor of the O2 position, perhaps because of less steric hinderance.

3.3.4. Migration in GGM

To show that the migration across the glycosidic bond also takes place in polysaccharides, a native polysaccharide, GGM, isolated from Norway spruce (*Picea abies*),⁵⁴ was used. The larger polysaccharides might not be able to uptake the right conformation to allow migration across the glycosidic bond to take place. Mannans usually uptake a two-fold screw conformation, similar to cellulose, but will be more flexible due to the axial O2.¹⁶⁸⁻¹⁷⁰ Glucose in the backbone do not induce any major conformational effect.¹⁷¹ The α -(1 \rightarrow 6)-linked galactose units will have the largest impact on the conformation, where the ratio of galactose and type of polymer (block, alternating or random) will affect the rigidity of the polysaccharide.¹⁵⁴

The Man:Glc:Gal ratio is approximately 4:1:0.1 in the GGM used,^{172,173} which should not have a significant impact on the linearity of the backbone, putting the O2 and O6 close in space to each other. The degree of acetylation of the mannose units is approximately 65%,⁵⁴ which is sufficient to investigate whether the acetyl groups could migrate across the glycosidic linkage.

The migration is, as expected, slow and several weeks were needed before the migration products could be analyzed. A peak grew in the same area where the acetyl group at O6 in the trisaccharides resides (Figure 3.14). With the help of water-suppressed HSQC and 1D HMBC NMR spectroscopic measurements, it could be determined that the signals, corresponding to the acetylated O6 in mannose, grew with time. These signals also match the corresponding signals of **58** in the HSQC spectrum. Considering that the O2 \rightarrow O6 migration in the trisaccharide model compounds takes place between two adjacent saccharides, towards the reducing end, the same is undoubtedly taking place in GGM.

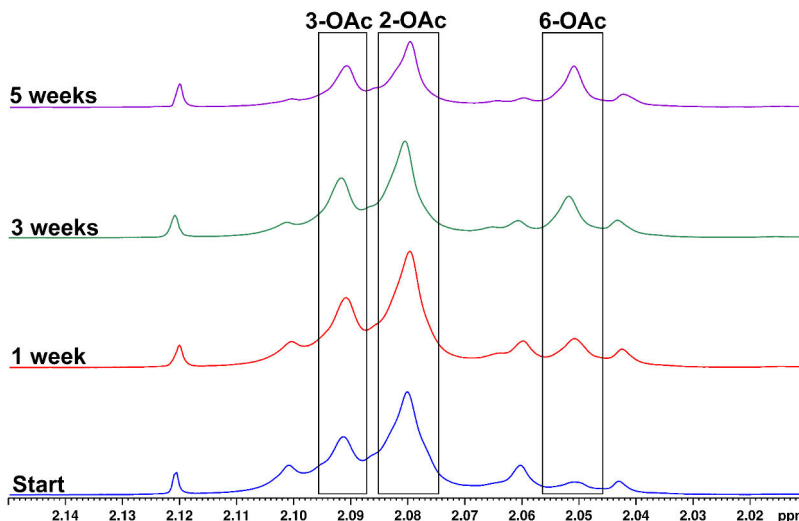


Figure 3.14. ^1H -NMR spectra of the acetyl group migration in GGM. The areas where the corresponding acetyl groups in the trisaccharides were located are marked with boxes. Conditions: 100 mM phosphate solution with 10% D_2O , starting pH = 8, 25 $^\circ\text{C}$.

A simplified model had to be used to calculate the rate constants, because of the complexity of the polysaccharide. The model is broken down into monosaccharide units based on the acetyl group peaks in the ^1H NMR spectra, where the peaks have similar position as the model compounds. The acetylated O2 and O3 positions are already in equilibrium at the start, which is why the rate constant for the $\text{O2} \rightarrow \text{O3}$ migration is set to 1 h^{-1} , allowing the $\text{O3} \rightarrow \text{O2}$ rate constant to uphold the equilibrium. Different concentrations of GGM (2, 10 and 20 mg/ml) were also employed because of possible interaction between the long polysaccharide chains.

It becomes apparent that there is some coordination between the polysaccharide chains, especially at higher concentrations. At lower concentration, the $\text{O2} \rightarrow \text{O6}$ migration rate is closer to that of the mannan trisaccharides compared to higher concentration. At 2 mg/ml, residue C reaches a constant concentration of 15%, but at 10 and 20 mg/ml residue C only reaches 11% (Figure 3.15). The slower $\text{O2} \rightarrow \text{O6}$ migration at higher concentrations is also supported by the rate constants (Table 3.6). The coordination between the polysaccharide chains could hinder the $\text{O2} \rightarrow \text{O6}$ migration, either by not allowing the right conformation or by hydrogen bonding, or both.

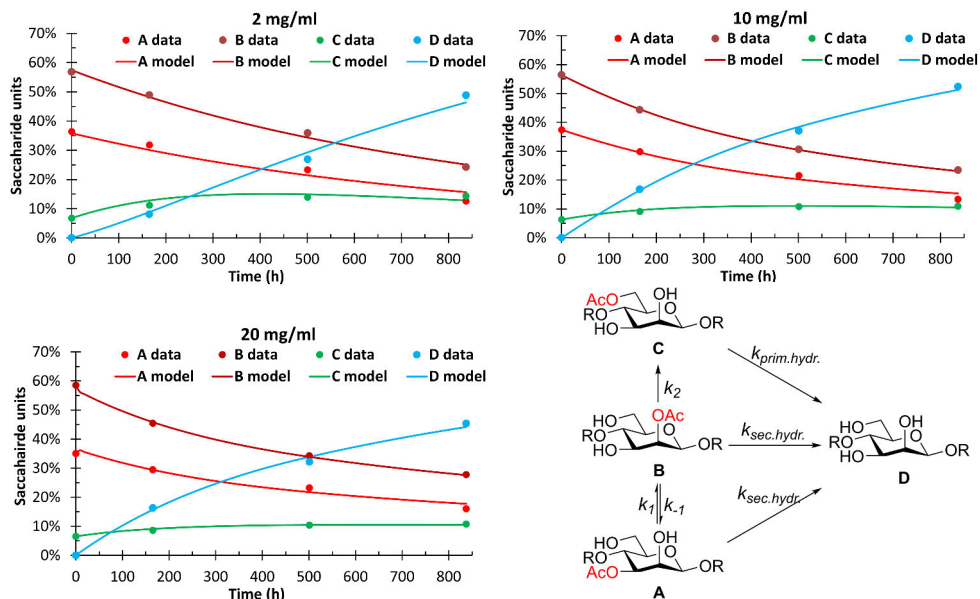


Figure 3.15. The acetyl group migration in GGM at different concentrations, displaying the experimental data and kinetic model. Conditions: 100 mM phosphate solution with 10% D₂O, pH = 8, 25 °C.

Table 3.6. The rate constants at pH = 8 for the kinetic model in Figure 3.15 at concentrations of 2, 10 and 20 mg/ml.^a

	2 mg/ml (h ⁻¹)	10 mg/ml (h ⁻¹)	20 mg/ml (h ⁻¹)
k_1	1.60E+0 ± 1.65E-1	1.51E+0 ± 8.28E-2	1.56E+0 ± 8.42E-2
k_{-1}	1.00E+0 ^b	1.00E+0 ^b	1.00E+0 ^b
k_2	1.50E-3 ± 8.36E-4	8.41E-4 ± 4.54E-4	7.08E-4 ± 5.88E-4
$k_{prim.hydr}$	3.72E-3 ± 2.46E-3	2.35E-3 ± 1.72E-3	2.06E-3 ± 2.58E-3
$k_{sec.hydr}$	2.60E-4 ± 5.22E-4	1.16E-3 ± 2.76E-4	1.24E-3 ± 3.60E-4

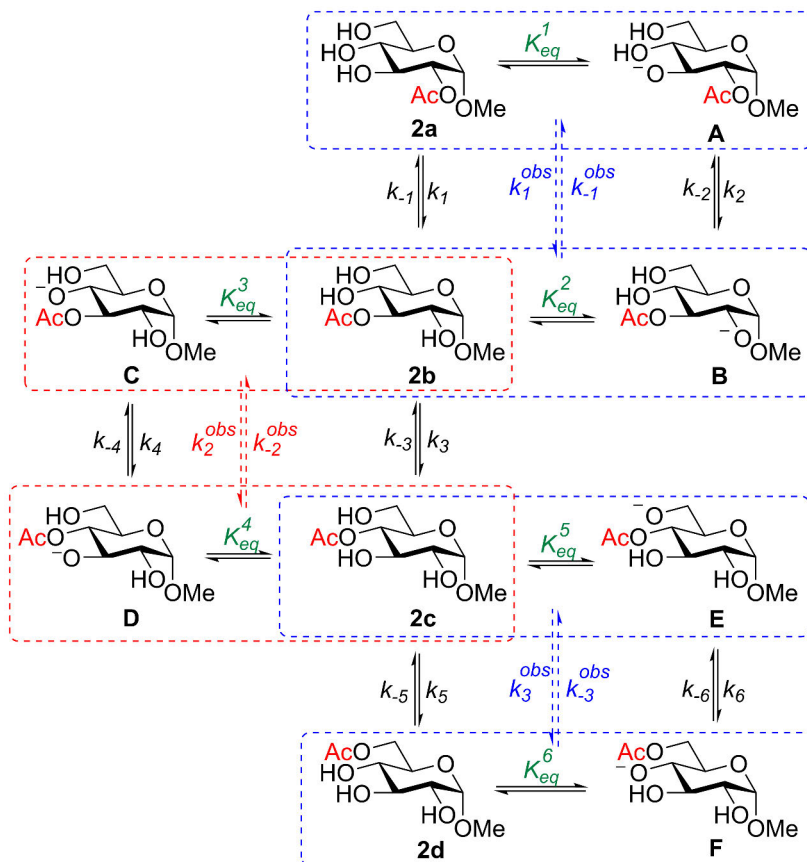
^a Conditions: 100 mM phosphate solution with 10% D₂O at 25 °C, starting pH = 8. ^b Locked.

The rate of hydrolysis from the primary positions decreases with increasing concentration and the hydrolysis from the secondary positions increases with increasing concentration. At 10 and 20 mg/ml concentrations the hydrolysis at the start is noticeably faster than at 2 mg/ml. This could be a consequence of the slower O2→O6 migration at higher concentrations. Because of the lower O6 concentration, the hydrolysis from the secondary positions will become more prominent. Due to the simplified model, these rate constants should be taken as an approximation, which becomes evident from the large calculated errors, especially for the hydrolysis constants. Nevertheless, these constants provide preliminary estimations of the range of the rate constants.

The migration in other β -(1 \rightarrow 4)-linked mannans should also be able to take place since the galactose content in GGM is low and the glucose in the backbone has no impact on the conformation. Since the migration in the glucan trisaccharide is much faster than the mannan trisaccharide, the migration in glucans should also be possible and migration could be the reason glucans are mostly acetylated at O6 in nature. The degree of acetylation and the position of the acetyl groups could change how the polysaccharides, and oligosaccharides, interact with other compounds. Therefore, it can be speculated that the migration could be a way to regulate the biological activity of the polysaccharides. During cell growth and development, the pH increases in the cells, meaning that the rate of migration would increase, implying that more acetyl groups in mannans and glucans would migrate to O6, which could increase the cell signaling. The role of the migration is also an important part for the biological activity of polysaccharides for pharmaceutical purposes,⁶⁹⁻⁷² since knowing what role the migration has is important to know whether to enhance or suppress the migration to prolong and increase biological activity. The migration might be active during the cell expansion by breaking the interactions between the polysaccharides, such as hydrogen bonding.

3.4. Elucidation of the migration mechanism

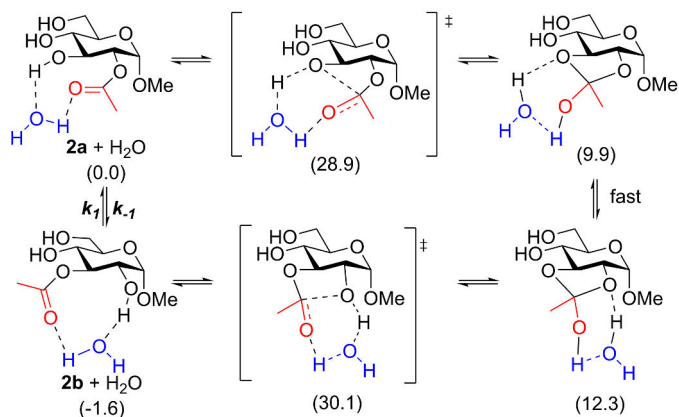
The deprotonation followed by the nucleophilic attack at the carbonyl carbon, forming an orthoester intermediate, is usually the accepted mechanism in buffer. The anion is usually assumed when calculations are made, giving energies that do not correlate to the observed migration rate. A neutral mechanism will also contribute to the overall rate (Scheme 3.7). The anionic and neutral mechanisms are competitive, and both will depend on the protonated and deprotonated species. The ratio of the deprotonated and protonated species is influenced by the pH of the solution and the pK_a of the hydroxyl group to where the acyl group is migrating. Most of the previous computational studies have not considered the pK_a of the hydroxyl groups when calculating the energies, resulting in too low energies compared to the experimentally observed rates.



Scheme 3.7. Acetyl group migration in Me α -D-glucopyranoside (2a – 2d).

3.4.1. Neutral mechanism

The neutral mechanism must involve some type of H-transfer. Without any aid the transfer would form a highly strained four membered cycle, which is why the transfer is usually mediated by water molecules. The energies of the neutral migration mechanism, mediated by one water molecule, were calculated (Scheme 3.8), which resulted in energies that are clearly too large when comparing them to the experimental rate constants. By applying two water molecules, the barriers increased, corresponding to a slower rate of migration. The calculations were further extended to the whole migration process in the Me α -D-glucopyranoside, which resulted in similar energy barriers (Table 3.7). The high barriers indicate that the neutral mechanism is not responsible for the observed migration rates.



Scheme 3.8. Acetyl group migration (**2a** → **2b**) under neutral conditions mediated by one water molecule. Calculated relative energies (kcal/mol) are given.

Table 3.7. Calculated energy barriers and rate constants for the acetyl group migration in Me α -D-glucopyranoside under the neutral mechanism with one water molecule in Scheme 3.7.

	ΔG (kcal/mol)	rate constant (h^{-1})
k_1	30.2	1.71E-06
k_{-1}	31.8	1.10E-07
k_3	36.3	5.62E-11
k_{-3}	32.3	4.61E-08
k_5	30.9	5.54E-07
k_{-5}	29.7	3.85E-06

3.4.2. Anionic Mechanism

The most used model is the naked anion, which results in energies that are much lower than the experimentally observed. The pK_{a} s should be considered in this mechanism since the resulted anion from the deprotonation is the starting point, but this step is often neglected. Water molecules, one, two, and three, surrounding the alkoxide anion were introduced in this study. The model, with three water molecules, was the path selected (Scheme 3.9), since three water molecules were used for the calculations of the pK_{a} s (see section 3.4.4). Several conformations had to be evaluated. The calculations resulted in low energy barriers with the conclusion that the resulting rate constants are too high compared to the observed ones (Table 3.8).

isotope effect was not really observed as the $k(^{12}\text{C})/k(^{13}\text{C})$ ratio was on average close to one and some was even under one.

Table 3.9. The $^{12}\text{C}/^{13}\text{C}$ and $^1\text{H}/^2\text{H}$ isotope effects in **26**.

	$k(^{12}\text{C})^a/k(^{13}\text{C})^a$	$k(^1\text{H})^b/k(^2\text{H})^a$
k_1	1.02	1.75
k_{-1}	0.97	1.70
k_2	0.89	1.83
k_{-2}	0.85	2.21
k_3	1.16	3.82
k_{-3}	1.15	1.21

^a 10 mM phosphate D₂O buffer pD = 8 and 25 °C. ^b 10 mM phosphate buffer (10% D₂O) pH = 8 and 25 °C.

3.4.3.2. pH dependence

There is a clear relationship between the pH and the rates constants.¹³⁰ To investigate the potential linear relationship between rate constants and concentration of $[\text{OH}^-]$, the migrations in buffers with the pHs 6, 7, 7.5, and 9 were compared to the rate constants in the buffer with pH 8. If the rate of migration is linear to the concentration of $[\text{OH}^-]$, the rate constants should follow the theoretical factors, which are calculated as $[\text{OH}^-]_{\text{pH}=x}/[\text{OH}^-]_{\text{pH}=8}$ (Table 3.10). The calculated experimental factors have small differentiations from the theoretical but is within the expected error. This demonstrates that the rate of migration is linear with the concentration of $[\text{OH}^-]$. This means that when the rate of migration is known at one pH it can be estimated at another pH.

Table 3.10. The theoretical and experimental pH factors for the migration in **2**.^a

pH	Theoretical	Experimental
9	10	7.1
8	1	1
7.5	0.32	0.35
7	0.1	0.085
6	0.01	0.0082

^a Conditions: 100 mM phosphate buffer with 10% D₂O, 25 °C.

3.4.4. The real model

As mentioned earlier the pK_as of the involved hydroxyl groups must be determined to evaluate the concentration of the starting components for both the anion and neutral mechanism. The pK_as are challenging to calculate because the values can have variations of a couple of units with very small differences in

energy.¹⁷⁵ The pK_a of hydroxyl groups in carbohydrates are in the range of 10 – 14. When a neighboring hydroxyl group has an acetyl group attached, it can be expected that the pK_a is 1 – 2 units lower. The method to calculate the pK_a s chosen here has been used on thiols in aqueous solutions.¹⁷⁶ This model uses three explicit water molecules and a continuum solvent model and provides values that are in the range of what is expected (Figure 3.16).

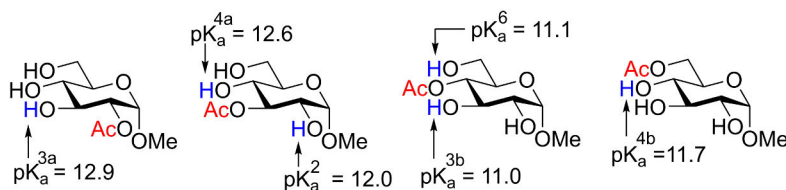


Figure 3.16. Calculated pK_a s in **2a**, **2b**, **2c** and **2d**.

It is possible to disregard the neutral mechanism at pH 8, because of the difference of five orders of magnitude between the mechanisms. Leaving out the neutral mechanism is possible at pH > 6, but at pH ≤ 6 the rate of the neutral mechanism should be considered. Therefore, a general equation for the rate constants can be written as:

$$\text{when } \text{pH} \leq 6: \quad k^{obs} = k^{neutral} + \frac{k^{anion} \cdot K_{eq}}{[H]^+}$$

$$\text{and when } \text{pH} > 6: \quad k^{obs} = \frac{k^{anion} \cdot K_{eq}}{[H]^+}$$

Obviously, one should evaluate which equation gives the correct values for each carbohydrate individually, because in some cases the $k^{neutral}$ might be large enough to affect the total rate of migration at higher pH.

The first calculations were performed on the acetyl group migration in Me α -D-glucopyranoside (**2**) and to assess the model, in this case for pH > 6, energies and rate constants for several carbohydrates were calculated (Table 3.11). The rate constants can vary greatly due to the logarithmic dependence of the calculated energies. The errors between the experimental and calculated energies are within the expected errors for DFT, 1–2 kcal/mol,¹⁷⁷ meaning that the calculations are in good agreement with the experimental values and the model can be considered valid. This model explains the fact that the pH dictates the rate of migration significantly and that it is linear to the concentration of $[OH^-]$ as shown experimentally. The resulted energies are in good agreement with the

experimental values for the selected level of theory, as all are within the range of 2 kcal/mol.

Table 3.11. Calculated formal energy barriers and rate constants for the acetyl group migration in **2**, **7**, **12**, **17**, **27**, and **32** at pH=8.

		Experimental		Calculated		ΔG error (kcal/mol)
		rate constant (h ⁻¹)	ΔG (kcal/mol)	rate constant (h ⁻¹)	ΔG (kcal/mol)	
α -Glc (2)	k_1	2.26E-01	23.2	1.21E+00	22.2	1.0
	k_{-1}	1.84E-01	23.3	1.45E-01	23.5	0.2
	k_2	1.82E-01	23.3	1.13E-02	25.0	1.6
	k_{-2}	3.64E-01	22.9	1.62E-02	24.8	1.8
	k_3	4.34E+00	21.4	2.28E+00	21.8	0.4
	k_{-3}	2.82E-01	23.1	2.93E-01	23.1	0.0
β -Glc (7)	k_1	7.28E-01	22.5	9.79E-02	23.7	1.2
	k_{-1}	4.00E-01	22.9	1.54E+00	22.1	0.8
	k_2	4.14E-01	22.8	1.29E+00	22.2	0.7
	k_{-2}	4.62E-01	22.8	1.70E-02	24.7	2.0
	k_3	3.95E+00	21.5	1.97E+01	20.6	1.0
	k_{-3}	1.64E-01	23.4	1.44E+00	22.1	1.3
α -Gal (12)	k_1	1.19E-01	23.6	1.08E+00	22.3	1.3
	k_{-1}	9.55E-02	23.7	5.62E-01	22.7	1.1
	k_2	8.74E-01	22.4	2.43E+01	20.4	2.0
	k_{-2}	8.73E-01	22.4	1.06E-01	23.7	1.3
	k_3	1.02E+00	22.3	1.74E+00	22.0	0.3
	k_{-3}	1.97E-01	23.3	8.42E-01	22.4	0.9
β -Gal (17)	k_1	5.28E-01	22.7	4.28E-01	22.8	0.1
	k_{-1}	2.19E-01	23.2	1.42E-01	23.5	0.3
	k_2	8.73E-01	22.4	6.77E-01	22.6	0.2
	k_{-2}	6.20E-01	22.6	3.16E-02	24.4	1.8
	k_3	7.55E-01	22.5	5.36E+00	21.3	1.2
	k_{-3}	2.06E-01	23.3	1.99E-01	23.3	0.0
α -Xyl (32)	k_1	2.11E-01	23.2	8.17E-01	22.4	0.8
	k_{-1}	1.53E-01	23.4	3.40E+00	21.6	1.8
	k_2	7.30E-02	23.9	5.29E-02	24.1	0.2
	k_{-2}	8.41E-02	23.8	4.50E-01	22.8	1.0
β -Xyl (27)	k_1	5.94E-01	22.6	1.03E-01	23.7	1.0
	k_{-1}	2.64E-01	23.1	1.27E+00	22.2	0.9
	k_2	3.28E-01	23.0	1.18E+00	22.2	0.8
	k_{-2}	2.81E-01	23.1	6.84E+00	21.2	1.9

3.4.5. Applying the mechanistic model to trisaccharides

The new model was applied to the migration in the glucan and mannan trisaccharide compounds, to investigate the applicability of the proposed mechanism to the migration over the glycosidic bond. Starting off, the model was applied to the acetyl group migration in the glucan trisaccharides **59a-59f**. One serious issue with the trisaccharides is the flexibility of the conformation and the ability to form hydrogen bonds that stabilizes the conformations, which results in many conformations within a range of 5 kcal/mol. Therefore, a conformational study must be performed to determine the preferred conformations and the

possible interactions between saccharide units. Molecular dynamics (MD) studies and conformational searches with Macromodel were used for this purpose.¹⁷⁸ Structures that were within 2 kcal/mol, when comparing the two methods, were optimized at DFT level. All minima corresponding to protonated and deprotonated substrates were located and characterized. These minima were used to calculate the pK_as of the different hydroxyl groups involved in an acetyl group migration. The same protocol, which was implemented for monosaccharides, was used (Figure 3.17).

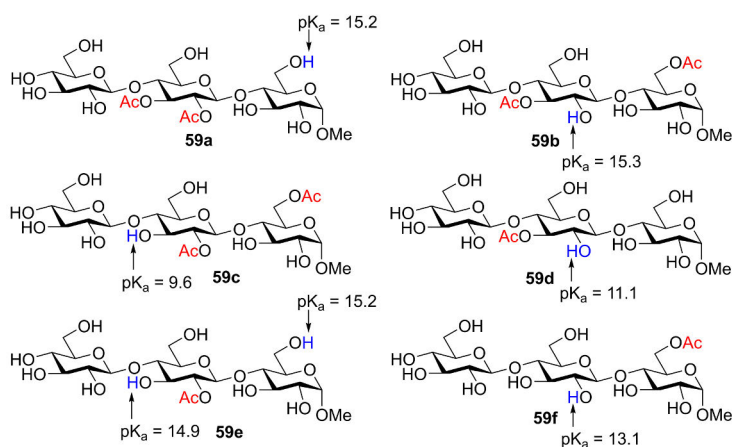


Figure 3.17. Calculated pK_as of hydroxyl groups involved in acetyl group migration processes in the glucan trisaccharides **59a-59f**.

The transitions between the saccharide units form a nine-membered ring, much different from the migration within the saccharide unit. The large ring gives rise to a substantial conformational flexibility, requiring a significant computational effort to consider the conformational variability of both the transition structures (Figure 3.18) and the intermediates. The preferred conformation in the rest of the trisaccharide was conserved during the migration process to avoid fluctuating energy values. Differences within 2 kcal/mol should be considered under that uncertainty, because the method cannot discriminate between values less than 2 kcal/mol.

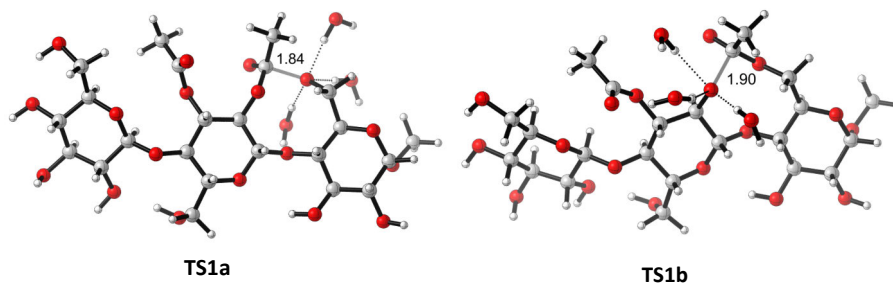


Figure 3.18. Optimized geometries of transition structures **TS1a** (**59a** → **59b**) and **TS1b** (**59b** → **59a**).

Following the same protocol as for the monosaccharides the energy barriers could be calculated (Table 3.12). The calculations were first applied to the glucan trisaccharides and later to the mannan trisaccharide. The predicted values are in an acceptable agreement with experimental results. The k_{-1} and k_{-4} values are calculated to be low, in agreement with the nonexistent experimental values. The next values are k_1 and k_4 that are the slowest migration rates calculated, which is supported by the computational calculations. All barriers match the experimental values well, especially for the mannan trisaccharide. This new protocol can be deemed as valid even for migration between saccharide units. The reason for the migration not going back (O6→O2) is because the acetyl group is so stable at the primary position that it does not migrate back, meaning that the reason is thermodynamic.

Table 3.12. Calculated formal energy barriers and rate constants for the acetyl group migration in the glucan and mannan trisaccharides at pH=8.

		Experimental		Calculated		ΔG error
		rate constants (h ⁻¹)	ΔG (kcal/mol)	rate constants (h ⁻¹)	ΔG (kcal/mol)	
Glucan	$k_{59a \rightarrow 59b}$	3.33E-02	24.3	5.62E-04	26.7	2.4
	$k_{59b \rightarrow 59a}$	< 3.60E-11 ^a	>36.0	1.01E-08	33.2	^b
	$k_{59b \rightarrow 59c}$	4.92E-01	22.7	7.24E-02	23.9	1.2
	$k_{59c \rightarrow 59b}$	4.82E-01	22.7	9.07E-02	23.7	1.0
	$k_{59d \rightarrow 59e}$	4.92E-01	22.7	3.23E-01	23.0	0.3
	$k_{59e \rightarrow 59d}$	4.82E-01	22.7	2.44E-03	25.9	3.2
	$k_{59e \rightarrow 59f}$	4.85E-03	25.5	2.97E-05	28.5	3.0
	$k_{59f \rightarrow 59e}$	< 3.60E-11 ^a	>36.0	2.42E-10	35.4	^b
Mannan	$k_{1a \rightarrow 1b}$	2.06E-03	26.0	1.05E-04	27.7	1.7
	$k_{1b \rightarrow 1a}$	< 3.60E-11 ^a	> 36.0	2.95E-09	33.9	^b
	$k_{1b \rightarrow 1c}$	1.88E+00	21.9	7.02E-02	23.9	2.0
	$k_{1c \rightarrow 1b}$	1.01E+00	22.3	2.08E-01	23.2	0.9
	$k_{1d \rightarrow 1e}$	1.88E+00	21.9	6.70E+00	21.2	0.3
	$k_{1e \rightarrow 1d}$	1.01E+00	22.3	4.18E-02	24.2	0.9
	$k_{1e \rightarrow 1f}$	2.06E-03	26.0	9.25E-06	29.2	3.2
	$k_{1f \rightarrow 1e}$	< 3.60E-11 ^a	> 36.0	7.09E-10	34.8	^b

^a Since this constant has not been observed experimentally it is considered very low. ^b This error cannot be considered because the experimental value has not been measured.

4. Concluding discussion

4.1. Summary and conclusions

It is demonstrated in this thesis that an acetyl group can migrate between two saccharide units, towards the reducing end. The acetyl group migration across the glycosidic bond takes place when it can migrate from a secondary to a primary hydroxyl group, since no migration between saccharide units was observed in the xylan model compounds. Furthermore, the migration across the glycosidic bond is also observed in a polysaccharide, GGM, showing that the migration can take place in large polysaccharide chains. The migration in polysaccharides could have a significant impact on how the polysaccharides interact with other compounds close to them and consequently the cell signaling and biological activity of them could be changed with migration.

A comprehensive study of the acyl group migration in common monosaccharides, with five different acyl groups, has been performed, resulting in some interesting conclusions. The stereochemistry at the anomeric position affects the migration in the whole unit. When the anomeric substituent is axial, the migration over *trans* hydroxyl groups is significantly slower compared to when the anomeric substituent is equatorial. The steric hindrance affects the rate of migration over *trans* hydroxyl groups more than over *cis* hydroxyl groups, most likely due to the strain of the transition state for migration between *trans* hydroxyl groups. The buffer strength will affect the rate of migration significantly as stronger buffers will increase the migration rate. The difference in the rate of migration indicates that studies where different buffers have been used, cannot be directly compared.

With the help of experimental evidence and computational means a new, more realistic mechanism is proposed. This mechanism combines neutral and anionic mechanisms and accounts for the pK_a of the hydroxyl groups. This mechanism is highly pH dependent and increasing the pH by one unit, will increase the rate of migration by a factor of ten, as demonstrated experimentally. Since the migration takes place in water, it is expected that water participates in the mechanism. By applying the mechanistic model to several carbohydrates, the model is confirmed to fit well with the experimental values, within the expected errors for computational calculations, even in the model trisaccharides.

4.2. Future perspectives

In this thesis only the naturally acetylated hemicelluloses were in focus, but there are several other poly- and oligosaccharides with other linkages that have important biological roles. Investigations of the migration over other linkages could give insight to potential regulation mechanisms of the biological activity in many more biologically active carbohydrates. Furthermore, the migration in furanosides have barely been investigated. At the time of writing, only one article covers some migration in furanosides.

The migration across the glycosidic linkage could be significant for the regulation of the biological activity of natural polysaccharides. Studies regarding the effects of the migration must be performed, to know for certain what role the migration plays. Whether the migration activates or deactivates the biological activity would be crucial for optimizing the polysaccharides for pharmaceutical use. Furthermore, the migration could also change the properties of the polysaccharides, changing the way the polysaccharide chain interacts with other compounds around it. Knowing whether the migration has a significant role in the plant cell walls would help to better understand the mechanism of cell walls. Further studies are required to tell how significant the migration phenomenon is regarding the regulation of biological activity and the properties of the polysaccharides.

5. References

- (1) Fischer, E. Synthesen in Der Zuckergruppe II. *Ber. Dtsch. Chem. Ges.* **1894**, 27, 3189–3232.
- (2) Hudson, C. S. Emil Fischer's Discovery of the Configuration of Glucose. A Semicentennial Retrospect. *J. Chem. Educ.* **1941**, 18, 353–357.
- (3) Kunz, H. Emil Fischer—Unequalled Classicist, Master of Organic Chemistry Research, and Inspired Trailblazer of Biological Chemistry. *Angew. Chem. Int. Ed.* **2002**, 41, 4439–4451.
- (4) Isbell, H. S.; Pigman, W. Mutarotation of Sugars in Solution: Part II. Catalytic Processes, Isotope Effects, Reaction Mechanisms, and Biochemical Aspects. *Adv. Carbohydr. Chem. Biochem.* **1970**, 24 (C), 13–65.
- (5) Angyal, S. J.; Pickles, V. A. Equilibria between Pyranoses and Furanoses. II. Aldoses. *Aust. J. Chem.* **1972**, 25, 1695–1710.
- (6) Rönnols, J.; Manner, S.; Ellervik, U.; Widmalm, G. Conformational Effects Due to Stereochemistry and C3-Substituents in Xylopyranoside Derivatives as Studied by NMR Spectroscopy. *Org. Biomol. Chem.* **2014**, 12 8031–8035.
- (7) Edward, J. T. Stability of Glycosides to Acid Hydrolysis. *Chem. Ind. London* **1955**, 1102–1104.
- (8) Lemieux, R. U. In *Molecular Rearrangements*; de Mayo, P., Ed.; Interscience Publisher, 1964; p 709.
- (9) Durette, P. L.; Horton, D. Conformational Studies on Pyranoid Sugar Derivatives by N.M.R. Spectroscopy. The Conformational Equilibria of Some Alkyl Tri-O-Acetyl- and Tri-O-Benzoyl- β -D-Ribopyranosides in Solution. *Carbohydr. Res.* **1971**, 18, 289–301.
- (10) Durette, P. L.; Horton, D. Conformational Studies on Pyranoid Sugar Derivatives by N.M.R. Spectroscopy. The Conformational Equilibria of Some Peracetylated Aldopentopyranosyl Halides in Solution. *Carbohydr. Res.* **1971**, 18, 57–80.
- (11) Durette, P. L.; Horton, D. Conformational Studies on Pyranoid Sugar Derivatives by N.M.R. Spectroscopy. The Conformational Equilibria of the 1,2-Trans Peracetylated Aldopentopyranosyl Benzoates and Perbenzoylated Aldopentopyranosyl Acetates in Solution. *Carbohydr. Res.* **1971**, 18, 389–401.
- (12) Durette, P. L.; Horton, D. Conformational Studies on Pyranoid Sugar Derivatives by N.M.R. Spectroscopy. Conformational Equilibria of the Peracetylated and Some Perbenzoylated Methyl D-Aldopentopyranosides in Solution. *Carbohydr. Res.* **1971**, 18, 403–418.
- (13) Romers, C.; Altona, C.; Buys, H. R.; Havinga, E. Geometry and Conformational Properties of Some Five- and Six-Membered Heterocyclic Compounds Containing Oxygen or Sulfur. In *Topics in Stereochemistry*; Topics in Stereochemistry; 2007; pp 39–97.
- (14) Ellervik, U.; Magnusson, G. Anomeric Effect in Furanosides. Experimental Evidence from Conformationally Restricted Compounds. *J. Am. Chem. Soc.* **1994**, 116, 2340–2347.
- (15) Nishida, Y.; Hori, H.; Ohru, H.; Meguro, H. ¹H NMR Analyses of Rotameric Distribution of C5-C6 Bonds of D-Glucopyranoses in Solution. *J. Carbohydr. Chem.* **1988**, 7, 239–250.
- (16) Hori, H.; Nishida, Y.; Ohru, H.; Meguro, H. Conformational Analysis of Hydroxymethyl Group of D-Mannose Derivatives Using (6S)- and (6R)-(6-²H₁)-D-Mannose. *J. Carbohydr. Chem.* **1990**, 9, 601–618.
- (17) Nishida, Y.; Ohtaki, E.; Ohru, H.; Meguro, H. Calculations of Cotton Effects in the Vacuum UV Region in the Non-Anomeric Part of Pyranoses: Correlations with the Absolute Stereochemistries. *J. Carbohydr. Chem.* **1990**, 9, 287–305.
- (18) Haines, A. H. Relative Reactivities of Hydroxyl Groups in Carbohydrates. *Adv. Carbohydr. Chem. Biochem.* **1976**, 33, 11–109.
- (19) de Belder, A. N. Cyclic Acetals of the Aldoses and Aldosides. *Adv. Carbohydr. Chem. Biochem.* **1965**, 20, 219–302.
- (20) Dimakos, V.; Taylor, M. S. Site-Selective Functionalization of Hydroxyl Groups in Carbohydrate Derivatives. *Chem. Rev.* **2018**, 118, 11457–11517.

- (21) Hung, S.-C.; Wang, C.-C. Protecting Group Strategies in Carbohydrate Synthesis. In *Glycochemical Synthesis*; Wiley Online Books; John Wiley & Sons, Inc.: Hoboken, NJ, USA, 2016; pp 35–68.
- (22) Vidal, S. *Protecting Groups: Strategies and Applications in Carbohydrate Chemistry*; Vidal, S., Ed.; Wiley-VCH: Weinheim, Germany, 2019.
- (23) Michael, A. On the Synthesis of Helicin and Phenolglucoside. *Am. Chem. J.* **1879**, *1*, 305–312.
- (24) Fischer, E. Ueber Die Glucoside Der Alkohole. *Ber. Dtsch. Chem. Ges.* **1893**, *26*, 2400–2412.
- (25) Koenigs, W.; Knorr, E. Ueber Einige Derivate Des Traubenzuckers Und Der Galactose. *Ber. Dtsch. Chem. Ges.* **1901**, *34*, 957–981.
- (26) Bohé, L.; Crich, D. A Propos of Glycosyl Cations and the Mechanism of Chemical Glycosylation; The Current State of the Art. *Carbohydr. Res.* **2015**, *403*, 48–59.
- (27) van der Vorm, S.; Hansen, T.; Overkleeft, H. S.; van der Marel, G. A.; Codée, J. D. C.; Pedersen, C. M.; Kim, K. S.; Codée, J. D. C. The Influence of Acceptor Nucleophilicity on the Glycosylation Reaction Mechanism. *Chem. Sci.* **2017**, *8*, 1867–1875.
- (28) van der Vorm, S.; Overkleeft, H. S.; van der Marel, G. A.; Codée, J. D. C. Stereoselectivity of Conformationally Restricted Glucosazide Donors. *J. Org. Chem.* **2017**, *82*, 4793–4811.
- (29) Hagen, B.; Ali, S.; Overkleeft, H. S.; van der Marel, G. A.; Codée, J. D. C. Mapping the Reactivity and Selectivity of 2-Azidofucosyl Donors for the Assembly of N-Acetylfucosamine-Containing Bacterial Oligosaccharides. *J. Org. Chem.* **2017**, *82*, 848–868.
- (30) Igarashi, K. The Koenigs-Knorr Reaction. *Adv. Carbohydr. Chem. Biochem.* **1977**, *34* (C), 243–283
- (31) Zeng, Y.; Ning, J.; Kong, F. Remote Control of α - or β -Stereoselectivity in (1 \rightarrow 3)-Glucosylations in the Presence of a C-2 Ester Capable of Neighboring-Group Participation. *Carbohydr. Res.* **2003**, *338*, 307–311.
- (32) Zeng, Y.; Ning, J.; Kong, F. Pure α -Linked Products Can Be Obtained in High Yields in Glycosylation with Glucosyl Trichloroacetimidate Donors with a C2 Ester Capable of Neighboring Group Participation. *Tetrahedron Lett.* **2002**, *43*, 3729–3733.
- (33) Kim, J.-H.; Yang, H.; Park, J.; Boons, G.-J. A General Strategy for Stereoselective Glycosylations. *J. Am. Chem. Soc.* **2005**, *127*, 12090–12097.
- (34) Boltje, T. J.; Kim, J.-H. H.; Park, J.; Boons, G.-J. J. Stereoelectronic Effects Determine Oxacarbenium vs β -Sulfonium Ion Mediated Glycosylations. *Org. Lett.* **2011**, *13*, 284–287.
- (35) Hansen, T.; Lebedel, L.; Remmerswaal, W. A.; van der Vorm, S.; Wander, D. P. A.; Somers, M.; Overkleeft, H. S.; Filippov, D. v.; Désiré, J.; Mingot, A.; Bleriot, Y.; van der Marel, G. A.; Thibaudeau, S.; Codée, J. D. C. Defining the SN1 Side of Glycosylation Reactions: Stereoselectivity of Glycopyranosyl Cations. *ACS Cent. Sci.* **2019**, *5*, 781–788.
- (36) Demchenko, A.; Stauch, T.; Boons, G.-J. Solvent and Other Effects on the Stereoselectivity of Thioglycoside Glycosidations. *Synlett* **1997**, 818–820.
- (37) Demchenko, A. v.; Rousson, E.; Boons, G. Neighboring Group Participation and Solvent Effects. *Tetrahedron Lett.* **1999**, *40*, 6523–6526.
- (38) Ishiwata, A.; Munemura, Y.; Ito, Y. Synergistic Solvent Effect in 1,2-Cis-Glycoside Formation. *Tetrahedron* **2008**, *64*, 92–102.
- (39) Adero, P. O.; Amarasekara, H.; Wen, P.; Bohé, L.; Crich, D. The Experimental Evidence in Support of Glycosylation Mechanisms at the S_N1–S_N2 Interface. *Chem. Rev.* **2018**, *118*, 8242–8284.
- (40) Sasaki, K.; Tohda, K. Recent Topics in β -Stereoselective Mannosylation. *Tetrahedron Lett.* **2018**, *59*, 496–503.
- (41) Mydock, L. K.; Demchenko, A. v. Mechanism of Chemical O-Glycosylation: From Early Studies to Recent Discoveries. *Org. Biomol. Chem.* **2010**, *8*, 497–510.
- (42) Crich, D. Mechanism of a Chemical Glycosylation Reaction. *Acc. Chem. Res.* **2010**, *43*, 1144–1153.
- (43) Landsteiner, K. Zur Kenntnis Der Antifermentativen, Lytischen Und Agglutininierenden Wirkung Des Blutserums Und Der Lymphe. *Zentralblatt Bakteriologie* **1900**, *27*, 357–362.

- (44) von Decastello, A.; Sturli, A. Ueber Die Isoagglutinine Im Serum Gesunder Und Kranker Menschen. *Munch Med. Wochenschr.* **1902**, *49*, 1090–1095.
- (45) Watkins, W. M.; Morgan, W. T. J. Neutralization of the Anti-H Agglutinin in Eel Serum by Simple Sugars. *Nature* **1952**, *169*, 825–826.
- (46) Watkins, W. M.; Morgan, W. T. J. Specific Inhibition Studies Relating to the Lewis Blood-Group System. *Nature* **1957**, *180*, 1038–1040.
- (47) Morgan, W. T. J. The Human AB0 Blood Group Substances. *Experientia* **1947**, *3*, 257–267.
- (48) McLean, J. A. Y. The Discovery of Heparin. *Circulation* **1959**, *19*, 75–78.
- (49) van Boeckel, C. A. A.; Beetz, T.; Vos, J. N.; de Jong, A. J. M.; van Aelst, S. F.; van den Bosch, R. H.; Mertens, J. M. R.; van der Vlugt, F. A. Synthesis of a Pentasaccharide Corresponding to the Antithrombin III Binding Fragment of Heparin. *J. Carbohydr. Chem.* **1985**, *4*, 293–321.
- (50) Petitou, M.; Duchaussoy, P.; Lederman, I.; Choay, J.; Sinaÿ, P.; Jacquinet, J.-C.; Torri, G. Synthesis of heparin fragments. A chemical synthesis of the pentasaccharide O-(2-deoxy-2-sulfamido-6-O-sulfo- α -D-glucopyranosyl)-(1 \rightarrow 4)-O-(β -D-glucopyranosyluronic acid)-(1 \rightarrow 4)-O-(2-deoxy-2-sulfamido-3,6-di-O-sulfo- α -D-glucopyranosyl)-(1 \rightarrow 4)-O-(2-O-sulfo- α -L-idopyranosyluronic acid)-(1 \rightarrow 4)-2-deoxy-2-sulfamido-6-O-sulfo-D-glucopyranose decasodium salt, a heparin fragment having high affinity for antithrombin III. *Carbohydr. Res.* **1986**, *147*, 221–236.
- (51) Ernst, B.; Magnani, J. L. From Carbohydrate Leads to Glycomimetic Drugs. *Nat. Rev. Drug Discovery* **2009**, *8*, 661–677.
- (52) Femenia, A.; Sánchez, E. S.; Simal, S.; Rosselló, C. Compositional Features of Polysaccharides from Aloe Vera (Aloe Barbadensis Miller) Plant Tissues. *Carbohydr. Polym.* **1999**, *39*, 109–117.
- (53) Kenne, L.; Rosell, K.-G.; Svensson, S. Studies on the Distribution of the O-Acetyl Groups in Pine Glucomannan. *Carbohydr. Res.* **1975**, *44*, 69–76.
- (54) Willför, S.; Sjöholm, R.; Laine, C.; Roslund, M.; Hemming, J.; Holmbom, B. Characterisation of Water-Soluble Galactoglucomannans from Norway Spruce Wood and Thermomechanical Pulp. *Carbohydr. Polym.* **2003**, *52*, 175–187.
- (55) Nunes, F. M.; Domingues, M. R.; Coimbra, M. A. Arabinosyl and Glucosyl Residues as Structural Features of Acetylated Galactomannans from Green and Roasted Coffee Infusions. *Carbohydr. Res.* **2005**, *340*, 1689–1698.
- (56) Xing, X.; Cui, S. W.; Nie, S.; Phillips, G. O.; Goff, H. D.; Wang, Q. Study on Dendrobium Officinale O-Acetyl-Glucomannan (Dendronan®): Part II. Fine Structures of O-Acetylated Residues. *Carbohydr. Polym.* **2015**, *117*, 422–433.
- (57) Xing, X.; Cui, S. W.; Nie, S.; Phillips, G. O.; Goff, H. D.; Wang, Q. Study on Dendrobium Officinale O-Acetyl-Glucomannan (Dendronan®): Part I. Extraction, Purification, and Partial Structural Characterization. *Bioact. Carbohydr. Diet. Fibre* **2014**, *4*, 74–83.
- (58) Liepman, A. H.; Nairn, C. J.; Willats, W. G. T.; Sørensen, I.; Roberts, A. W.; Keegstra, K.; Sorensen, I.; Roberts, A. W.; Keegstra, K. Functional Genomic Analysis Supports Conservation of Function Among Cellulose Synthase-Like A Gene Family Members and Suggests Diverse Roles of Mannans in Plants. *Plant Physiol.* **2007**, *143*, 1881–1893.
- (59) Huang, X.; Nie, S.; Cai, H.; Zhang, G.; Cui, S. W.; Xie, M.; Phillips, G. O. Study on Dendrobium Officinale O-Acetyl-Glucomannan (Dendronan®): Part VI. Protective Effects against Oxidative Stress in Immunosuppressed Mice. *Food Res. Int.* **2015**, *72*, 168–173.
- (60) Liang, J.; Wu, Y.; Yuan, H.; Yang, Y.; Xiong, Q.; Liang, C.; Li, Z.; Li, C.; Zhang, G.; Lai, X.; Hu, Y.; Hou, S. Dendrobium Officinale Polysaccharides Attenuate Learning and Memory Disabilities via Anti-Oxidant and Anti-Inflammatory Actions. *Int. J. Biol. Macromol.* **2019**, *126*, 414–426.
- (61) Huang, X.; Nie, S.; Cai, H.; Zhang, G.; Cui, S. W.; Xie, M.; Phillips, G. O. Study on Dendrobium Officinale O-Acetyl-Glucomannan (Dendronan®): Part IV. Immunomodulatory Activity in Vivo. *J. Funct. Foods* **2015**, *15*, 525–532.
- (62) He, T.-B.; Huang, Y.-P.; Yang, L.; Liu, T.-T.; Gong, W.-Y.; Wang, X. J.; Sheng, J.; Hu, J.-M. Structural Characterization and Immunomodulating Activity of Polysaccharide from Dendrobium Officinale. *Int. J. Biol. Macromol.* **2016**, *83*, 34–41.

- (63) Ebringerová, A.; Hromádková, Z.; Hříbalová, V.; Xu, C.; Holmbom, B.; Sundberg, A.; Willför, S. Norway Spruce Galactoglucomannans Exhibiting Immunomodulating and Radical-Scavenging Activities. *Int. J. Biol. Macromol.* **2008**, *42*, 1–5.
- (64) Xing, H.-B.; Tong, M.-T.; Wang, J.; Hu, H.; Zhai, C.-Y.; Huang, C.-X.; Li, D. Suppression of IL-6 Gene by ShRNA Augments Gemcitabine Chemosensitization in Pancreatic Adenocarcinoma Cells. *Biomed Res. Int.* **2018**, 1–10.
- (65) Yu, W.; Ren, Z.; Zhang, X.; Xing, S.; Tao, S.; Liu, C.; Wei, G.; Yuan, Y.; Lei, Z. Structural Characterization of Polysaccharides from *Dendrobium Officinale* and Their Effects on Apoptosis of HeLa Cell Line. *Molecules* **2018**, *23*, 2484.
- (66) Ge, J.-C.; Zha, X.-Q.; Nie, C.-Y.; Yu, N.-J.; Li, Q.-M.; Peng, D.-Y.; Duan, J.; Pan, L.-H.; Luo, J.-P. Polysaccharides from *Dendrobium Huoshanense* Stems Alleviates Lung Inflammation in Cigarette Smoke-Induced Mice. *Carbohydr. Polym.* **2018**, *189*, 289–295.
- (67) Wang, C.; Li, B.; Chen, T.; Mei, N.; Wang, X.; Tang, S. Preparation and Bioactivity of Acetylated Konjac Glucomannan Fibrous Membrane and Its Application for Wound Dressing. *Carbohydr. Polym.* **2020**, *229*, 115404.
- (68) Tabandeh, M. R.; Oryan, A.; Mohammadalipour, A. Polysaccharides of Aloe Vera Induce MMP-3 and TIMP-2 Gene Expression during the Skin Wound Repair of Rat. *International Journal of Biological Macromolecules* **2014**, *65*, 424–430.
- (69) Shi, X.-D.; Yin, J.-Y.; Cui, S. W.; Wang, Q.; Wang, S.-Y.; Nie, S.-P. Plant-Derived Glucomannans: Sources, Preparation Methods, Structural Features, and Biological Properties. *Trends Food Sci. Technol.* **2020**, *99*, 101–116.
- (70) Chokboribal, J.; Tachaboonyakiat, W.; Sangvanich, P.; Ruangpornvisuti, V.; Jettanacheawchankit, S.; Thunyakitpisal, P. Deacetylation Affects the Physical Properties and Bioactivity of Acemannan, an Extracted Polysaccharide from Aloe Vera. *Carbohydr. Polym.* **2015**, *133*, 556–566.
- (71) Salah, F.; Ghoul, Y. el; Mahdhi, A.; Majdoub, H.; Jarroux, N.; Sakli, F. Effect of the Deacetylation Degree on the Antibacterial and Antibiofilm Activity of Acemannan from Aloe Vera. *Ind. Crops Prod.* **2017**, *103*, 13–18.
- (72) Li, M.; Feng, G.; Wang, H.; Yang, R.; Xu, Z.; Sun, Y.-M. Deacetylated Konjac Glucomannan Is Less Effective in Reducing Dietary-Induced Hyperlipidemia and Hepatic Steatosis in C57BL/6 Mice. *J. Agric. Food Chem.* **2017**, *65*, 1556–1565.
- (73) Ebringerová, A.; Hromádková, Z.; Heinze, T. Hemicellulose. In *Polysaccharides I*; Springer-Verlag: Berlin/Heidelberg, 2005; Vol. 186, pp 1–67.
- (74) Ebringerová, A.; Heinze, T. Xylan and Xylan Derivatives - Biopolymers with Valuable Properties, 1. Naturally Occurring Xylans Structures, Isolation Procedures and Properties. *Macromol. Rapid Commun.* **2000**, *21*, 542–556.
- (75) Zhou, X.; Li, W.; Mabon, R.; Broadbelt, L. J. A Critical Review on Hemicellulose Pyrolysis. *Energy Technol.* **2017**, *5*, 52–79.
- (76) Keppler, B. D.; Showalter, A. M. IRX14 and IRX14-LIKE, Two Glycosyl Transferases Involved in Glucuronoxylan Biosynthesis and Drought Tolerance in Arabidopsis. *Mol. Plant* **2010**, *3*, 834–841.
- (77) Scheller, H. V.; Ulvskov, P. Hemicelluloses. *Annu. Rev. Plant Biol.* **2010**, *61*, 263–289.
- (78) Pauly, M.; Gille, S.; Liu, L.; Mansoori, N.; de Souza, A.; Schultink, A.; Xiong, G. Hemicellulose Biosynthesis. *Planta* **2013**, *238*, 627–642.
- (79) Teleman, A.; Lundqvist, J.; Tjerneld, F.; Stålbrand, H.; Dahlman, O. Characterization of Acetylated 4-O-Methylglucuronoxylan Isolated from Aspen Employing ¹H and ¹³C NMR Spectroscopy. *Carbohydr. Res.* **2000**, *329*, 807–815.
- (80) Ishii, T. Acetylation at O-2 of Arabinofuranose Residues in Feruloylated Arabinoxylan from Bamboo Shoot Cell-Walls. *Phytochemistry* **1991**, *30*, 2317–2320.
- (81) Kabel, M. A.; de Waard, P.; Schols, H. A.; Voragen, A. G. J. Location of O-Acetyl Substituents in Xylo-Oligosaccharides Obtained from Hydrothermally Treated Eucalyptus Wood. *Carbohydr. Res.* **2003**, *338*, 69–77.

- (82) Grantham, N. J.; Wurman-Rodrich, J.; Terrett, O. M.; Lyczakowski, J. J.; Stott, K.; Iuga, D.; Simmons, T. J.; Durand-Tardif, M.; Brown, Steven. P.; Dupree, R.; Busse-Wicher, M.; Dupree, P. An Even Pattern of Xylan Substitution Is Critical for Interaction with Cellulose in Plant Cell Walls. *Nat. Plants* **2017**, *3*, 859–865.
- (83) Yuan, Y.; Teng, Q.; Zhong, R.; Ye, Z. H. Roles of Arabidopsis TBL34 and TBL35 in Xylan Acetylation and Plant Growth. *Plant Sci.* **2016**, *243*, 120–130.
- (84) Fooks, L. J.; Fuller, R.; Gibson, G. R. Prebiotics, Probiotics and Human Gut Microbiology. *Int. Dairy J.* **1999**, *9*, 53–61.
- (85) Popper, Z. A. Evolution and Diversity of Green Plant Cell Walls. *Curr. Opin. Plant Biol.* **2008**, *11*, 286–292.
- (86) Popper, Z. A.; Fry, S. C. Primary Cell Wall Composition of Bryophytes and Charophytes. *Ann. Bot.* **2003**, *91*, 1–12.
- (87) Moller, I.; Sørensen, I.; Bernal, A. J.; Blaukopf, C.; Lee, K.; Øbro, J.; Pettolino, F.; Roberts, A.; Mikkelsen, J. D.; Knox, J. P.; Bacic, A.; Willats, W. G. T. High-Throughput Mapping of Cell-Wall Polymers within and between Plants Using Novel Microarrays. *Plant J.* **2007**, *50*, 1118–1128.
- (88) Caffall, K. H.; Mohnen, D. The Structure, Function, and Biosynthesis of Plant Cell Wall Pectic Polysaccharides. *Carbohydr. Res.* **2009**, *344*, 1879–1900.
- (89) Sims, I. M.; Munro, S. L. A.; Currie, G.; Craik, D.; Bacic, A. Structural Characterisation of Xyloglucan Secreted by Suspension-Cultured Cells of *Nicotiana Plumbaginifolia*. *Carbohydr. Res.* **1996**, *293*, 147–172.
- (90) Jia, Z.; Cash, M.; Darvill, A. G.; York, W. S. NMR Characterization of Endogenously O-Acetylated Oligosaccharides Isolated from Tomato (*Lycopersicon Esculentum*) Xyloglucan. *Carbohydr. Res.* **2005**, *340*, 1818–1825.
- (91) Kiefer, L. L.; York, W. S.; Darvill, A. G.; Albersheim, P. Xyloglucan Isolated from Suspension-Cultured Sycamore Cell Walls Is O-Acetylated. *Phytochemistry* **1989**, *28*, 2105–2107.
- (92) Hoffman, M.; Jia, Z.; Peña, M. J.; Cash, M.; Harper, A.; Blackburn, A. R.; Darvill, A.; York, W. S. Structural Analysis of Xyloglucans in the Primary Cell Walls of Plants in the Subclass Asteridae. *Carbohydr. Res.* **2005**, *340*, 1826–1840.
- (93) Gibeaut, D. M.; Pauly, M.; Bacic, A.; Fincher, G. B. Changes in Cell Wall Polysaccharides in Developing Barley (*Hordeum Vulgare*) Coleoptiles. *Planta* **2005**, *221*, 729–738.
- (94) Hayashi, T. Xyloglucans in the Primary Cell Wall. *Annu. Rev. Plant Physiol. Plant Mol. Biol.* **1989**, *40*, 139–168.
- (95) Pauly, M.; Albersheim, P.; Darvill, A.; York, W. S. Molecular Domains of the Cellulose/Xyloglucan Network in the Cell Walls of Higher Plants. *Plant J.* **1999**, *20*, 629–639.
- (96) Pauly, M.; Andersen, L. N.; Kauppinen, S.; Kofod, L. v.; York, W. S.; Albersheim, P.; Darvill, A. A Xyloglucan-Specific Endo- β -1,4-Glucanase from *Aspergillus Aculeatus*: Expression Cloning in Yeast, Purification and Characterization of the Recombinant Enzyme. *Glycobiology* **1999**, *9*, 93–100.
- (97) Somerville, C. Toward a Systems Approach to Understanding Plant Cell Walls. *Science* **2004**, *306*, 2206–2211.
- (98) Park, Y. B.; Cosgrove, D. J. A Revised Architecture of Primary Cell Walls Based on Biomechanical Changes Induced by Substrate-Specific Endoglucanases. *Plant Physiol.* **2012**, *158*, 1933–1943.
- (99) McDougall, G. J.; Fry, S. C. Structure-Activity Relationships for Xyloglucan Oligosaccharides with Antiauxin Activity. *Plant Physiol.* **1989**, *89*, 883–887.
- (100) Takeda, T.; Furuta, Y.; Awano, T.; Mizuno, K.; Mitsuishi, Y.; Hayashi, T. Suppression and Acceleration of Cell Elongation by Integration of Xyloglucans in Pea Stem Segments. *Proc. Natl. Acad. Sci.* **2002**, *99*, 9055–9060.
- (101) Stone, B. A.; Clarke, A. E. *Chemistry and Biology of (1 \rightarrow 3)- β -Glucans*; La Trobe University Press, 1992.
- (102) Cosgrove, D. J. Expansive Growth of Plant Cell Walls. *Plant Physiol. Biochem.* **2000**, *38*, 109–124.

- (103) Obel, N.; Porchia, A. C.; Scheller, H. V. Dynamic Changes in Cell Wall Polysaccharides during Wheat Seedling Development. *Phytochemistry* **2002**, *60*, 603–610.
- (104) Gille, S.; Pauly, M. O-Acetylation of Plant Cell Wall Polysaccharides. *Front. Plant Sci.* **2012**, *3*, 1–7.
- (105) Pauly, M.; Ramírez, V. New Insights into Wall Polysaccharide O-Acetylation. *Front. Plant Sci.* **2018**, *9*, 1210.
- (106) Kohla, G.; Stockfleth, E.; Schauer, R. Gangliosides with O-Acetylated Sialic Acids in Tumors of Neuroectodermal Origin. *Neurochem. Res.* **2002**, *27*, 583–592.
- (107) Mandal, C.; Mandal, C. Identification and Analysis of O-Acetylated Sialoglycoproteins. In *Protein Acetylation*; Hake, S. B., Janzen, C. J., Eds.; Humana Press: Totowa, NJ, 2013; pp 57–93.
- (108) Kamerling, J. P.; Schauer, R.; Shukla, A. K.; Stoll, S.; Halbeek, H.; Vliegthart, J. Migration of O-Acetyl Groups in N,O-Acetylneuraminic Acids. *Eur. J. Biochem.* **1987**, *162*, 601–607.
- (109) Reinhard, B.; Faillard, H. Regioselective Acetylations of Sialic Acid α -Ketosides. *Liebigs Ann. Chem.* **1994**, 193–203.
- (110) Portaleone, P. Acetylation. In *Encyclopedia of Endocrine Diseases, Volym 1*; Martini, L., Ed.; Elsevier: New York, 2004; pp 9–12.
- (111) Papackova, Z.; Cahova, M. Fatty Acid Signaling: The New Function of Intracellular Lipases. *Int. J. Mol. Sci.* **2015**, *16*, 3831–3855.
- (112) Badenhorst, C. P. S.; van der Sluis, R.; Erasmus, E.; van Dijk, A. A. Glycine Conjugation: Importance in Metabolism, the Role of Glycine N-Acyltransferase, and Factors That Influence Interindividual Variation. *Expert Opin. Drug Metab. Toxicol.* **2013**, *9*, 1139–1153.
- (113) Badenhorst, C. P. S.; Erasmus, E.; van der Sluis, R.; Nortje, C.; van Dijk, A. A. A New Perspective on the Importance of Glycine Conjugation in the Metabolism of Aromatic Acids. *Drug Metab. Rev.* **2014**, *46*, 343–361.
- (114) Chan, J. M. Drug Metabolism and Pharmacogenetics. In *Pharmacology and Physiology for Anesthesia*; Hemmings, H. C., Egan, T. D., Eds.; Elsevier, 2019; pp 70–90.
- (115) Di, L.; Kerns, E. H.; Di, L.; Kerns, E. H. Chapter 10 – Blood-Brain Barrier. In *Drug-Like Properties*; Academic Press, 2016; pp 141–159.
- (116) Liners, F.; Gaspar, T.; van Cutsem, P. Acetyl- and Methyl-Esterification of Pectins of Friable and Compact Sugar-Beet Calli: Consequences for Intercellular Adhesion. *Planta* **1994**, *192*, 545–556.
- (117) Pauly, M.; Eberhard, S.; Albersheim, P.; Darvill, A.; York, W. S. Effects of the Mur1 Mutation on Xyloglucans Produced by Suspension-Cultured Arabidopsis Thaliana Cells. *Planta* **2001**, *214*, 67–74.
- (118) Obel, N.; Erben, V.; Schwarz, T.; Kühnel, S.; Fodor, A.; Pauly, M. Microanalysis of Plant Cell Wall Polysaccharides. *Mol. Plant* **2009**, *2*, 922–932.
- (119) Doerschuk, A. P. Acyl Migrations in Partially Acylated, Polyhydroxylic Systems. *J. Am. Chem. Soc.* **1952**, *74*, 4202–4203.
- (120) Bruce Martin, R.; Hedrick, R. I. Intramolecular S-O and S-N Acetyl Transfer Reactions. *J. Am. Chem. Soc.* **1962**, *84*, 106–110.
- (121) Fischer, E. Wanderung von Acyl Bei Den Glyceriden. *Ber. Dtsch. Chem. Ges.* **1920**, *53*, 1621–1633.
- (122) Angyal, S. J.; Melrose, G. J. H. Cyclitols. Part X VIII. Acetyl Migration: Equilibrium between Axial and Equatorial Acetates. *J. Chem. Soc.* **1965**, 6494–6500.
- (123) Ekholm, F. S.; Ardá, A.; Eklund, P.; André, S.; Gabius, H. J.; Jiménez-Barbero, J.; Leino, R. Studies Related to Norway Spruce Galactoglucomannans: Chemical Synthesis, Conformation Analysis, NMR Spectroscopic Characterization, and Molecular Recognition of Model Compounds. *Chem. Eur. J.* **2012**, *18*, 14392–14405.
- (124) Oesterling, T. O.; Metzler, C. M. Acidic and Alkaline Isomerization and Hydrolysis of Lincomycin Monoesters. *Carbohydr. Res.* **1970**, *15*, 285–290.
- (125) Horrobin, T.; Tran, C. H.; Crout, D. Esterase-Catalysed Regioselective 6-Deacylation of Hexopyranose per-Acetates, Acid-Catalysed Rearrangement to the 4-Deprotected Products and Conversions of These into Hexose 4- and 6-Sulfates. *J. Chem. Soc., Perkin Trans. 1* **1998**, 1069–1080.

- (126) Deng, S.; Chang, C. W. T. Cesium Trifluoroacetate or Silver Oxide Mediated Acyl Migration for the Construction of Disaccharide Building Blocks. *Synlett* **2006**, 756–760.
- (127) Petrović, V.; Tomić, S.; Matanović, M. Synthesis and Intramolecular Transesterifications of Pivaloylated Methyl α -D-Galactopyranosides. *Carbohydr. Res.* **2002**, 337, 863–867.
- (128) Illing, H. P. A.; Wilson, I. D. pH Dependent Formation of B-Glucuronidase Resistant Conjugates from the Biosynthetic Ester Glucuronide of Isoxepac. *Biochem. Pharmacol.* **1981**, 30, 3381–3384.
- (129) Brecker, L.; Manut, M.; Schwarz, A.; Nidetzky, B. In Situ Proton NMR Study of Acetyl and Formyl Group Migration in Mono-O-Acyl D-Glucose. *Magn. Reson. Chem.* **2009**, 47, 328–332.
- (130) Mortensen, R. W.; Sidelmann, U. G.; Tjørnelund, J.; Hansen, S. H. Stereospecific pH-Dependent Degradation Kinetics of R- and S-Naproxen- β -1-O-Acyl-Glucuronide. *Chirality* **2002**, 14, 305–312.
- (131) Rangelov, M. A.; Vayssilov, G. N.; Petkov, D. D. Quantum Chemical Model Study of the Acyl Migration in 2'(3')-Formylnucleosides. *Int. J. Quantum Chem.* **2006**, 106, 1346–1356.
- (132) Nicholls, A. W.; Akira, K.; Lindon, J. C.; Farrant, R. D.; Wilson, I. D.; Harding, J.; Killick, D. A.; Nicholson, J. K. NMR Spectroscopic and Theoretical Chemistry Studies on the Internal Acyl Migration Reactions of the 1-O-Acyl- β -D-Glucopyranuronate Conjugates of 2-, 3-, and 4-(Trifluoromethyl)Benzoic Acids. *Chem. Res. Toxicol.* **1996**, 9, 1414–1424.
- (133) Bradshaw, P. R.; Richards, S. E.; Wilson, I. D.; Stachulski, A. v.; Lindon, J. C.; Athersuch, T. J. Kinetic Modelling of Acyl Glucuronide and Glucoside Reactivity and Development of Structure–Property Relationships. *Org. Biomol. Chem.* **2020**, 18, 1389–1401.
- (134) Khan, S.; Teitz, D. S.; Jemal, M. Kinetic Analysis by HPLC - Electrospray Mass Spectrometry of the pH-Dependent Acyl Migration and Solvolysis as the Decomposition Pathways of Ifetroban 1-O-Acyl Glucuronide. *Anal. Chem.* **1998**, 70, 1622–1628.
- (135) Kefurt, K.; Kefurtová, Z.; Jarý, J.; Horáková, I.; Marek, M. Enzymic Deacetylation of Derivatives of 1,2-O-Isopropylidene- α -D-Hexofuranoses. *Carbohydr. Res.* **1992**, 223, 137–145.
- (136) Roslund, M. U.; Aitio, O.; Wärnå, J.; Maaheimo, H.; Murzin, D. Y.; Leino, R. Acyl Group Migration and Cleavage in Selectively Protected β -D-Galactopyranosides as Studied by NMR Spectroscopy and Kinetic Calculations. *J. Am. Chem. Soc.* **2008**, 130, 8769–8772.
- (137) Hasegawa, H.; Akira, K.; Shinohara, Y.; Kasuya, Y.; Hashimoto, T. Kinetics of Intramolecular Acyl Migration of 1 β -O-Acyl Glucuronides of (R)- and (S)-2-Phenylpropionic Acids. *Biol. Pharm. Bull.* **2001**, 24, 852–855.
- (138) Iddon, L.; Richards, S. E.; Johnson, C. H.; Harding, J. R.; Wilson, I. D.; Nicholson, J. K.; Lindon, J. C.; Stachulski, A. v. Synthesis of a Series of Phenylacetic Acid 1- β -O-Acyl Glucosides and Comparison of Their Acyl Migration and Hydrolysis Kinetics with the Corresponding Acyl Glucuronides. *Org. Biomol. Chem.* **2011**, 9, 926–934.
- (139) Blanckaert, N.; Compernelle, F.; Leroy, P.; van Houtte, R.; Fevery, J.; Heirwegh, K. P. The Fate of Bilirubin-IXa Glucuronide in Cholestasis and during Storage in Vitro: Intramolecular Rearrangement to Positional Isomers of Glucuronic Acid. *Biochem. J.* **1978**, 171, 203–214.
- (140) Yoshioka, T.; Baba, A. Structure-Activity Relationships for Degradation Reaction of 1- β -O-Acyl Glucuronides: Kinetic Description and Prediction of Intrinsic Electrophilic Reactivity under Physiological Conditions. *Chem. Res. Toxicol.* **2009**, 22, 158–172.
- (141) Berry, N. G.; Iddon, L.; Iqbal, M.; Meng, X.; Jayapal, P.; Johnson, C. H.; Nicholson, J. K.; Lindon, J. C.; Harding, J. R.; Wilson, I. D.; Stachulski, A. v. Synthesis, Transacylation Kinetics and Computational Chemistry of a Set of Arylacetic Acid 1 β -O-Acyl Glucuronides. *Org. Biomol. Chem.* **2009**, 7, 2525–2533.
- (142) Stachulski, A. v.; Harding, J. R.; Lindon, J. C.; Maggs, J. L.; Park, B. K.; Wilson, I. D. Acyl Glucuronides: Biological Activity, Chemical Reactivity, and Chemical Synthesis. *J. Med. Chem.* **2006**, 49, 6931–6945.
- (143) Filice, M.; Bavaro, T.; Fernandez-Lafuente, R.; Pregnolato, M.; Guisan, J. M.; Palomo, J. M.; Terreni, M. Chemo-Biocatalytic Regioselective One-Pot Synthesis of Different Deprotected Monosaccharides. *Catal. Today* **2009**, 140, 11–18.
- (144) Ren, B.; Wang, M.; Liu, J.; Ge, J.; Dong, H. Enhanced Basicity of Ag₂O by Coordination to Soft Anions. *ChemCatChem* **2015**, 7, 761–765.

- (145) Ahn, Y.-H.; Chang, Y.-T. Molecular Evolution Using Intramolecular Acyl Migration on Myo-Inositol Benzoates with Thermodynamic and Kinetic Selectors. *Chem. Eur. J* **2004**, *10*, 3543–3547.
- (146) Ahn, Y. H.; Chang, Y. T. Molecular Evolution on Chiro-Inositol Dibenzoate Using Intramolecular Acyl Migration and Selection by Phenyl Boronic Acid. *J. Comb. Chem.* **2004**, *6*, 293–296.
- (147) James, T. D.; Sandanayake, K. R. A. S.; Shinkai, S. Saccharide Sensing with Molecular Receptors Based on Boronic Acid. *Angew. Chem. Int. Ed.* **1996**, *35*, 1910–1922.
- (148) Yang, W.; He, H.; Drueckhammer, D. G. Computer-Guided Design in Molecular Recognition: Design and Synthesis of a Receptor. *Angew. Chem. Int. Ed.* **2001**, *40*, 1714–1718.
- (149) Chevallier, O. P.; Migaud, M. E. Investigation of Acetyl Migrations in Furanosides. *Beilstein J. Org. Chem.* **2006**, *2*.
- (150) ChemAdder/SpinAdder. *Spin Discoveries Ltd.* (<http://www.chemadder.com>).
- (151) Puchart, V.; Agger, J. W.; Berrin, J. G.; Várnai, A.; Westereng, B.; Biely, P. Comparison of Fungal Carbohydrate Esterases of Family CE16 on Artificial and Natural Substrates. *J. Biotechnol.* **2016**, *233*, 228–236.
- (152) Ohara, K.; Lin, C. C.; Yang, P. J.; Hung, W. T.; Yang, W. bin; Cheng, T. J. R.; Fang, J. M.; Wong, C. H. Synthesis and Bioactivity of β -(1 \rightarrow 4)-Linked Oligomannoses and Partially Acetylated Derivatives. *J. Org. Chem.* **2013**, *78*, 6390–6411.
- (153) Woods, R. J.; Pathiaseril, A.; Wormald, M. R.; Edge, C. J.; Dwek, R. A. The High Degree of Internal Flexibility Observed for an Oligomannose Oligosaccharide Does Not Alter the Overall Topology of the Molecule. *Eur. J. Biochem.* **1998**, *258*, 372–386.
- (154) Petkowicz, C. L. O.; Reicher, F.; Mazeau, K. Conformational Analysis of Galactomannans: From Oligomeric Segments to Polymeric Chains. *Carbohydr. Polym.* **1998**, *37*, 25–39.
- (155) Geijtenbeek, T. B. H.; Torensma, R.; van Vliet, S. J.; van Duijnhoven, G. C. F.; Adema, G. J.; van Kooyk, Y.; Figdor, C. G. Identification of DC-SIGN, a Novel Dendritic Cell-Specific ICAM-3 Receptor That Supports Primary Immune Responses. *Cell* **2000**, *100*, 575–585.
- (156) van Vliet, S. J.; García-Vallejo, J. J.; van Kooyk, Y. Dendritic Cells and C-Type Lectin Receptors: Coupling Innate to Adaptive Immune Responses. *Immunol. Cell Biol.* **2008**, *86*, 580–587.
- (157) Valverde, P.; Martínez, J. D.; Cañada, F. J.; Ardá, A.; Jiménez-Barbero, J. Molecular Recognition in C-Type Lectins: The Cases of DC-SIGN, Langerin, MGL, and L-Sectin. *ChemBioChem* **2020**, *21*, 2999–3025.
- (158) Thépaut, M.; Guzzi, C.; Sutkeviciute, I.; Sattin, S.; Ribeiro-Viana, R.; Varga, N.; Chabrol, E.; Rojo, J.; Bernardi, A.; Angulo, J.; Nieto, P. M.; Fieschi, F. Structure of a Glycomimetic Ligand in the Carbohydrate Recognition Domain of C-Type Lectin DC-SIGN. Structural Requirements for Selectivity and Ligand Design. *J. Am. Chem. Soc.* **2013**, *135*, 2518–2529.
- (159) Martínez, J. D.; Valverde, P.; Delgado, S.; Romanò, C.; Linclau, B.; Reichardt, N. C.; Oscarson, S.; Ardá, A.; Jiménez-Barbero, J.; Cañada, F. J. Unraveling Sugar Binding Modes to DC-SIGN by Employing Fluorinated Carbohydrates. *Molecules* **2019**, *24*, 2337.
- (160) Nagae, M.; Yamaguchi, Y. Structural Aspects of Carbohydrate Recognition Mechanisms of C-Type Lectins. In *Current topics in microbiology and immunology*; Science and Business Media Deutschland GmbH, 2020; Vol. 429, pp 147–176.
- (161) Martínez, J. D.; Infantino, A. S.; Valverde, P.; Diercks, T.; Delgado, S.; Reichardt, N.-C.; Ardá, A.; Cañada, F. J.; Oscarson, S.; Jiménez-Barbero, J. The Interaction of Fluorinated Glycomimetics with DC-SIGN: Multiple Binding Modes Disentangled by the Combination of NMR Methods and MD Simulations. *Pharmaceuticals* **2020**, *13*, 179.
- (162) Mayer, M.; Meyer, B. Characterization of Ligand Binding by Saturation Transfer Difference NMR Spectroscopy. *Angew. Chem. Int. Ed.* **1999**, *38*, 1784–1788.
- (163) Meyer, B.; Peters, T. NMR Spectroscopy Techniques for Screening and Identifying Ligand Binding to Protein Receptors. *Angew. Chem. Int. Ed.* **2003**, *42*, 864–890.
- (164) Viegas, A.; Manso, J.; Nobrega, F. L.; Cabrita, E. J. Saturation-Transfer Difference (STD) NMR: A Simple and Fast Method for Ligand Screening and Characterization of Protein Binding. *J. Chem. Educ.* **2011**, *88*, 990–994.

- (165) Gimeno, A.; Valverde, P.; Ardá, A.; Jiménez-Barbero, J. Glycan Structures and Their Interactions with Proteins. A NMR View. *Curr. Opin. Struct. Biol.* **2020**, *62*, 22–30.
- (166) Feinberg, H.; Mitchell, D. A.; Drickamer, K.; Weis, W. I. Structural Basis for Selective Recognition of Oligosaccharides by DC-SIGN and DC-SIGNR. *Science* **2001**, *294*, 2163–2166.
- (167) Guo, Y.; Feinberg, H.; Conroy, E.; Mitchell, D. A.; Alvarez, R.; Blixt, O.; Taylor, M. E.; Weis, W. I.; Drickamer, K. Structural Basis for Distinct Ligand-Binding and Targeting Properties of the Receptors DC-SIGN and DC-SIGNR. *Nat. Struct. Mol. Biol.* **2004**, *11*, 591–598.
- (168) Rees, D. A.; Scott, W. E. Polysaccharide Conformation. Part VI. Computer Model-Building for Linear and Branched Pyranoglycans. Correlations with Biological Function. Preliminary Assessment of Inter-Residue Forces in Aqueous Solution. Further Interpretation of Optical Rotation in Terms of Chain Conformation. *J. Chem. Soc. B* **1971**, 469–479.
- (169) Preston, R. D. Polysaccharide Conformation and Cell Wall Function. *Annu. Rev. Plant Biol.* **1979**, *30*, 55–78.
- (170) Terrett, O. M.; Lyczakowski, J. J.; Yu, L.; Iuga, D.; Franks, W. T.; Brown, S. P.; Dupree, R.; Dupree, P. Molecular Architecture of Softwood Revealed by Solid-State NMR. *Nat. Commun.* **2019**, *10*, 4978.
- (171) Northcote, D. H. Chemistry of the Plant Cell Wall. *Annu. Rev. Plant Biol.* **1972**, *23*, 113–132.
- (172) Lundqvist, J.; Teleman, A.; Junel, L.; Zacchi, G.; Dahlman, O.; Tjerneld, F.; Stålbrand, H. Isolation and Characterization of Galactoglucomannan from Spruce (*Picea Abies*). *Carbohydr. Polym.* **2002**, *48*, 29–39.
- (173) Thornton, J.; Ekman, R.; Holmbom, B.; Örså, F. Polysaccharides Dissolved from Norway Spruce in Thermomechanical Pulping and Peroxide Bleaching. *J. Wood Chem. Technol.* **1994**, *14*, 159–175.
- (174) Anslyn, E. v.; Dougherty, D. A. *Modern Physical Organic Chemistry*; University Science Books: Sausalito, California, 2006.
- (175) Ho, J.; Coote, M. L. A Universal Approach for Continuum Solvent pK_a Calculations: Are We There Yet? *Theor. Chem. Acc.* **2010**, *125*, 3–21
- (176) Thapa, B.; Schlegel, H. B. Density Functional Theory Calculation of pK_a's of Thiols in Aqueous Solution Using Explicit Water Molecules and the Polarizable Continuum Model. *J. Phys. Chem. A* **2016**, *120*, 5726–5735.
- (177) Bootsma, A. N.; Wheeler, S. E. Popular Integration Grids Can Result in Large Errors in DFT-Computed Free Energies. *ChemRxiv*. **2019**.
- (178) Schrödinger Release 2020-1: MacroModel, Schrödinger, LLC, New York, NY, 2021.

